

SHRP-A-408

# **Level One Mix Design: Materials Selection, Compaction, and Conditioning**

Ronald Cominsky  
University of Texas at Austin

Rita B. Leahy  
Strategic Highway Research Program

Edward T. Harrigan  
Strategic Highway Research Program



**Strategic Highway Research Program**  
National Research Council  
Washington, DC 1994

SHRP-A-408  
Contract A-003A  
ISBN 0-309-05824-4  
Product no. 1012

Program Manager: *Edward T. Harrigan*  
Project Manager: *Rita B. Leahy*  
Program Area Secretary: *Juliet Narsiah*  
Copyeditor: *Katharyn L. Bine*  
Typesetter: *Laurie Dockendorf*  
Production Editor: *Katharyn L. Bine*

August 1994

keywords:  
age conditioning  
aging  
asphalt aggregate mixes  
asphalt concrete mix design  
Delphi method  
gyratory compaction  
mix conditioning  
moisture conditioning  
stripping  
water-sensitivity

Strategic Highway Research Program  
National Research Council  
2101 Constitution Avenue N.W.  
Washington, DC 20418

(202) 334-3774

The publication of this report does not necessarily indicate approval or endorsement by the National Academy of Sciences, the United States Government, or the American Association of State Highway and Transportation Officials or its member states of the findings, opinions, conclusions, or recommendations either inferred or specifically expressed herein.

©1994 National Academy of Sciences

## **Acknowledgments**

The research described herein was supported by the Strategic Highway Research Program (SHRP). SHRP is a unit of the National Research Council that was authorized by section 128 of the Surface Transportation and Uniform Relocation Assistance Act of 1987.

The patience and expertise of Laurie Dockendorf, Oregon State University, are gratefully acknowledged. It was largely through her tireless efforts at the keyboard that this report made it to press.

# Contents

Acknowledgments	iii
List of Figures	ix
List of Tables	xiii
Abstract	1
Executive Summary	3
1 Development of a Volumetric Mix Design Criteria for Aggregates and Mixes Through a Modified Delphi Group Process	7
1.1 Introduction	7
1.2 Overview of the Delphi Method	8
1.3 Use of a Modified Delphi Method to Develop Specifications	8
1.4 Round 1 Questionnaire	10
1.5 Round 2 Questionnaire	11
1.6 Round 3 Questionnaire	13
1.7 Round 4 Questionnaire	13
1.8 Round 5 Questionnaire	13
1.9 Summary of Delphi Group Results	16
1.9.1 Gradation Controls	18
1.9.2 Coarse Aggregate Angularity	20
1.9.3 Fine Aggregate Angularity	21
1.9.4 Aggregate Toughness	22
1.9.5 Aggregate Soundness	22

1.9.6	Aggregate Deleterious Material . . . . .	22
1.9.7	Clay Content . . . . .	23
1.9.8	Thin Elongated Particles . . . . .	24
1.9.9	Dust Proportion . . . . .	24
1.9.10	Air Voids . . . . .	25
1.9.11	Voids in Mineral Aggregate . . . . .	26
1.9.12	Voids Filled with Asphalt . . . . .	26
<b>2</b>	<b>Compaction in the Superpave System: Mix Design and Field Control . . . . .</b>	<b>29</b>
2.1	Introduction . . . . .	29
2.2	Simulation of Field Compaction . . . . .	30
2.2.1	Related Research . . . . .	30
2.2.2	Consideration of Alternative Methods . . . . .	31
2.2.3	Conclusions and Recommendations . . . . .	32
2.3	Basis for Selection of the SHRP Gyratory Compactor for Mix Design and Field Control . . . . .	33
2.3.1	Laboratoire Central des Ponts et Chaussées (LCPC) Gyratory Compactor Approach . . . . .	34
2.3.2	Regional Laboratory of Augers Gyratory Compactor Approach . . . . .	39
2.3.3	SHRP's Gyratory Compactor Approach . . . . .	48
2.3.4	Gyratory Compaction Characteristics—Relation to Service Densities of Asphalt Mixes . . . . .	62
2.4	SHRP Gyratory Compactor in Relation to Field Control . . . . .	77
2.4.1	Experiment Design . . . . .	78
2.4.2	Summary of Effects on $C_{10}$ , $C_{230}$ , and K . . . . .	86
2.4.3	Volumetric Properties . . . . .	86
2.4.4	Summary and Recommendations . . . . .	87
2.5	Field Validation of SHRP Gyratory Compactor . . . . .	88
2.6	Comparison of Experimental Results with Technical Criteria . . . . .	88
<b>3</b>	<b>Mix Conditioning Procedures in the Superpave System . . . . .</b>	<b>93</b>
3.1	Aging . . . . .	93
3.1.1	Experimental Design . . . . .	94
3.1.2	Discussion of Results . . . . .	95
3.1.3	Conclusions and Recommendations . . . . .	104

3.2	Moisture Sensitivity . . . . .	105
3.2.1	Hypothesis . . . . .	106
3.2.2	Experimental Design . . . . .	107
3.2.3	Discussion of Results . . . . .	108
3.3	Conclusions and Recommendations . . . . .	117
References	. . . . .	119

## List of Figures

Figure 1.1	Typical gradation control for 12.5 mm (1/2 in.) mix . . . . .	19
Figure 2.1	Principle of compacting with the gyratory shear compacting press . . . . .	35
Figure 2.2	Variation in void content with number of gyrations . . . . .	36
Figure 2.3	Compaction curves illustrating different workability for three bituminous mixes . . . . .	38
Figure 2.4	Variation in force during compaction . . . . .	39
Figure 2.5	Comparison of compaction curves for field and gyratory compactors . . . . .	41
Figure 2.6	Compaction curves for transformations . . . . .	41
Figure 2.7	Change in compaction curves by horizontal transformation . . . . .	42
Figure 2.8	Compaction curves from a gyratory compactor . . . . .	44
Figure 2.9	Measured profile and apparent volume at $n$ passes . . . . .	44
Figure 2.10	Evolution of the profile . . . . .	46
Figure 2.11	Results with gyratory compactor . . . . .	46
Figure 2.12	Results with compaction bed . . . . .	48
Figure 2.13	Percent compaction as a function of simulator passes . . . . .	49
Figure 2.14	Comparison of maximum density versus number of gyrations at optimum asphalt content . . . . .	50
Figure 2.15	Comparison of maximum density versus number of gyrations at 1 percent greater than optimum asphalt content . . . . .	50
Figure 2.16	Comparison of maximum density versus number of gyrations at 1 percent less than optimum asphalt content . . . . .	51
Figure 2.17	Air voids and VMA as a function of gyratory speed . . . . .	52

Figure 2.18	VFA and density as a function of gyratory speed . . . . .	53
Figure 2.19	Number of gyrations to define construction and traffic compaction . . . . .	58
Figure 2.20	Typical gyratory compaction curve . . . . .	58
Figure 2.21	Effect of asphalt content on mix compactability . . . . .	59
Figure 2.22	Design gyrations as a function of temperature . . . . .	68
Figure 2.23	Design gyrations as a function of traffic . . . . .	70
Figure 2.24	Compaction curve for 90-1802 blend . . . . .	71
Figure 2.25	Compaction curve for 04-1022 blend . . . . .	71
Figure 2.26	Compaction curve for 06-8535 blend . . . . .	72
Figure 2.27	Design gyrations ( $N_{\text{design}}$ ) for various temperatures . . . . .	76
Figure 2.28	Design gyrations for various traffic levels . . . . .	76
Figure 2.29	Gradation of baseline mix for field control experiment . . . . .	79
Figure 2.30	Gradation of mixes with variable percent passing the 75 $\mu\text{m}$ sieve . . . . .	80
Figure 2.31	Gradation of mixes with variable percent passing the 2.36 mm sieve . . . . .	81
Figure 2.32	Gradation of mix with variable nominal maximum size . . . . .	82
Figure 2.33	Gradation of mixes with variable percent natural sand . . . . .	84
Figure 2.34	Typical compaction curve for gyratory compacted specimen . . . . .	85
Figure 2.35	Densification curve for Arizona SPS-9-blend 1 . . . . .	89
Figure 2.36	Densification curve for Arizona SPS-9-blend 2 . . . . .	89
Figure 2.37	Densification curve for Arizona SPS-9-blend 3 . . . . .	90
Figure 3.1	Short-term oven aging (high voids) . . . . .	96
Figure 3.2	Short-term oven aging (low voids) . . . . .	96
Figure 3.3	Aging by extended mixing . . . . .	97



Figure 3.4	Long-term oven aging . . . . .	97
Figure 3.5	Comparison of short-term aging of binders and mixes . . . . .	99
Figure 3.6	Comparison of long-term aging of binders and mixes . . . . .	99
Figure 3.7	Comparison of pavement age and resilient modulus . . . . .	101
Figure 3.8	Comparison of field core and unaged core moduli . . . . .	101
Figure 3.9	Comparison of field core and short-term oven-aged core moduli . . . . .	102
Figure 3.10	Comparison of field core and long-term oven-aged core moduli . . . . .	102
Figure 3.11	Comparison of pavement age and resilient modulus ratio . . . . .	103
Figure 3.12	Comparison of unaged and short-term oven-aged moduli . . . . .	103
Figure 3.13	Comparison of unaged and long-term oven-aged moduli . . . . .	104
Figure 3.14	Air void distribution in compacted mix . . . . .	106
Figure 3.15	Environmental Conditioning System test results with binder AAG . . . . .	109
Figure 3.16	Environmental Conditioning System test results with aggregate RD . . . . .	109
Figure 3.17	Environmental Conditioning System test results with aggregate RC . . . . .	110
Figure 3.18	Comparison of AASHTO T 283 and Environmental Conditioning System results for resilient modulus ratio . . . . .	112
Figure 3.19	Comparison of AASHTO T 283 and Environmental Conditioning System results for tensile strength and resilient modulus ratios . . . . .	112
Figure 3.20	Comparison of AASHTO T 283 and Environmental Conditioning System results normalized for percent air voids . . . . .	113
Figure 3.21	Environmental Conditioning System field validation—wheel track data . . . . .	115
Figure 3.22	Environmental Conditioning System field validation—performance criterion . . . . .	115
Figure 3.23	Net adsorption test results by binder . . . . .	116
Figure 3.24	Net adsorption test results by aggregate . . . . .	116
Figure 3.25	Environmental Conditioning System resilient modulus results by binder . . . . .	118

**Figure 3.26 Environmental Conditioning System resilient modulus results by  
aggregate . . . . . 118**

## List of Tables

Table 1.1	Average ratings from the first questionnaire . . . . .	11
Table 1.2	Average ratings from the second questionnaire . . . . .	12
Table 1.3	Average ratings from the third questionnaire . . . . .	14
Table 1.4	Average ratings and measurements identified as "best" by statistically significant agreement of the experts (based on responses to the fourth questionnaire . . . . .	15
Table 1.5	List of statistically significant external factors for each measurement . . . . .	16
Table 1.6	Average, low and high values for the measurements (based on responses to the fifth questionnaire) . . . . .	17
Table 1.7	Coarse aggregate angularity criteria . . . . .	21
Table 1.8	Fine aggregate angularity criteria . . . . .	21
Table 1.9	Clay content criteria . . . . .	23
Table 1.10	Thin elongated particles criteria . . . . .	24
Table 1.11	Dust proportion criteria . . . . .	25
Table 1.12	Air void criteria . . . . .	25
Table 1.13	Voids in mineral aggregate criteria . . . . .	26
Table 1.14	Voids filled with asphalt criteria . . . . .	27
Table 2.1	Comparison of laboratory compaction methods to field compaction . . . . .	31
Table 2.2	Summary of gyratory compaction data for 6, 15, and 30 rpm . . . . .	51
Table 2.3	Controlled variables in compactor comparison experiment . . . . .	54

Table 2.4	Cells of experiment . . . . .	57
Table 2.5	Cells of USACOE compactor comparison experiment . . . . .	60
Table 2.6	Comparison of densification parameters from gyratory compactors . . . . .	60
Table 2.7	Final core selection—experiment matrix . . . . .	66
Table 2.8	Design gyrations determined from monthly maximum air temperature . . . . .	68
Table 2.9	Temperature conversion . . . . .	69
Table 2.10	Superpave traffic levels . . . . .	69
Table 2.11	Results from $N_{\text{design}}$ experiment . . . . .	74
Table 2.12	Design gyrations for various traffic levels and environmental zones . . . . .	75
Table 2.13	Controlled variables in compactor field control experiment . . . . .	78
Table 2.14	Definition of asphalt content levels . . . . .	79
Table 2.15	Definition of levels for percent passing 75 $\mu\text{m}$ sieve . . . . .	80
Table 2.16	Definition of levels for percent passing 2.36 mm sieve . . . . .	81
Table 2.17	Definition of levels for nominal maximum size . . . . .	82
Table 2.18	Definitions of levels for percent natural sand . . . . .	84
Table 2.19	Array of conditions used in the field control experiment . . . . .	85
Table 2.20	Response of design compaction curve to variables . . . . .	86
Table 2.21	Volumetric properties at 100 gyrations . . . . .	87
Table 2.22	Response of parameters to input variables . . . . .	88
Table 2.23	Density as a function of angle of gyration . . . . .	90
Table 3.1	Factors considered in the water sensitivity experiment plan . . . . .	108
Table 3.2	Conditioning information chart for warm and cold climates . . . . .	108

## **Abstract**

**This report summarizes the research devoted to three key aspects of the Superpave Level I mix design: volumetric mix design criteria for aggregates and mixes; compaction; and mix conditioning. The first chapter describes the Delphi group process that was used to select aggregate properties and specification values included in the Level I mix design procedure. Chapter 2 addresses the rationale for the selection of the gyratory compactor, its relation to field control and validation. The final chapter summarizes the research associated with the development and validation of laboratory conditioning procedures for asphalt concrete mixes. It describes the procedures used to simulate both short- and long-term aging, as well as moisture sensitivity under repeated loading.**

## **Executive Summary**

The purpose of this report is to provide a technical summary of the asphalt research input to Superpave Level 1 mix design relative to the materials selection, compaction, and specimen conditioning.

Superpave (Superior Performing Asphalt Pavements) is the name for the final product of the SHRP Asphalt Research Program. The Superpave mix design system is a comprehensive method of designing paving mixes tailored to the unique performance requirements dictated by the traffic, environment (climate), and structural section at a particular pavement site. It facilitates selecting and combining asphalt binder, aggregate, and any necessary modifier to achieve the required level of pavement performance.

The Superpave system is applicable to virgin and recycled, dense-graded, hot mix asphalt (HMA), with or without modification. In addition, the Superpave performance tests are applicable to the characterization of a variety of specialized paving mixes such as stone matrix asphalt (SMA). It can be used when constructing new surface, binder, and base layers, as well as overlays on existing pavements. Through materials selection (aggregate and asphalt) and mix design, it directly addresses the reduction and control of permanent deformation, fatigue cracking, and low-temperature cracking. It also explicitly considers the effects of aging and moisture sensitivity in promoting or arresting the development of these three distresses.

One of the goals of the Strategic Highway Research Program (SHRP) was to develop specifications for aggregates and asphalt aggregate mixtures. Based on the results of a modified Delphi process, SHRP developed the aggregate and mix characteristics, and the corresponding values, to be included in the mix specifications. The characteristics chosen were as follows:

### **Aggregate Characteristics**

- (a) gradation
- (b) crushed faces
- (c) natural sand content
- (d) Los Angeles abrasion
- (e) aggregate soundness
- (f) deleterious materials
- (g) sand equivalent

## Asphalt-Aggregate Characteristics

- a) air voids
- b) voids in the mineral aggregate (VMA)
- c) voids filled with asphalt (VFA)

SHRP also recognized the need for laboratory compaction equipment that would be relatively simple, economical, and representative of in-place compaction at the construction site. The equipment should also provide the potential for field quality control purposes. The entire mix design system, including field control, is based on the use of the Superpave gyratory compactor. The SHRP gyratory compactor was developed from the French gyratory protocol. The compactor is relatively inexpensive, portable, and capable of quickly molding specimens with minimal specimen to specimen variation. Of primary importance is the performance properties of the compacted specimen simulate the performance properties of cores from pavement constructed with the same asphalt aggregate combination. The compactor allows the compactability of the mix to be evaluated, including an estimate of the final air void content under traffic (the probability of the mix becoming plastic under traffic) and a measure of the structuring of the aggregate in the mix.

The Superpave gyratory compactor has the following characteristics:

- an angle of gyration of  $1.25 \pm 0.02^\circ$ ,
- a gyration rate of 30 gyrations per minute,
- a vertical pressure during gyration of 600 kPa (87 lb/in<sup>2</sup>), and
- the capability of producing cylindrical specimens 150 mm (6 in.) in diameter and height.

Other gyratory compactors can be utilized if capable of meeting the requirements outlined in SHRP Method of Test M-002.

The SHRP Superpave mix design system also includes procedures to evaluate the effects of aging and moisture sensitivity.

Principal control on aging in the Superpave mix design system is through the combined use of the rolling film oven test and the pressure aging vessel to measure the long-term aging of the asphalt. Since laboratory mixtures are made with unaged asphalt binders, the conditioning procedure must simulate both plant and pavement aging.

In the short-term aging procedure, loose mix is placed in a tray (immediately after mixing) to a uniform depth. The mix is held in a forced draft oven for 4 hours at 135°C, after which the mix is brought to the appropriate compaction temperature and the specimen compacted. This procedure simulates the aging that takes place during hot mix asphalt production and the pavement construction process.

In the optimal long-term aging procedure, compacted specimens are placed (prepared from loose mix which has undergone short-term aging) in a forced draft oven at 85°C. The time of exposure in the oven varies depending on the length of pavement service to be simulated.

The recommended exposure time is 2 days which is equivalent to about 10 years of pavement service. Longer periods can be utilized at the designer's discretion.

Either AASHTO T 283, *Resistance of Compacted Bituminous Mixture to Moisture Induced Damage*, or SHRP Method of Test M-006, *Determining the Moisture Susceptibility of Modified and Unmodified Hot Mix asphalt with the Environmental Conditioning System*, is used in the Superpave mix design system to evaluate the moisture sensitivity of trial mix designs.

Use of SHRP method M-006 requires an environmental conditioning system. This is a modified triaxial test unit in which the dynamic resilient modulus of cylindrical or prismatic mixture specimen can be continually measured as moisture forced through it. Moisture susceptibility is characterized by the resilient modulus ratio of conditioned to unconditioned specimens.



# 1

## **Development of Volumetric Mix Design Criteria for Aggregates and Mixes Through a Modified Delphi Group Process**

### **1.1 Introduction**

Specifications for aggregates and for asphalt aggregate mixes must be based on engineering theory and data. However, development of the specifications also requires the more subjective knowledge of experts. This chapter describes the use of a modified Delphi procedure to draw upon the opinions of a group of experts to assist in the development of the specifications for the volumetric mix design contained in the Superpave system.

One of the goals of the Strategic Highway Research Program (SHRP) was to develop specifications for aggregates and for asphalt aggregate mixes. The objective of the study described in this report was to use the combined knowledge of 14 experts, selected by SHRP, to assist in that development. These experts comprised what is known as the Aggregate Expert Task Group (ETG).

One way to obtain the experts' knowledge is to form a committee. There are a number of problems with such an approach. One major problem is group dynamics. For example, one strong-willed individual may dominate the committee meetings. Other problems are the cost and logistics of convening frequent committee meetings of a geographically dispersed group of participants.

One alternative to the committee process is the Delphi method, developed by the RAND Corporation in the 1950s and 1960s (Brown 1968, Dalkey 1967, Dalkey and Helmer 1951). This method evolved from PROJECT DELPHI, an Air Force-sponsored study of the use of expert opinion, which was named after the Greek oracle at Delphi. The Delphi method attempts to avoid the negative effects that may result from group dynamics while retaining the strengths of joint decisions. It does this by avoiding face-to-face meetings to preserve the anonymity of the participants.

This chapter discusses the application of a modified Delphi method to aid in the development of specifications. A statistically designed fractional factorial experiment was incorporated into the overall process to obtain the experts' opinions of the possible effects of environmental conditions on the specification limits (Linstone and Turoff 1975, Smith et al. 1992). The results of the Delphi application described in this chapter were used by the SHRP office to specify the criteria to be used in the volumetric mix design (Kennedy et al. 1994).

## **1.2 Overview of the Delphi Method**

One of the major aspects of the Delphi method is that the group members remain anonymous to each other (Dalkey and Helmer 1951, Linstone and Turoff 1975). This is usually accomplished through the use of questionnaires which are administered by a coordinator. The experts deal only with the coordinator, and not with other group members. The process is evolutionary, proceeding through a series of rounds (typically four to six), which begin with general issues and converge toward more specific findings. After each round, the group members usually receive tabulated responses and statistics calculated from the questionnaire results.

In general, the initial questionnaire is used to formulate the issues and solicit possible options. The coordinator collects these questionnaires and summarizes the information contained therein. The summary is disseminated to the participants, together with a follow-up questionnaire. The participants are asked to reconsider their previous responses in view of the information, and to then complete the follow-up questionnaire.

This process, which continues through a number of rounds, tends to narrow the spread of the responses, but does not necessarily guarantee a consensus.

## **1.3 Use of a Modified Delphi Method to Develop Specifications**

To arrive at the most useful information in the shortest amount of time, without an overwhelming amount of paperwork, a modified Delphi procedure was used. The modification retained the evolutionary nature of the Delphi process and some of its anonymity, but also permitted the experts to meet face-to-face once during the overall process. It was thought that this would permit SHRP to obtain as much useful information as possible for use in the establishment of specifications (Smith et al. 1992).

Based on the results of the modified Delphi process, SHRP developed the aggregate and mix characteristics, and the corresponding values, to be included in the mix specifications.

The aggregate characteristics chosen were

- (a) *Gradation controls*, defined by control points and a restricted zone for the gradation.

- (b) *Coarse aggregate angularity*, defined as the percent by weight of aggregate particles larger than 4.75 mm (No. 4 sieve) with one or more fractured faces.
- (c) *Fine aggregate angularity*, defined as the percentage of air voids of loosely compacted aggregate as measured in the National Aggregates Association Test Method A.
- (d) *Aggregate toughness*, defined as a percentage loss from the Los Angeles abrasion test.
- (e) *Aggregate soundness*, defined as a percentage of degradation from the sodium or magnesium soundness test.
- (f) *Aggregate deleterious materials*, defined as a percentage by weight of undesirable contaminants.
- (g) *Clay content*, defined by the use of the sand equivalent test on the portion of blended aggregates passing a 2.36 mm (No.8) sieve.
- (h) *Thin elongated particles*, defined as the percentage by weight of coarse aggregate particles that have a ratio of maximum to minimum dimensions greater than 5.

The asphalt aggregate mix characteristics chosen were

- (a) *Air voids*, defined as the percent by volume of compacted aggregate asphalt mix of air between coated aggregate particles.
- (b) *Voids in mineral aggregate (VMA)*, defined as the percent by volume of effective asphalt binder plus air voids in a compacted aggregate asphalt mix.
- (c) *Voids filled with asphalt (VFA)*, defined as a percentage of the VMA filled with asphalt.
- (d) *Dust to asphalt ratio*, defined as the percentage by weight ratio of material passing the 75  $\mu\text{m}$  (No. 200) sieve to the percentage of effective asphalt binder.

The modified Delphi procedure involved five rounds of questionnaires. The first round was conducted by mail, as is usually done. However, the second and third rounds were conducted in Washington, DC during a meeting of all the experts. The fourth and fifth rounds were conducted by mail. The following subsections briefly describe the five rounds of questionnaires.

## 1.4 Round 1 Questionnaire

An initial questionnaire was developed and sent to the ETG. The questionnaire contained the following two sets of questions pertaining to: (1) aggregate characteristics and (2) asphalt aggregate mix characteristics. The questionnaire listed seven possible aggregate characteristics and three possible asphalt aggregate characteristics. These were as follows:

### *Aggregate Characteristics*

- (a) gradation limits
- (b) crushed faces
- (c) natural sand content
- (d) LA abrasion
- (e) aggregate soundness
- (f) deleterious materials
- (g) sand equivalent

### *Asphalt Aggregate Characteristics*

- (a) air voids
- (b) VMA
- (c) VFA

The experts were asked to rate their degree of agreement or disagreement with the inclusion of each characteristics as a specification by using a seven-point scale. Specifically, they were asked to respond to statements of the following type:

- (1) Gradation limits should be included as a specification in the mix design system.

Very Strongly Disagree	Strongly Disagree	Disagree	Neutral	Agree	Strongly Agree	Very Strongly Agree
---------------------------	----------------------	----------	---------	-------	-------------------	------------------------

In addition, an open-ended question provided opportunity for the respondent to suggest other characteristics. The initial questionnaire was completed by the experts and returned to SHRP. A summary of the results of the ratings is given in Table 1.1.

The experts were also asked to list the following: (a) suggested measurements for establishing the specification for each of the possible characteristics; (b) external factors such as traffic level or environmental conditions which would have an effect on each characteristics

**Table 1.1. Average ratings from the first questionnaire**

Specification	Average Rating*	Standard Deviation
<b>Aggregate characteristics:</b>		
(1) gradation limits	6.18	0.98
(2) crushed faces	6.04	1.00
(3) natural sand content	4.54	2.01
(4) Los Angeles abrasion	4.67	1.78
(5) aggregate soundness	5.45	1.04
(6) deleterious materials	5.33	1.61
(7) sand equivalent	4.17	1.40
<b>Asphalt aggregate mix characteristics:</b>		
(1) air voids	6.75	0.45
(2) VMA	6.08	1.24
(3) VFA	4.25	1.55

\*Scaled ratings: 1 - very strongly disagree  
2 - strongly disagree  
3 - disagree  
4 - neutral  
5 - agree  
6 - strongly agree  
7 - very strongly agree

specification limit; and (c) how the external factors would affect the specification limits. They provided numerous suggestions to (a) and (b).

## 1.5 Round 2 Questionnaire

For the second round, the ETG was convened in Washington, DC. A brief overview of the Delphi process was presented to the group and the results from the first round were discussed. The participants were then given a questionnaire that requested rankings of the seven aggregate characteristics and three asphalt aggregate characteristics that were included in the initial questionnaire.

A method to solicit information about the possible effects of five external factors was also included as part of the second questionnaire. These factors were as follows:

- (a) moisture level (annual inches of precipitation)
- (b) July mean daily high temperature (°F)
- (c) lowest expected annual temperature (°F)
- (d) traffic level (design ESALs)
- (e) pavement depth (inches from surface).

The questionnaire contained scenarios of different highway locations defined by eight combinations of levels of the five factors. The experts were asked to consider these eight

scenarios, and for each to indicate their best judgement of specification limit values. A 2<sup>5-2</sup> partial factorial design was used to generate the scenarios which involved highway locations of differing weather conditions and traffic loads. This type of design provides a basis for an efficient evaluation of whether the five factors have a statistically significant effect on the specification limit values.

The first part repeated the request for ratings on the seven-point scale used in the first questionnaire. The second part included the eight highway locations. Following the administration of this questionnaire, a more intensive discussion of specification limits was held. The results of the second questionnaire were analyzed the same day in order to incorporate the findings, as well as suggestions arising from the discussion, into the third questionnaire.

A summary of the results of the ratings for the characteristics is given in Table 1.2. Preliminary findings indicated that the external factor having the greatest effect on the specification limit values was traffic level. July mean daily high temperature, lowest expected annual temperature, and pavement depth also had a statistically significant effect on the values of at least one of the specification limits.

**Table 1.2. Average ratings from the second questionnaire**

Specification	Average Rating*	Standard Deviation
<b>Aggregate characteristics:</b>		
(1) gradation limits	6.15	1.69
(2) crushed faces	5.77	1.66
(3) natural sand content	4.92	1.56
(4) Los Angeles abrasion	4.65	2.02
(5) aggregate soundness	4.85	1.51
(6) deleterious materials	5.31	1.66
(7) sand equivalent	4.23	1.59
<b>Asphalt aggregate mix characteristics:</b>		
(1) air voids	6.85	0.36
(2) VMA	6.23	0.69
(3) VFA	4.46	1.51

\*Scaled ratings: 1 - very strongly disagree  
 2 - strongly disagree  
 3 - disagree  
 4 - neutral  
 5 - agree  
 6 - strongly agree  
 7 - very strongly agree

## 1.6 Round 3 Questionnaire

The discussion following round 2 suggested the inclusion of a few additional characteristics, which were a subset of those provided by the ETG in response to the first questionnaire. In addition, the discussion suggested that some characteristics be redefined or renamed (e.g., aggregate toughness instead of Los Angeles abrasion).

Based on these suggestions and on the results of the second questionnaire, a questionnaire was prepared for the third round. The questionnaire asked for ratings (on the seven-point scale used previously) of both possible characteristics and possible measurements for establishing specification limits. A summary of the ratings of the characteristics and measurements is given in Table 1.3.

In addition, another  $2^{5-2}$  fractional factorial was used to obtain more information about the effects of the external factors. Again, traffic level was the external factor that had the greatest effect.

## 1.7 Round 4 Questionnaire

After the third round, it was reasonably clear which characteristics should be included in the specifications. It was less clear, however, which measurement should be used for each characteristic. Therefore, it was decided to implement a "forced measurement choice" in the fourth questionnaire. This was done by requiring the experts to rank each proposed method of measurement for a characteristic as 1 (first choice), 2 (second choice), etc., assuming that the characteristic *would be included* as a specification (even if they disagreed with its inclusion).

An analysis of variance of the measurement ranks, based on the Friedman Test, was conducted. The results indicated that there was statistically significant agreement about the best measurement for a number of the characteristics. These measurements, as well as the ratings of the characteristics, are listed in Table 1.4.

## 1.8 Round 5 Questionnaire

Based on the results of the four Delphi rounds and the discussions during the meeting of the ETG, SHRP decided upon the characteristics and measurements to be incorporated. The fifth questionnaire had the following purposes: (1) to determine the values of the measurements that should serve to define specification limits, and (2) to assess the impact of external factors on these values.

The questionnaire used a set of highway scenarios based on a  $2^{4-1}$  fractional factorial which incorporated four of the five external factors listed in section 1.5. Moisture level was not included as a factor because it had never been found statistically significant in any of the preliminary studies. The use of the fractional factorial permitted an evaluation of the overall

**Table 1.3. Average ratings from the third questionnaire**

Specification/Measurement	Average Rating*	Standard Deviation
<b>Aggregate characteristics:</b>		
(1) gradation limits	6.57	0.76
a. minimum/maximum	4.50	1.95
b. control points/zone	4.14	1.79
c. control points only	5.29	1.68
(2) coarse aggregate angularity	6.43	0.76
a. % particles	4.79	1.72
b. % weight	5.21	1.37
(3) fine aggregate angularity	5.85	1.21
a. natural/manufactured	3.57	1.87
b. NAA method	5.29	1.49
(4) aggregate toughness (Los Angeles abrasion)	5.57 4.71	1.65 2.16
(5) aggregate soundness	5.43	1.28
a. ASTM C88	3.71	1.59
b. AASHTO T210	3.71	1.59
c. Washington State Degradation	3.14	1.61
d. freeze/thaw	5.14	1.65
(6) limit deleterious material	5.86	1.61
a. visual	4.93	1.86
b. % weight	5.64	1.08
(7) maximum clay content	6.07	1.00
a. sand equivalent	4.29	1.68
b. plasticity index	4.86	1.29
(8) thin, elongated pieces (ASTM D4791)	4.71 4.86	1.98 1.70
(9) Minus No. 200	3.77	2.35
a. compacted voids	3.93	1.94
b. gradation	3.50	1.83
(10) mineral identification (visual)	4.38 4.46	1.56 1.56
<b>Asphalt aggregate mix characteristics:</b>		
(1) air voids	6.79	0.43
(Rice TSG)	6.71	0.61
(2) VMA	6.36	0.84
a. bulk specific gravity	5.71	1.73
b. specific gravity of aggregate	3.71	1.77
(3) VFA	4.21	1.72
(4) dust asphalt ratio	3.36	1.69
(% wt No. 200/% asphalt)	4.08	2.06
(5) film thickness	3.57	1.79
(Asphalt Institute's MS-2 Procedure)	4.18	1.33

\*Scaled ratings: 1 - very strongly disagree  
2 - strongly disagree  
3 - disagree  
4 - neutral  
5 - agree  
6 - strongly agree  
7 - very strongly agree



**Table 1.4. Average ratings and measurements identified as "best" by statistically significant agreement of the experts (based on responses to the fourth questionnaire)**

Specification	Average Rating*	Standard Deviation	"Best" Measurement
<b>Aggregate characteristics:</b>			
(1) gradation limits	6.08	0.76	none identified
(2) coarse aggregate angularity	6.39	1.65	none identified
(3) fine aggregate angularity	5.62	1.38	NAA Method
(4) aggregate toughness	5.77	0.97	Los Angeles abrasion test
(5) aggregate soundness	5.23	1.50	ASTM C88 test
(6) limit deleterious materials	5.85	1.21	% weight of aggregate
(7) maximum clay content	5.76	1.01	sand equivalent test
(8) thin, elongated pieces	4.70	1.11	ASTM D4791
(9) minus No. 200	4.83	1.80	none identified
(10) mineral identification	3.85	1.99	none identified
<b>Asphalt aggregate mix characteristics:</b>			
(1) air voids	6.77	0.44	Rice specific gravity
(2) VMA	6.15	0.90	bulk specific gravity of aggregate
(3) VFA	4.00	1.68	none identified
(4) dust asphalt ratio	4.46	1.85	none identified
(5) film thickness	3.31	1.89	MS-2 procedure

\*Scaled ratings: 1 - very strongly disagree  
 2 - strongly disagree  
 3 - disagree  
 4 - neutral  
 5 - agree  
 6 - strongly agree  
 7 - very strongly agree

average value for any particular measurement, as well as an assessment of the differences between the experts and of the possible effects of the external factors.

The data from the fifth questionnaire indicated that only two (traffic level and pavement depth) of the four external factors examined had statistically significant effects on any of the measurement values specified by the experts. Although there was general agreement among the experts about the effects of the external factors, there was no overall agreement about what the measurement values should be. Some experts specified relatively high values while others specified relatively low values for a specific measurement. This is reflected by the large variability in the data.

In an attempt to decrease that variability, the observed data was trimmed to delete the responses of those experts who reported values at the high and the low end of the spectrum for each measurement. Table 1.5 lists the external factors that were found statistically significant for each measurement, together with the corresponding *p*-values (i.e., the observed level of significance).

**Table 1.5. List of statistically significant external factors from the fifth questionnaire**

Measurement	Statistically Significant External Effects
nominal maximum size	pavement depth (< .01)
coarse aggregate angularity	pavement depth (< .01) traffic level (< .01)
fine aggregate angularity	pavement depth (.04) traffic level (< .01)
aggregate toughness	pavement depth (.05) traffic level (< .05)
aggregate soundness	traffic level (< .01)
deleterious materials	pavement depth (.01) traffic level (< .01)
clay content	traffic level (< .01)
thin elongated particles	pavement depth (.01) traffic level (< .02)
air voids	traffic level (< .01)
VMA	traffic level (< .01)
VFA	traffic level (< .01)

Table 1.6 presents a summary of the *average* values from the experts (using the trimmed data) for each measurement. As mentioned previously, there are large differences between the values specified by the experts. As an indication of the size of these differences, low values and high values may be obtained from the average values by subtracting or adding the indicated amount to each of the average values. The low values correspond to the expert who provided the lowest values for the measurement (using the trimmed data), and the high values correspond to the expert who provided the highest values. Also given is the proportion of total variation in the trimmed data due to the differences among the experts.

The questionnaire also asked for an evaluation of restrictions on aggregate gradation for each of the highway locations. The majority of the experts specified aggregate gradation either above or below the restricted zone, although for the higher traffic level there was a tendency for about half of them to specify aggregate gradation only below the zone.

## 1.9 Summary of Delphi Group Results

The modified Delphi process used in this study provided four major contributions to the development of specifications. They were as follows:

- to provide quantified opinions about the importance of possible characteristics to be used in the specifications,

**Table 1.6. Average, low and high values for the measurements (based on responses to the fifth questionnaire)**

<b>Nominal maximum size:</b>		
Average value for 2 in. pavement depth: 0.63 in.		
Average value for 5 in. pavement depth: 1.08 in.		
For low values, subtract 0.17; for high values, add 0.30.		
Proportion of variation due to differences among experts: 20%		
<b>Coarse aggregate angularity:</b>		
	<u><math>3 \times 10^5</math> ESALs</u>	<u><math>10^7</math> ESALs</u>
Average value for 2 in. pavement depth	67.9%	83.8%
Average value for 5 in. pavement depth	56.3%	72.2%
For low values, subtract 0.17; for high values, add 0.30.		
Proportion of variation due to differences among experts: 20%		
<b>Fine aggregate angularity:</b>		
	<u><math>3 \times 10^5</math> ESALs</u>	<u><math>10^7</math> ESALs</u>
Average value for 2 in. pavement depth	42.8%	44.2%
Average value for 5 in. pavement depth	41.4%	42.8%
<b>Aggregate toughness:</b>		
	<u><math>3 \times 10^5</math> ESALs</u>	<u><math>10^7</math> ESALs</u>
Average value for 2 in. pavement depth	44.8%	43.5%
Average value for 5 in. pavement depth	46.0%	44.8%
For low values, subtract 0.17; for high values, add 0.30.		
Proportion of variation due to differences among experts: 20%		
<b>Aggregate soundness:</b>		
Average value for 2 in. pavement depth: 12.9%		
Average value for 5 in. pavement depth: 11.7%		
For low values, subtract 0.18; for high values, add 1.2%.		
Proportion of variation due to differences among experts: 39%		
<b>Deleterious materials</b>		
	<u><math>3 \times 10^5</math> ESALs</u>	<u><math>10^7</math> ESALs</u>
Average value for 2 in. pavement depth	2.0%	1.5%
Average value for 5 in. pavement depth	2.4%	1.9%
For low values, subtract 0.17; for high values, add 2.0%.		
Proportion of variation due to differences among experts: 60%		
<b>Clay content:</b>		
Average value for $3 \times 10^5$ ESALs: 38.8%		
Average value for $10^7$ ESALs: 42.2%		
For low values, subtract 6.7%; for high values, add 4.5%.		
Proportion of variation due to differences among experts: 50%		
<b>Thin elongated particles:</b>		
	<u><math>3 \times 10^5</math> ESALs</u>	<u><math>10^7</math> ESALs</u>
Average value for 2 in. pavement depth	11.5%	10.3%
Average value for 5 in. pavement depth	13.1%	11.9%
For low values, subtract 6.7%; for high values, add 3.3%.		
Proportion of variation due to differences among experts: 78%		

Continued on next page.

**Table 1.6 (continued). Average, low and high values for the measurements (based on responses to the fifth questionnaire)**

---

**Air voids:**

Average value for  $3 \times 10^5$  ESALs: 3.4% to 4.9%  
Average value for  $10^7$  ESALs: 3.5% to 4.9%  
For low values, subtract 0.6%; for high values, add 0.9%.  
Proportion of variation due to differences among experts: 67%

---

**VMA:**

Average value for  $3 \times 10^5$  ESALs: 14.6%  
Average value for  $10^7$  ESALs: 14.8%  
For low values, subtract 0.7%; for high values, add 0.8%.  
Proportion of variation due to differences among experts: 78%

---

**VFA:**

Average value for  $3 \times 10^5$  ESALs: 67.9% to 78.6%  
Average value for  $10^7$  ESALs: 66.2% to 77.2%  
For low values, subtract 2.2%; for high values, add 4.6%.  
Proportion of variation due to differences among experts: 45%

---

- to fine-tune the definitions of the characteristics,
- to obtain information about measurements to be used for specification limits,
- to estimate the effects of external factors on those limits.

SHRP used the information gained from this modified Delphi process to develop the criteria and specification limits for aggregates and asphalt aggregate mixes.

The following aggregate and mix characteristics are included in the mix specification.

### *1.9.1 Gradation Controls*

#### **1.9.1.1 Definition**

Gradation is to be controlled using control points and a restricted zone plotted with the sieve opening raised to the 0.45 power. A typical gradation control is shown in Figure 1.1.

Other definitions associated with gradation control are as follows:

- **Nominal maximum size:** one sieve size larger than the first sieve to retain more than 10 percent.
- **Maximum size:** one sieve size larger than the nominal maximum size.

### Typical Gradation Control for 12.5 mm (1/2 inch) Mixture

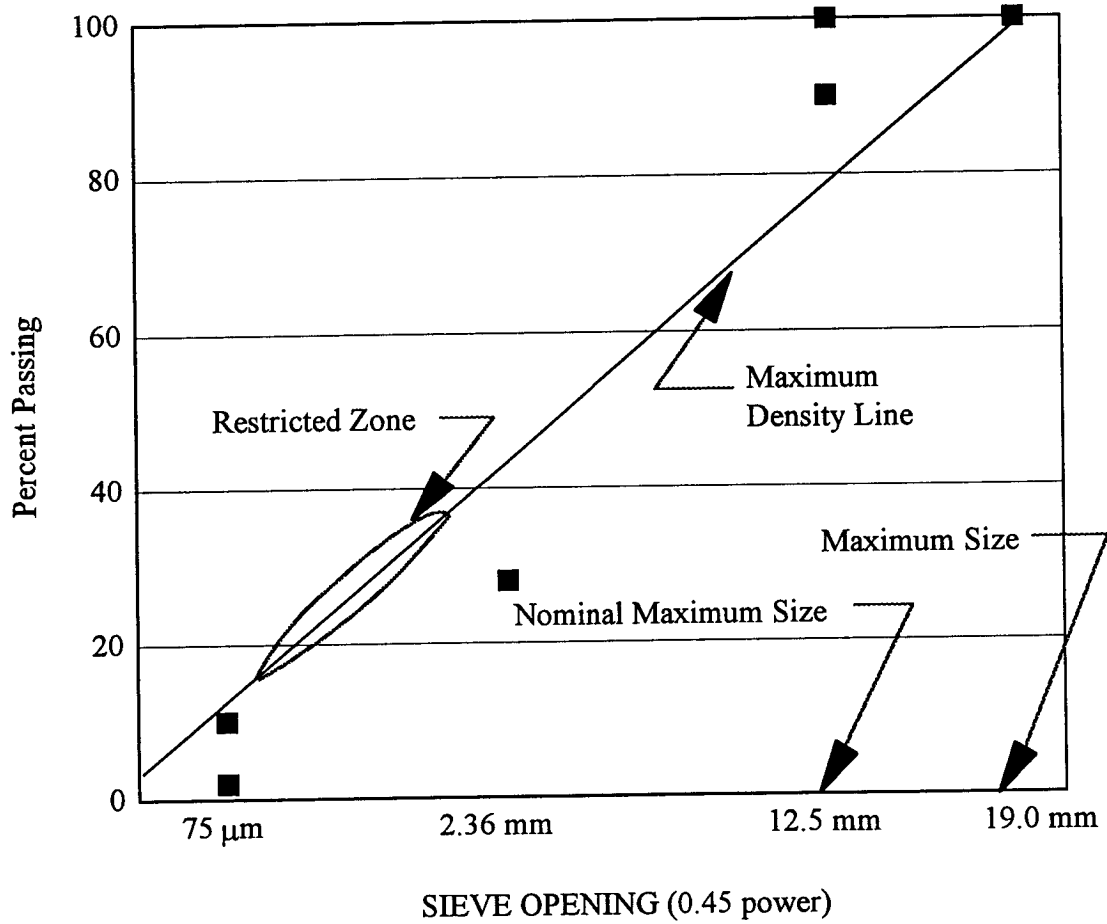


Figure 1.1. Typical gradation control for 12.5 mm (1/2 in.) mix

- **Maximum density line:** a maximum density line is drawn from the origin to the maximum size.
- **Restricted zone:** a zone lying on the maximum density line extending from the 300  $\mu\text{m}$  (No. 50 sieve) to the 2.36 mm (3/8 in.) sieve through which it is undesirable for the gradation to pass.

The Delphi group responses indicated that the location within the gradation controls depended on the level of traffic. As traffic levels increase, the experts moved the aggregate gradation toward the bottom of the gradation controls, below the restricted zone. Specification of gradation above or below the restricted zone will be left to the specifying agency.

The Delphi process identified only one external factor for nominal maximum size. Responses indicated that nominal maximum size of aggregate mix should increase with increasing distance from the pavement surface.

SHRP chose not to include nominal maximum size as a criteria. Specifying agencies are to select an aggregate nominal maximum size for surface, binder and base mixes according to their specific requirements.

## *1.9.2 Coarse Aggregate Angularity*

### 1.9.2.1 Definition

Coarse aggregate angularity is defined as the percent by weight of aggregate particles larger than 4.75 mm (No. 4 sieve) with one or more fractured faces. A fractured face is defined as a fractured surface larger than 25 percent of the maximum aspect ratio of the aggregate particle. Coarse aggregate angularity is to be measured on the coarse (plus 4.75 mm) particles of the blended aggregates.

### 1.9.2.2 Use

The test is to be used in the laboratory during mix design to determine acceptability as well as a field control tool to monitor production of aggregates. Acceptable values are shown in Table 1.7.

**Table 1.7. Coarse aggregate angularity criteria**

Traffic, ESALs	Depth from Surface	
	< 100 mm	> 100 mm
1. < 3×10 <sup>5</sup>	55/ -	-/ -
2. < 1×10 <sup>6</sup>	65/ -	-/ -
3. < 3×10 <sup>6</sup>	76/ -	50/ -
4. < 1×10 <sup>7</sup>	85/80	60/ -
5. < 3×10 <sup>7</sup>	95/90	80/75
6. < 1×10 <sup>8</sup>	100/100	95/90
7. < 1×10 <sup>8</sup>	100/100	100/100

Note: 85/80 means 85 percent one fractured face, 80 percent two fractured faces.

### 1.9.3 Fine Aggregate Angularity

#### 1.9.3.1 Definition

Fine aggregate angularity is defined as the percent air voids of loosely compacted aggregate as measured in the National Aggregate Association Test Method A. This test is done on the portion of blended aggregates passing the 2.36 mm (No. 8) sieve.

#### 1.9.3.2 Use

The test is to be used in the laboratory during mix design to determine acceptability but not as a field control too to monitor aggregate production. Acceptable values are shown in Table 1.8.

**Table 1.8. Fine aggregate angularity criteria**

Traffic, ESALs	Depth From Surface	
	< 100 mm	> 100 mm
1. < 3×10 <sup>5</sup>	-	-
2. < 1×10 <sup>6</sup>	40	-
3. < 3×10 <sup>6</sup>	40	40
4. < 1×10 <sup>7</sup>	45	40
5. < 3×10 <sup>7</sup>	45	40
6. < 1×10 <sup>8</sup>	45	45
7. < 1×10 <sup>8</sup>	45	45

## ***1.9.4 Aggregate Toughness***

### **1.9.4.1 Definition**

Aggregate toughness is defined as percentage loss from the Los Angeles abrasion test.

### **1.9.4.2 Use**

The test could be used in the laboratory during mix design to determine acceptability or could be used as source acceptance control for an aggregate supplier.

The SHRP mix design method does not specify criteria. Specifying agencies should determine the requirement for an aggregate toughness criteria in their local situation and apply such criteria as they are currently using or determine acceptable levels for the local situation.

## ***1.9.5 Aggregate Soundness***

### **1.9.5.1 Definition**

Aggregate soundness is defined as percentage degradation from the sodium or magnesium soundness test.

### **1.9.5.2 Use**

The test could be used in the laboratory during mix design to determine acceptability or could be used as source acceptance control for an aggregate supplier.

The SHRP mix design method does not specify criteria. Specifying agencies should determine the requirement for an aggregate toughness criteria in their local situation and apply such criteria as they are currently using or determine acceptable levels for the local situation.

## ***1.9.6 Aggregate Deleterious Materials***

### **1.9.6.1 Definition**

Deleterious material is defined as the percentage by weight of undesirable contaminants.



### 1.9.6.2 Use

The test could be used in the laboratory during mix design to determine acceptability. It also could be used as source acceptance control for an aggregate supplier.

Aggregate contaminants vary widely according to geographic location. Among many things, typical contaminants include soft shale, coal, wood, and mica. Specifying agencies should determine the requirements for a deleterious criteria for their local situation and apply such criteria as they may be currently using or determine acceptable levels for their local situation.

The SHRP mix design method does not specify criteria.

## 1.9.7 Clay Content

### 1.9.7.1 Definition

Clay content is measured using the sand equivalent test which is done on the portion of blended aggregate passing the 2.36 mm (No. 8) sieve.

### 1.9.7.2 Use

The test is to be used in the laboratory during mix design to determine aggregate acceptability and may also be used as a field control tool to monitor aggregate production. Acceptable values are shown in Table 1.9.

**Table 1.9. Clay content criteria**

Traffic, ESALs	Sand Equivalent
1. $< 3 \times 10^5$	40
2. $< 1 \times 10^6$	40
3. $< 3 \times 10^6$	40
4. $< 1 \times 10^7$	45
5. $< 3 \times 10^7$	45
6. $< 1 \times 10^8$	50
7. $< 1 \times 10^8$	50

## 1.9.8 Thin Elongated Particles

### 1.9.8.1 Definition

Thin, elongated particles are defined as the percentage by weight of coarse aggregate particles which have a ratio of maximum to minimum dimensions greater than 5. Thin elongated particles are measured using ASTM test method D4791 which is done on the portion of blended aggregates passing the 4.75 mm (No. 4) sieve.

### 1.9.8.2 Use

The test may be used in the laboratory during mix design to determine aggregate acceptability or may also be used as a method of source qualification. Acceptable values are shown in Table 1.10.

**Table 1.10. Thin elongated particles criteria**

Traffic, ESALs	Thin Elongated Particles, Maximum Percent
1. $< 3 \times 10^5$	-
2. $< 1 \times 10^6$	-
3. $< 3 \times 10^6$	10
4. $< 1 \times 10^7$	10
5. $< 3 \times 10^7$	10
6. $< 1 \times 10^8$	10
7. $< 1 \times 10^8$	10

## 1.9.9 Dust Proportion

### 1.9.9.1 Definition

Dust proportion is defined as the percentage by weight ratio of material passing the 75  $\mu\text{m}$  (No. 200) sieve to the percentage of effective asphalt binder.

### 1.9.9.2 Use

Dust proportion is calculated in the laboratory during mix design to determine acceptability. Acceptable values are shown in Table 1.11.

**Table 1.11. Dust proportion criteria**

Traffic, ESALs	Dust Proportion
1. $< 3 \times 10^5$	0.6 - 1.2
2. $< 1 \times 10^6$	0.6 - 1.2
3. $< 3 \times 10^6$	0.6 - 1.2
4. $< 1 \times 10^7$	0.6 - 1.2
5. $< 3 \times 10^7$	0.6 - 1.2
6. $< 1 \times 10^8$	0.6 - 1.2
7. $< 1 \times 10^8$	0.6 - 1.2

### 1.9.10 *Air Voids*

#### 1.9.10.1 Definition

Air voids are defined as the total volume of air between the coated aggregate particles throughout a compacted mix, expressed as a percent of the bulk volume of the compacted mix.

#### 1.9.10.2 Use

The test is to be used in the laboratory during mix design to select asphalt content. It may also be used in the field to monitor the production of the mix. Acceptable values are shown in Table 1.12.

**Table 1.12. Air void criteria**

Traffic, ESALs	Design, Percent	Field Control, Percent
1. $< 3 \times 10^5$	4	3 - 5
2. $< 1 \times 10^6$	4	3 - 5
3. $< 3 \times 10^6$	4	3 - 5
4. $< 1 \times 10^7$	4	3 - 5
5. $< 3 \times 10^7$	4	3 - 5
6. $< 1 \times 10^8$	4	3 - 5
7. $< 1 \times 10^8$	4	3 - 5

## **1.9.11 Voids in Mineral Aggregate (VMA)**

### **1.9.11.1 Definition**

Voids in mineral aggregate (VMA) are defined as the percent by volume of effective asphalt binder plus air voids in a compacted aggregate asphalt mix. Voids in mineral aggregate are calculated using bulk specific gravity of the aggregate.

### **1.9.11.2 Use**

The test is to be used in the laboratory during mix design to determine acceptability. It may also be used as a field control tool to monitor production of mix. Acceptable values are shown in Table 1.13.

**Table 1.13. Voids in mineral aggregate criteria**

<b>Nominal Maximum Size of Aggregate</b>	<b>Voids in the Mineral Aggregate, Percent</b>
9.5 mm	15.0
12.5 mm	14.0
19.0 mm	13.0
25.0 mm	12.0
37.5 mm	11.0

## **1.9.12 Voids Filled with Asphalt (VFA)**

### **1.9.12.1 Definition**

Voids filled with asphalt (VFA) is defined as percent of the VMA filled with asphalt.

### **1.9.12.2 Use**

Voids filled with asphalt does not require a separate test method but is calculated from values of air voids and VMA. Acceptable values are shown in Table 1.14.

**Table 1.14. Voids filled with asphalt criteria**

Traffic, ESALs	Voids Filled with Asphalt, Percent
1. $< 3 \times 10^5$	70 - 80
2. $< 1 \times 10^6$	65 - 78
3. $< 3 \times 10^6$	65 - 78
4. $< 1 \times 10^7$	65 - 75
5. $< 3 \times 10^7$	65 - 75
6. $< 1 \times 10^8$	65 - 75
7. $< 1 \times 10^8$	65 - 75

## 2

# Compaction in the Superpave System: Mix Design and Field Control

## 2.1 Introduction

Research has shown that volumetric properties have a greater influence than stability on the final performance of an asphalt mix (Busching 1963, Hughes 1989). It may be possible that a mix with adequate aggregate quality parameters and correct volumetric properties would produce a mix with stability values which meet current design criteria and that the mix would perform adequately in service. The opposite, however, is not necessarily correct. A mix can be designed that meets stability but does not meet volumetric criteria. This mix is not likely to perform well.

In addition the performance of structurally adequate asphalt pavements is affected by two factors: the mix design and compaction. Neither of these factors can assure satisfactory pavement life. Even the best-designed mix will be subject to reduced performance if not compacted sufficiently. For this reason, compaction is considered to be the single most important factor affecting the performance of asphalt pavements.

Compaction is the process of reducing the air void content of an asphalt concrete mix. The solid aggregate particles within a viscoelastic medium are placed and oriented into a more dense and effective arrangement. This process should take place during construction rather than under traffic. Experience and research have shown that the air voids present in a pavement decrease by 2 to 8 percent from the time of construction (Consuegra 1988, Hughes 1989, Hughes 1964).

If the initial air voids after construction are high, or the layer is thicker, or the traffic is heavier, there will be more rutting after several years of traffic. The percentage of air voids obtained during construction, therefore, should be as close as possible to the percentage of air voids found in the pavement after several years of service.

It is equally important that the density of laboratory-compacted specimens approximate that obtained in the field in terms of (a) the structure of the mix and (b) the quantity, size, and distribution of the air voids (Conseugra 1988, Hughes 1989). The most important aspect of relating laboratory density to field density is the time at which the field density is determined. In addition, the method of laboratory compaction affects the fundamental mix properties important to pavement performance. This chapter describes how SHRP selected the gyratory compactor for mix design and field control.

## **2.2 Simulation of Field Compaction**

Different compaction techniques produce asphalt concrete specimens with different particle orientations and thus differing physical properties. When evaluating asphalt concrete mixes in the laboratory, it is desirable to produce test specimens that duplicate, as nearly as possible, the compacted mix as it exists (or will exist) in an actual pavement layer.

### ***2.2.1 Related Research***

Several studies have focused on comparing the properties of mixes compacted with different laboratory compaction devices. The most extensive and most relevant studies to this effort are the National Cooperative Highway Research Program (NCHRP) (Von Quintus et al. 1991) and the SHRP A-003A studies (Sousa et al. 1991).

In the Von Quintus study, *Asphalt Aggregate Mix Analysis System (AAMAS)*, the effects of five different laboratory compactors on the selected properties of the compacted mixes were investigated. Field cores and laboratory compacted samples were subjected to indirect tensile testing (strength, strain at failure, resilient modulus and creep) and aggregate particle orientation evaluation. The results of these mechanical tests performed at three different temperatures were pooled. The relative similarities between laboratory compaction technique and field compaction found are shown in Table 2.1.

Researchers at the University of California at Berkeley, evaluated three compaction devices: Texas gyratory, kneading, and rolling wheel (Sousa et al. 1991). The study determined the extent to which the method of laboratory compaction affects pavement performance in terms of permanent deformation and fatigue. The most important findings were:

1. Samples prepared with the Texas gyratory compactor are expected to be more sensitive to asphalt type (and perhaps binder content) than samples prepared by the kneading compactor.
2. Samples prepared using the kneading compaction device are more resistant to permanent deformation primarily due to the development of a more complete interparticle contact structure, at least for densely graded aggregates. Mixes prepared with kneading compaction are more sensitive to aggregate angularity and surface texture.

**Table 2.1. Comparison of laboratory compaction methods to field compaction**

Compaction Device	Closest to the Field Cores	Percent of Cells with Properties Indifferent from the Field Cores
Texas gyratory	45	63
Rolling wheel compactor*	25	49
Kneading compactor	23	52
Arizona vibratory/kneading	7	41
Standard Marshall hammer	7	35

Source: Von Quintus et al. 1991

\*The rolling wheel compactor was the Mobil Steel Wheel Simulator.

3. Specimens prepared using the rolling wheel compactor were ranked between specimens prepared by kneading and gyratory methods in terms of their resistance to permanent deformation. They were stiffer under transient loading and more fatigue resistant than either gyratory or kneading specimens.

Based on these findings, Sousa et al. indicated that the compaction method has a profound impact on fundamental mix properties. They summarized their recommendations by indicating that the rolling wheel compactor seems to best duplicate field-compacted mixes. A criticism of this study is that it is not correlated to field results. Although the study performed mix property tests which have been shown to be related to field performance, the link between laboratory-compacted and field-compacted mix properties is absent.

It should be noted that the Sousa et al. and the Von Quintus et al. studies both concluded that the kneading compactor produced specimens with greater resistance to rutting, than either the rolling wheel compactor or the Texas gyratory compactor. Specimens produced by the Texas gyratory compactor were found to have properties most susceptible to rutting. It may be argued that, since the Texas gyratory compactor is the most sensitive to asphalt type and asphalt cement properties, it is an appropriate device for mix analysis. SHRP research clearly underscores the need to discriminate among asphalts with various physical properties.

### *2.2.2 Consideration of Alternative Methods*

Based on the findings of Von Quintus et al. and Sousa et al., SHRP initiated a study under contract A-001 to evaluate the correlation of selected laboratory compaction methods with field compaction. The work was performed by the Texas Transportation Institute at Texas A&M University (Button et al. 1992).



The objective of this research study was to determine which of four compaction devices more closely simulated actual field compaction. Detailed studies were conducted to compare the properties of specimens made using the Texas gyratory compactor and the Exxon rolling wheel compactor with pavement cores. An abbreviated study was performed using selected test procedures to similarly evaluate mixes prepared using the rotating base Marshall hammer. The Elf linear kneading compactor was also evaluated, but only for two types of paving mixes.

Paving mixes from five different locations and comprised of different aggregates and asphalts were used in the study. These materials provided a wide range of engineering properties and test values for the compacted mixes. An attempt was made to compact laboratory specimens to air void contents simulating those of the field cores.

Laboratory test procedures employed in the study included the following: compressive creep at 40°C (104°F), direct compression at 40°C (104°F), indirect tension at 25°C (77°F), resilient modulus at 0°C and 25°C (32°F and 77°F), Marshall stability, and Hveem stability. Limited work was performed in an effort to quantify particle orientation in the compacted mixes using fractal analysis.

The experiment was designed to determine the extent to which the method of laboratory compaction affects certain fundamental and commonly measured properties of asphalt concrete. Statistical analyses of the test results were performed to determine whether statistical differences existed between the field core and the different compaction methods.

### *2.2.3 Conclusions and Recommendations*

The research was designed to compare specimens compacted using the Exxon rolling wheel compactor and the gyratory compactor with field cores. Additional limited work was performed on specimens prepared using the rotating base Marshall compactor and the Elf linear kneading compactor. Button et al. came to the following conclusions:

- Statistical analyses indicated that the gyratory method most often produced specimens similar to pavement cores (73 percent of the tests performed). Exxon and Elf compactors had the same probability of producing specimens similar to pavement cores (64 percent of the tests performed). The Marshall rotating base compactor had the least probability of producing specimens similar to pavement cores (50 percent of the tests performed).
- When all the data are considered collectively, the differences in specimens, as reflected by mix properties, produced by the four laboratory compaction methods compared in this study are relatively small. The types of tests selected to evaluate mix properties were not ideal but were dictated by the size of the field cores.
- The Exxon rolling wheel compactor did not control air voids in the finished specimens nearly as easily as the other compaction methods. The Exxon compactor

requires about 100 kg (220 lb) of mix to prepare one set of specimens (one slab) at one air void level. This makes it a very labor-intensive and material-intensive operation to prepare samples with various air void contents.

- For producing small samples of specific void contents as in this study, the gyratory compactor is cheaper, much more convenient, and faster than the Exxon compactor.
- The Marshall compactor breaks aggregate more often during compaction than the other three compactors. This phenomenon apparently had little effect on the measured properties of the compacted mixes.
- The Elf compactor easily produces a 17 kg (38 lb) slab with a predictable air void content. It is convenient and offers a great deal of versatility.

The researchers recommended the following based on the previous conclusions:

- When compared with the Exxon rolling wheel compactor, the Texas gyratory compactor appears to be the better choice for preparing laboratory specimens for routine mix design testing of asphalt concrete. It should be pointed out that, based on other studies, air void distribution of gyratory compacted specimens may be less similar to pavement cores than rolling wheel compacted specimens. This difference, however, did not adversely affect the mix properties measured herein.
- The rolling wheel compactor may be the method of choice for fabrication of certain specialized samples such as those for beam fatigue or thermal cracking studies.
- Additional research is needed to investigate in detail the size and distribution of air voids within hot mix asphalt specimens compacted by different methods and the effect on fundamental engineering properties.
- Testing in this study was limited to dense-graded mixes. Stone mastic or other nonconventional mixes were not evaluated. Therefore, an evaluation of laboratory compactibility of nonconventional mixes, including stone mastic and porous mixes, is needed.

### **2.3 Basis for Selection of the SHRP Gyratory Compactor for Mix Design and Field Control**

Based on the studies previously identified, SHRP decided to support the use of the gyratory compactor for mix design and field control. Button et al. (1992) and Von Quintus et al. (1991) reported that the Texas gyratory compactor reasonably simulated field compaction and provided quick and economical means for a laboratory compaction procedure. The relationship between the number of gyrations (revolutions per minute) and the expected or design traffic level was still lacking.

In France, two researchers (Bonnot 1986 and Moultier 1977) have recommended the gyratory to evaluate the compactability of the mix.

### *2.3.1 Laboratoire Central des Ponts et Chaussées (LCPC) Gyratory Compactor Approach*

Bonnot (1986) and Moultier (1977) developed a procedure that is presently being used by the LCPC. A gyratory shear compactor press (PCG) test was devised for the purpose of studying the compacting performance of bituminous mixes. The press applies a compacting pressure close to that applied by rubber-tire compactors simultaneously with a kneading action obtained by gyratory shearing of the bituminous mixes in its mold, simulating the effect of job-site compactors. Not all conventional compacting tests give a good idea of the voids content values observed on the job site. Thus, Marshall or LCPC void contents are obtained relatively easily where the pavement is thick (7 to 8 cm [2.8 to 3.2 in.] for a wearing course), but are extremely difficult, or even impossible to obtain in the case of a thin course (wearing course of 3 to 4 cm [1.2 to 1.6 in.]).

On the other hand, the PCG test makes it possible to evaluate compaction performance, and also estimate the voids content which could be obtained in situ, according to course thickness. This is the test most widely used in France for optimizing the composition of hot laid bituminous concretes. It is conducted ahead of the mechanical tests, which are also more costly. The PCG test can at least be used to make a preliminary selection or screening of mixes.

**Test and Operating Conditions.** The bituminous mix is enclosed in a cylindrical mold, the axis of which describes a cone during the test. As shown in Figure 2.1, the form of the sample is an oblique cylinder, with parallel ends, one end is fixed while the other describes a circle.

The values of two principal parameters imposed for the test are set as follows:

1. The vertical compressive load gives a mean applied vertical pressure of 0.6 MPa (87 psi).
2. Angle of inclination  $\phi$  is  $1^\circ$  (constant during compacting).

In addition, temperature is regulated during the test, and rotational speed is set at 6 rpm. Mold diameter is 160 mm (6.4 in.), and final sample height is approximately 150 mm (6 in.).

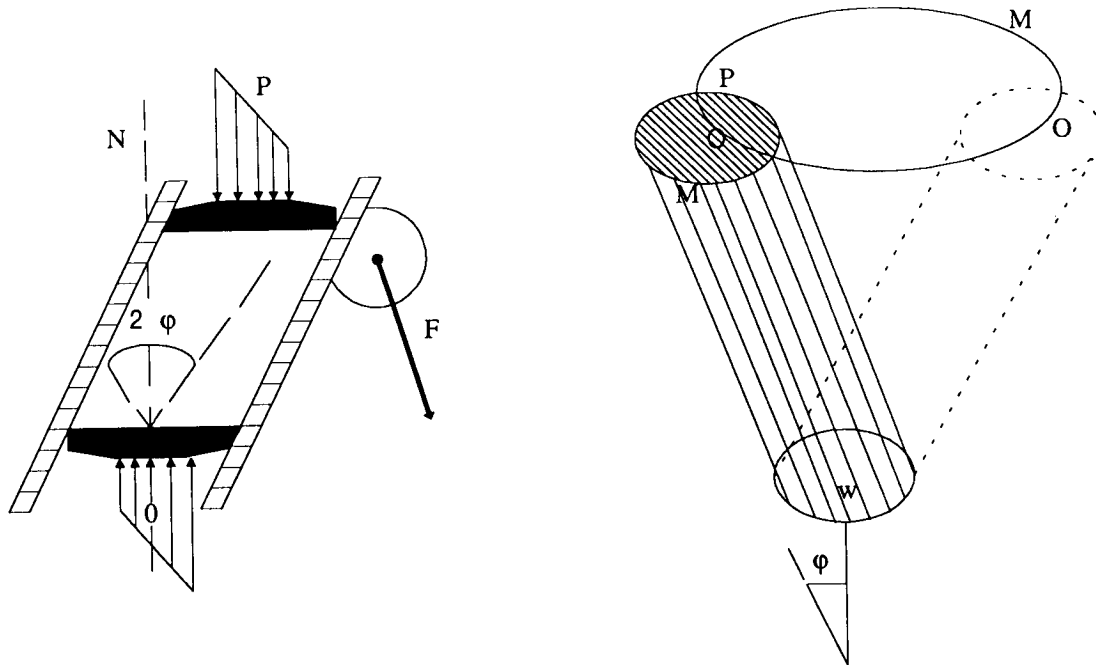


**Figure 2.1. Principle of compacting with the gyratory shear compacting press**

The following values are measured during the test:

- Reduction in sample height, giving percent voids,  $V\%$ , versus number of gyrations  $N$  (Figure 2.2).
- Evolution of inclination force  $F$ , the load required to maintain angle  $\phi$  constant at  $1^\circ$ .

The test is stopped automatically after 200 gyrations. Half a day is required to execute four test sequences.

**Relation Between PCG Test Curves and Pilot Compactor Curves.** Correlation studies between the voids contents given by the gyratory shear compaction and those produced by a pilot compactor (rubber-tire) operating under normal conditions, have been run on a full-scale basis.

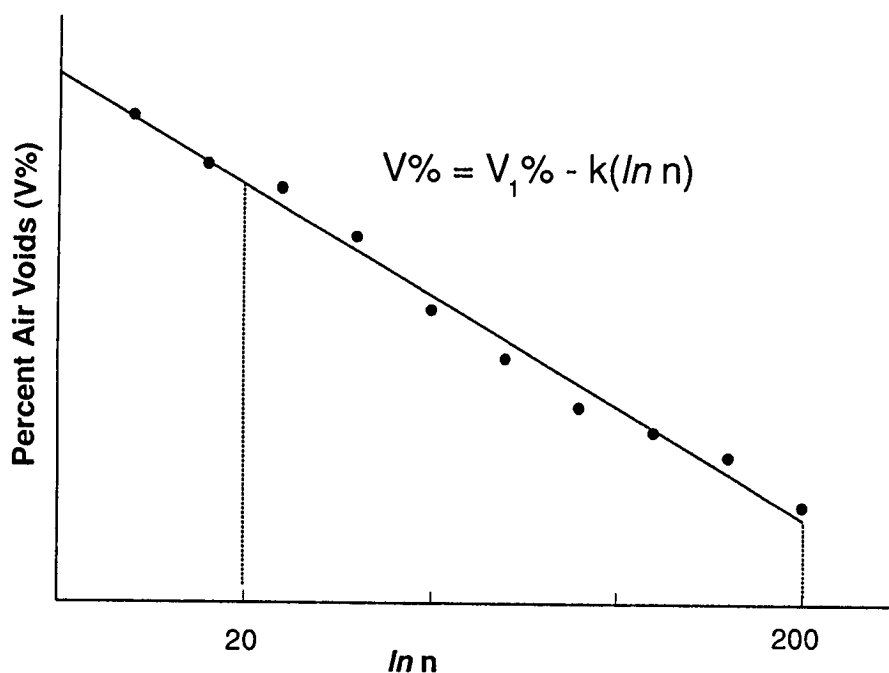


**Figure 2.2. Variation in void content with number of gyrations**

For the bituminous concrete with thicknesses between 3 and 12 cm (1.2 and 4.8 in.), the number of gyrations corresponding to the number of passes executed by the rubber-tire compactor, is given reasonably accurately by:

$$N_g = 0.0625 e N_p \quad (2.1)$$

where:

$e$	=	job site pavement thickness in mm,
$N_g$	=	number of PCG press gyrations, and
$N_p$	=	number of compactor passes.

This expression allows one to calculate the number of gyrations needed to achieve a laboratory-compacted void content equivalent to that of the pavement in the field. Thus, if the intended job site thickness is 100 mm (4 in.) and the number of passes is 16, the reference number of gyrations is 100. Therefore, it is possible to verify if the predicted void content in situ is correct, and to adjust the mix composition if necessary.

This formula is frequently applied taking the mean number of compactor passes as 16, reducing the expression to the following form, which is largely confirmed by experience:

$$N_g = e \quad (2.2)$$

Vibratory compactors are more efficient than rubber-tire compactors. Thus, the number of gyrations given by equation 2.1 frequently gives a conservative estimate of void content.

Nevertheless, the correlation appears to take the following form for these materials:

$$N_g = k e N_p \quad (2.3)$$

where  $k$  is a factor depending essentially on the nature of the compaction increasing with compactor efficiency. Globally a vibrating drum with a linear static load of 3.5 kN/mm, subjected to the action of a cam wheel of about 10 tons and a frequency of 25 to 30 Hz, gives a  $k$  factor value of about 0.25. The expression then becomes:

$$N_g = 0.25 e N_p \quad (2.4)$$

**Repeatability and Reproducibility.** A study of the repeatability and reproducibility of the PCG test, involving 19 laboratories and three different materials, led to the calculation of repeatability and reproducibility variances for the test. For the measurement of void content at given numbers of gyrations  $N_g$  (40, 80, and 120) the repeatability variance = 0.24 and the reproducibility variance = 0.49.

The repeatability variance is obtained by repetitions executed in the same laboratory. The reproducibility variance is the sum of repeatability variance and inter-laboratory variance.

*For this test, a laboratory is selected for which repeatability is assumed correct. This laboratory obtains four results with arithmetic mean  $x$  for the same material. The true inter-laboratory value  $m$  for this material falls within the following confidence interval with a probability of 95 percent.*

$$x \pm 1.09\% \quad (2.5)$$

Comparison of the two means  $m_1$  and  $m_2$ , in two different laboratories is as follows:

$$m_1 = m_2 \text{ if } 0 < x_1 - x_2 < 1.54 \quad (2.6)$$

**Utilization of PCG Test.** The thickness of the bituminous concrete course is a parameter known to the mix designer who sets an initial in situ void-content target according to the type of bituminous concrete, traffic and climate. Thus LCPC looks for a void content of the order of 3 to 4 percent for a bituminous concrete subjected to severe winter constraints. The target differs slightly for a bituminous concrete used in a hot region, with need for a stiffer mix, giving voids content values of around 6 to 7 percent.

Figure 2.3 illustrates gyratory compaction curves depicting different workability for three bituminous mixes. For example, a wearing course is to be applied with a thickness of 6 cm

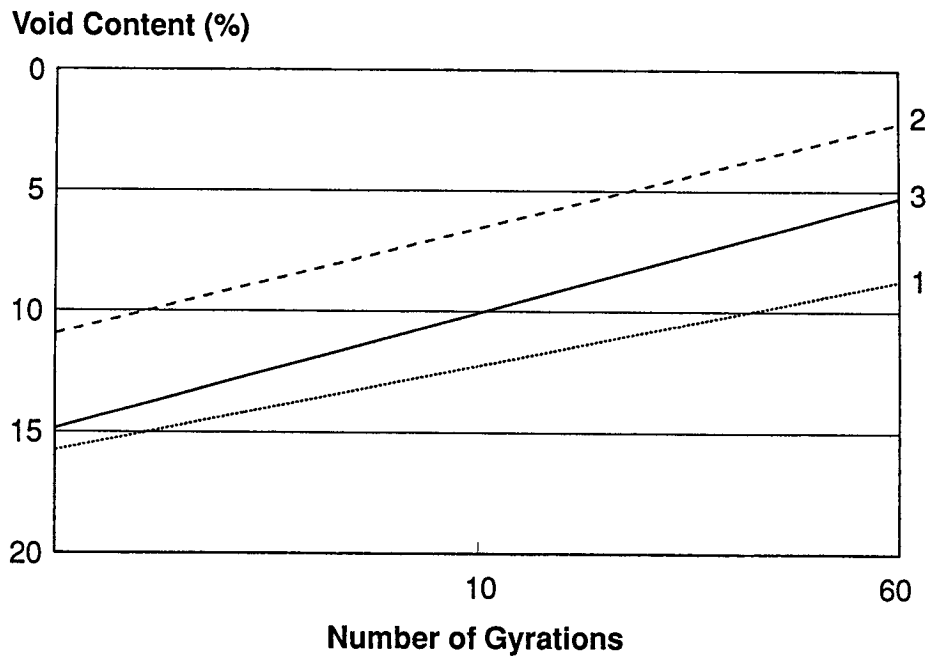


**Figure 2.3. Compaction curves illustrating different workability for three bituminous mixes**

(2.4 in.) and in situ void content target of 5 percent. The PCG compaction curve for the mix selected should give a PCG void content of the order of 5 percent at 60 gyrations as shown by compaction curve 3.

Compaction curve 1 gives a void content exceeding 5 percent at 60 gyrations, and is considered insufficiently workable. It must therefore be modified to improve its compacting characteristics. The methods most frequently employed for this purpose include:

- increased bitumen content,
- increased filler content,
- utilization of rounded river sand, and
- decreased percentage of medium-sized aggregate fractions or even gap grading.

On the other hand, if the mix appears too easily workable (as in the case of curve 2), reverse formulation factors are then applied, to obtain a compaction curve like curve 3.

Interpretation of the PCG test can be completed by qualitative analysis of force (F) during the compaction process.

The curves obtained are generally grouped in two main types (Figure 2.4). For curve A, the force, F, increases at the start of compaction, then stabilizes near the end of the compaction process. This type of curve is generally obtained with mixes having low workability.

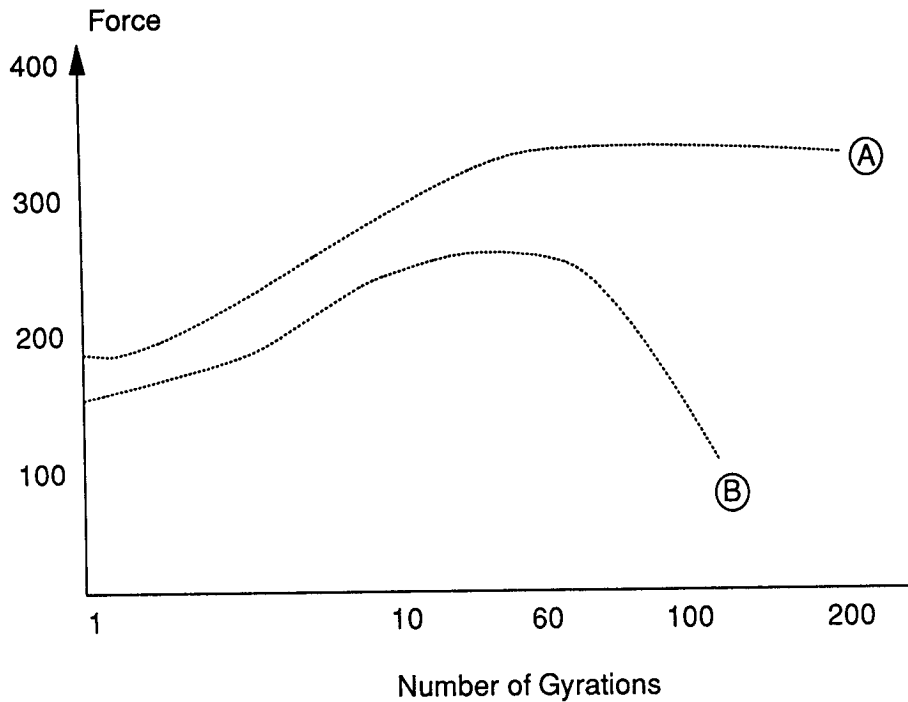


**Figure 2.4. Variation in force during compaction**

For curve B, there is a drop in force,  $F$ , above a certain level of compaction. This reflects a change of state in the bituminous mix due to reduced internal friction. This type of curve is encountered with gap-graded bituminous concrete with a high mastic content. To minimize the occurrence of this phenomenon, the mix is modified by reducing the percentage of sand or fines.

### *2.3.2 Regional Laboratory of Augers Gyrotory Compactor Approach*

Moultier (1977) provided another unique research approach employing the gyrotory compactor. Moultier hypothesized that the mix with the best laboratory compaction also will compact best on site for a given thickness, whatever the rolling equipment.

If this hypothesis is not valid, the methodology in altering the mix parameters in order to modify the mix compactness, and testing corresponding mixes with the gyrotory compactor, does not seem justified.

Some inconsistencies have been found between laboratory and construction site results. These can stem from the variety of compaction equipment, production of mixes quite different from those studied in the laboratory, and possibly a faulty use of the laboratory tool. It was urgent therefore to compare laboratory test results to those of compaction equipment to establish possible correlations between gyrotory compaction curves and those



resulting from a pneumatic roller. A comparison of laboratory results to field results from every type of compaction method was not within the scope of this project.

### 2.3.2.1 Correlation Approach

By experience, curves representing compaction as a function of the number of passes or gyrations can be likened to straight lines on a semi-log grid (logarithmic abscissa, linear ordinate). If these two lines are drawn, for the same mix, on the same grid, the roller-related line will be on the left and the gyratory compactor-related line will be on the right (Figure 2.5).

In other respects, thickness plays a key role in compaction. The compactness of a material will vary with the thickness compacted (thick sections always lead to greater compaction than thin ones, for the same material). Establishing relations between compaction curves from the simulator and gyratory compactor without taking this into account can only lead to rejection of the hypothesis to be verified. Gyratory compactor curves do not take thickness into account, while simulator curves are dependent on it.

Therefore, the French decided that establishing a correlation would consist of finding a horizontal transformation providing an approach to go from the first curve to the second, independent of thickness.

Among the simplest transformations are the following:

- In the horizontal translation (Figure 2.6) there is proportionality between the number of pneumatic roller passes and the number of gyrations of the gyratory compactor:

$$n_g = kn_p$$

- In the horizontal translation (Figure 2.7) if  $\ln \alpha$  is the abscissa and  $K$  the ratio characterizing the affinity:

$$\frac{\ln(n_g/\alpha)}{\ln(n_p/\alpha)} = K \quad (2.7)$$

and

$$n_g = \frac{n_p^k}{\alpha K - 1} \quad (2.8)$$

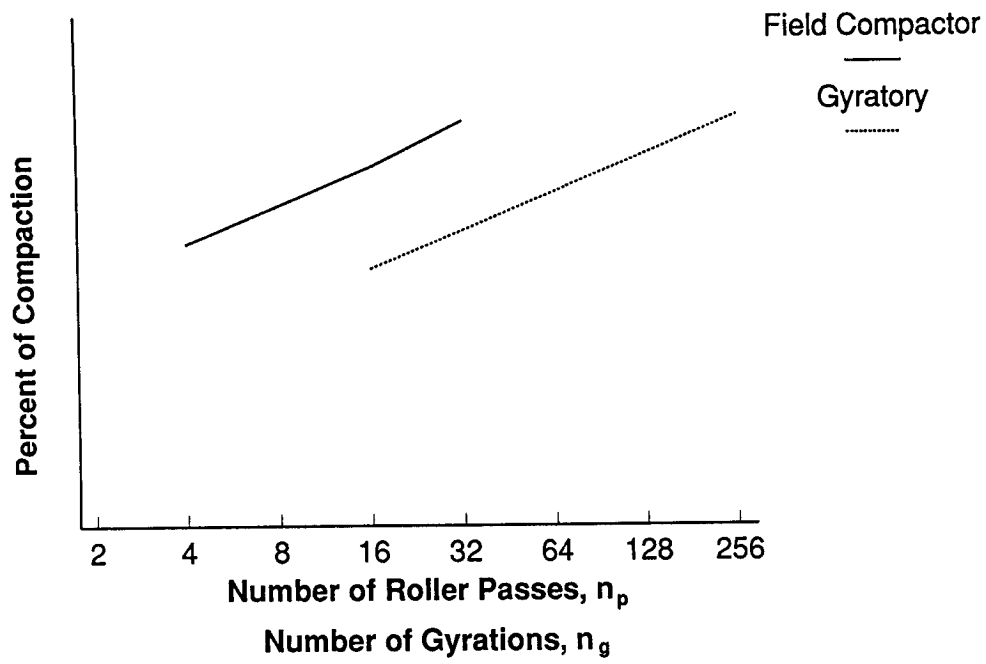


**Figure 2.5. Comparison of compaction curves for field and gyratory compactors**

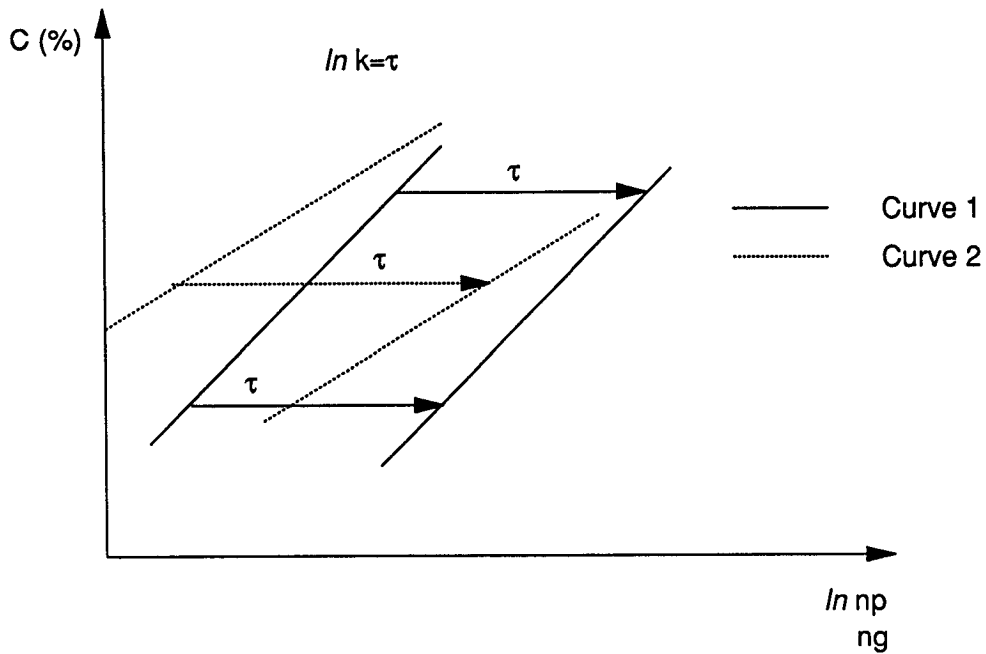


**Figure 2.6. Compaction curves for transformations**

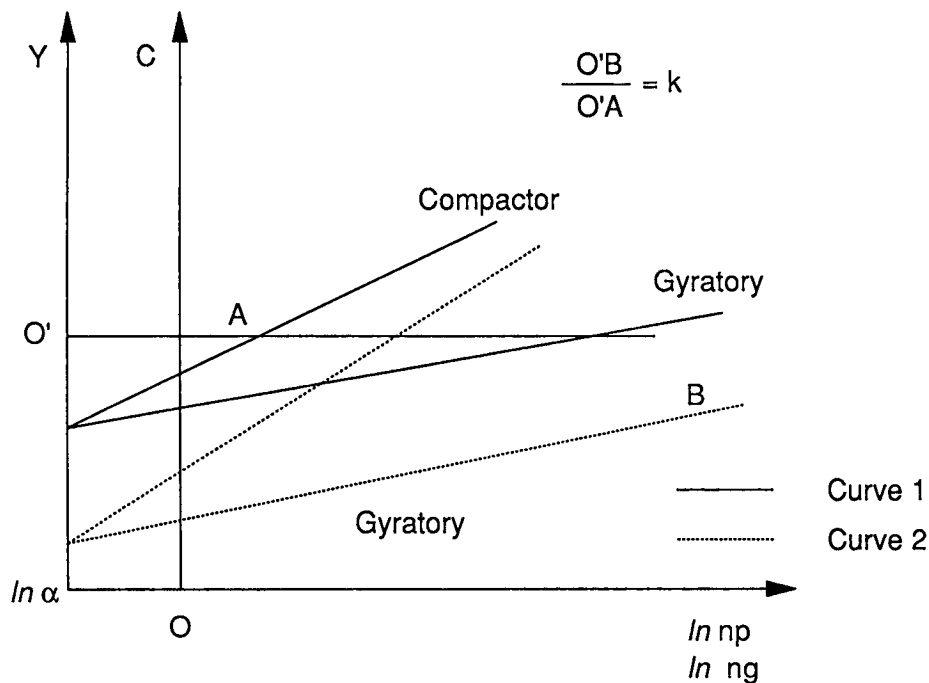


**Figure 2.7. Change in compaction curves by horizontal transformation**

### 2.3.2.2 Gyratory Equipment

Representative samples were subjected to kneading action combined with a small static compression simulating the effect of construction site compactors. This action was achieved by using a gyratory compactor to compress a sample inside a cylindrical mold. The shape of the sample at every moment is an oblique cylinder with parallel ends. One end is fixed while the center of the other end follows a circle. The following are the gyratory details:

- Inclination angle = 1°.
- Vertical pressure = 0.6 MPa (87 psi).
- Rotation speed = 6 gyrations per minute.
- Test temperature = 160°C (320°F).

With each complete rotation (gyration) of the incline plane (plane containing the vertical axis and the sample axis), the material is compacted and its volume decreases. To monitor the compaction of the material, only the sample height and the number of gyrations have to be measured and recorded during the test. From the sample height the compactness can be found from the following:

$$C\% = 100 \left[ 1 - \frac{v}{V_{ap}} \right] = 100 \frac{V_{min}}{V_{ap}} = 100 \frac{M_{va}}{M_{vr}} \quad (2.9)$$

$$C\% = 100 \frac{h_{min}}{h_{ap}} = 100 \frac{M}{M_{vr} \times S \times h_{ap}} \quad (2.10)$$

where:

C%	=	percent compaction,
$V_{ap}$	=	apparent volume of the material,
$V_{min}$	=	minimal volume (without void),
$v$	=	volume of void,
$M_{vr}$	=	real volumetric mass,
$M_{va}$	=	apparent volumetric mass of the sample,
$S$	=	transverse area of the sample,
$h_{ap}$	=	apparent height of the sample,
$h_{min}$	=	minimal height of the sample, and
$M$	=	mass of the sample.

Knowing  $h_{ap}$  is sufficient for finding C% since  $M$ ,  $M_{vr}$  and  $S$  are constant during the test. For a given number of gyrations ( $n_j$ ), compaction is calculated by drawing the compaction curves on a semi-logarithmic grid:

$$C\% = f(\ln \cdot n_j) \quad (2.11)$$

Generally, points on this curve (Figure 2.8) are on a straight line, which permits the calculation of two coefficients ( $C1$ ,  $k$ ) representing the potential for compaction of the tested mix:

$$C\% = C1 + k \ln \cdot n \quad (2.12)$$

### 2.3.2.3 Laboratory Compaction Bed

To simulate field compaction Moutier (1977) compacted bituminous concrete profiles of various thicknesses, by using a rolling wheel compactor. Several roller passes were used.

It is necessary to calculate the corresponding compaction for each profile. For this calculation, the mass of the material is assumed constant between 2 and 16 passes. This is shown in Figure 2.9.

If  $N$  is the total number of gyrations at the end of compaction, the apparent volume of the compacted material is  $V_{apN}$ . By coring in this profile, and after passing a gamma density gauge over the profile, it is possible to measure the average compaction of each core and then the compaction of the slice by averaging the average compactness of all cores. This number will only represent the average compaction in the slice if thicknesses are not too

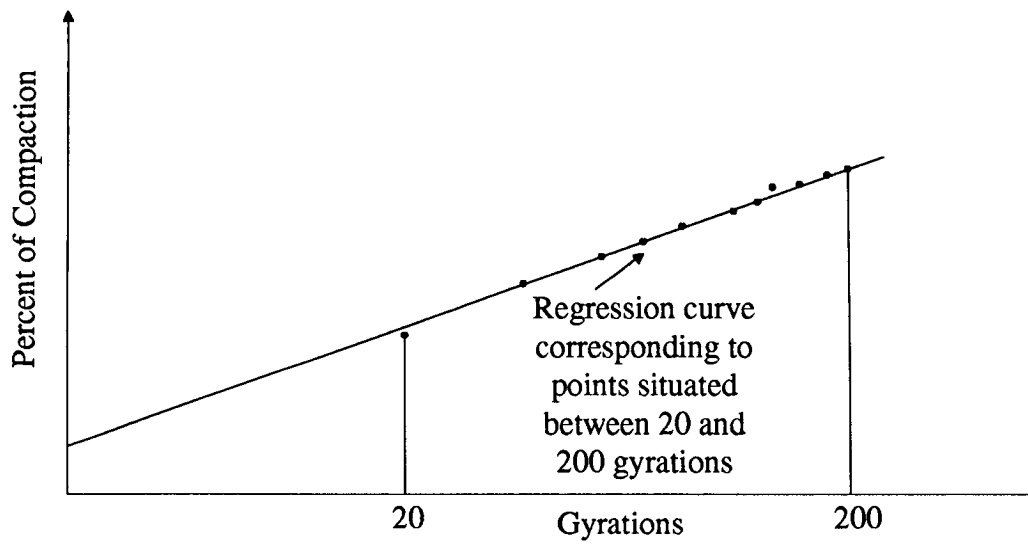


**Figure 2.8. Compaction curves from a gyratory compactor**

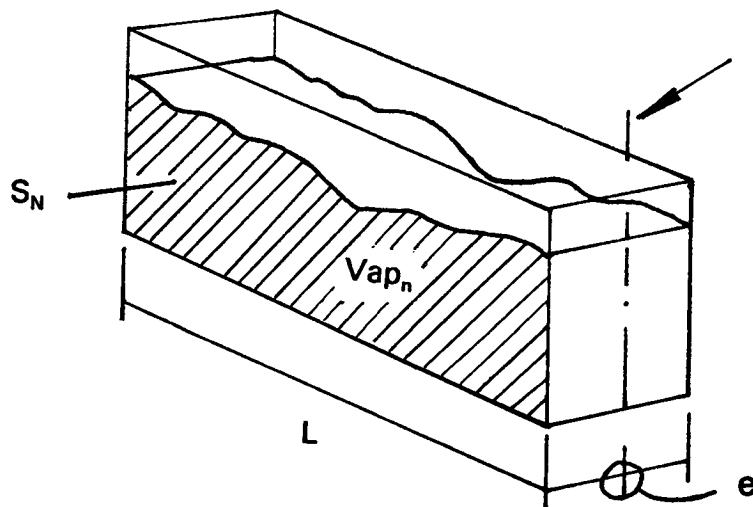


**Figure 2.9. Measured profile and apparent volume at  $n$  passes**

scattered, so gradients are quite similar.  $C_n$  represents the average of the compaction gradients among cores of a material of uniform thickness.

From the knowledge of  $C_n$  and the real volumetric mass  $M_{vr}$  of the mix, it is possible to calculate the mass  $M$  of the material corresponding to the volume  $V_{sp_n}$ .

Compaction  $C_n$  and  $M$  are related by the following:

$$C_n = \frac{M}{M_{vr} V_{sp_n}} 100 \quad (2.13)$$

$M$  is calculated from this as follows

$$M = \frac{C_n M_{vr} V_{sp_n}}{100} \quad (2.14)$$

If the mass  $M$  is considered constant throughout the compaction sequence, and  $C_n$  and  $C_{ni}$  represent compaction percentages at  $n$  and  $n_1$  passes, respectively, and

$$\begin{aligned} M \text{ and } M_{vr} &= \text{constants,} \\ V_{sp_i} &= \text{the apparent volume occupied by the material at } n_i \\ &\text{passes, } V_{sp_i} \text{ being calculated from } N_{ni}, \text{ and} \\ (V_{sp_i} = S_{ni} \cdot e) S_{ni} &= \text{the area of the section of the plate given by the profile} \\ &\text{measured for the same number of passes } N_i \text{ (Figure 2.10)} \end{aligned}$$

by substitution

$$\frac{C_{ni}}{C_n} = \frac{V_{sp_n}}{V_{sp_{ni}}} = \frac{S_n e}{S_{ni} e} = \frac{S_n}{S_{ni}} \quad (2.15)$$

or

$$C_{ni} = \frac{S_n}{S_{ni}} C_n \quad (2.16)$$

If  $l$  = length of the profile (see Figure 2.11), and  $h_{ni}$  and  $h_n$  = average heights of the profile at  $n_1$  and  $n$  passes, then

$$S_n = h_n l \quad S_{ni} = h_{ni} l \quad (2.17)$$

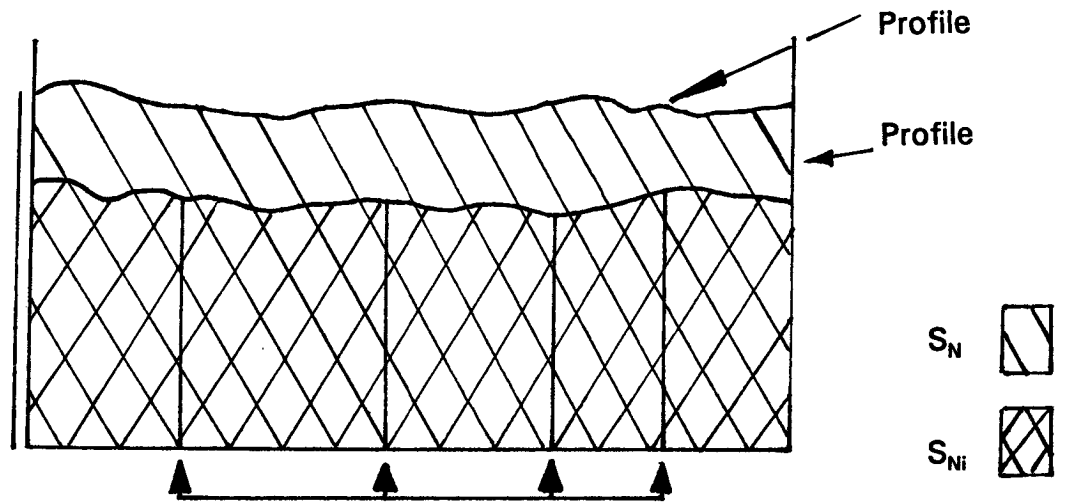


**Figure 2.10. Evolution of the profile**

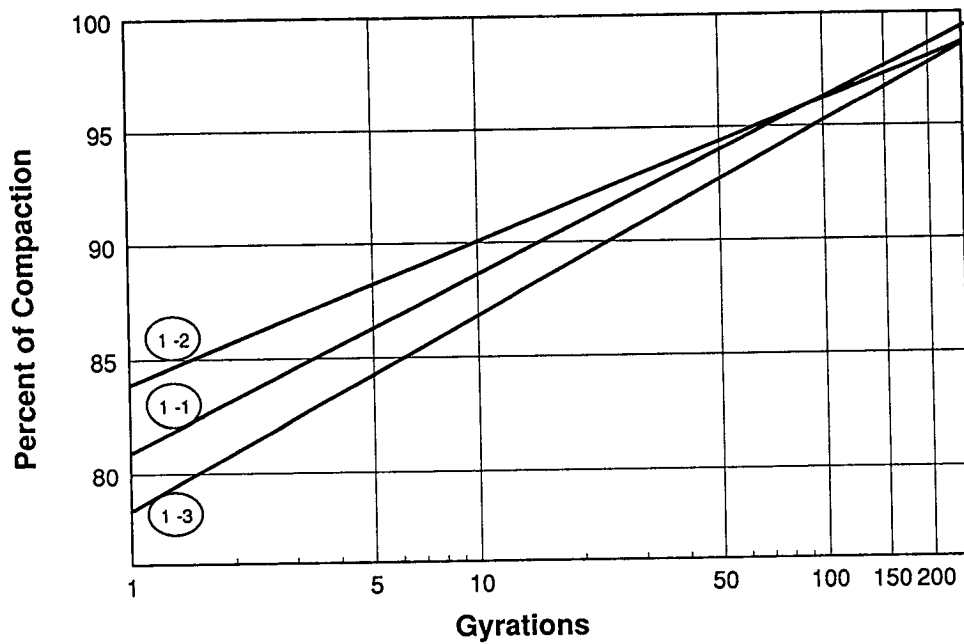


**Figure 2.11. Results with gyratory compactor**

which allows the previous relation to be written in the following simplified way:

$$C_{ni} = \frac{h_n}{h_{ni}} C_n \quad (2.18)$$

For example, profiles measured during the actual test bed monitoring were as follows:

- calculation of average areas ( $S_i$ ),
- calculation of heights at  $n_i$  passes ( $H_i$ ), and
- calculation of compactness ( $C_i$ ).

### 2.3.2.4 Experiment Design

Three pavement thicknesses were chosen: 4, 8, and 12 cm (1.6, 3.2, 4.8 in.). For the correlation to have a distinct meaning, a minimum of three types of materials quite different were chosen for each thickness class. Therefore, nine different mixes were used for the tests. Each mix was used for two plates on the compaction bed with the following average compaction characteristics:

- load per wheel = 30 kN (6750 lb),
- tire pressure = 0.6 MPa (87 psi), and
- translation speed = 3 km/hr (1.8 mi/hr).

These same mixes were tested with the gyratory compactor according to the test procedure conditions listed earlier.

### 2.3.2.5 Results and Conclusions

Figure 2.11 illustrates the results with the gyratory compactor and Figure 2.12 shows the results of the compaction bed.

Analysis of variance indicated that curves 1.1 and 1.2, obtained from the gyratory compactor beyond 15 gyrations and from the simulator are not significantly different. Curve 1.3 is in both cases very different from the other two. It can be noted that 16 compactor passes are equivalent to 35 gyrations; 8 passes are equivalent to 17 gyrations; and 4 passes are equivalent to 8 gyrations.

There is a proportionality factor between the number of passes and the number of gyrations:

$$K = \frac{n_g}{n_p} = \frac{35}{16} = \frac{17}{8} = 2.2 \quad (2.19)$$



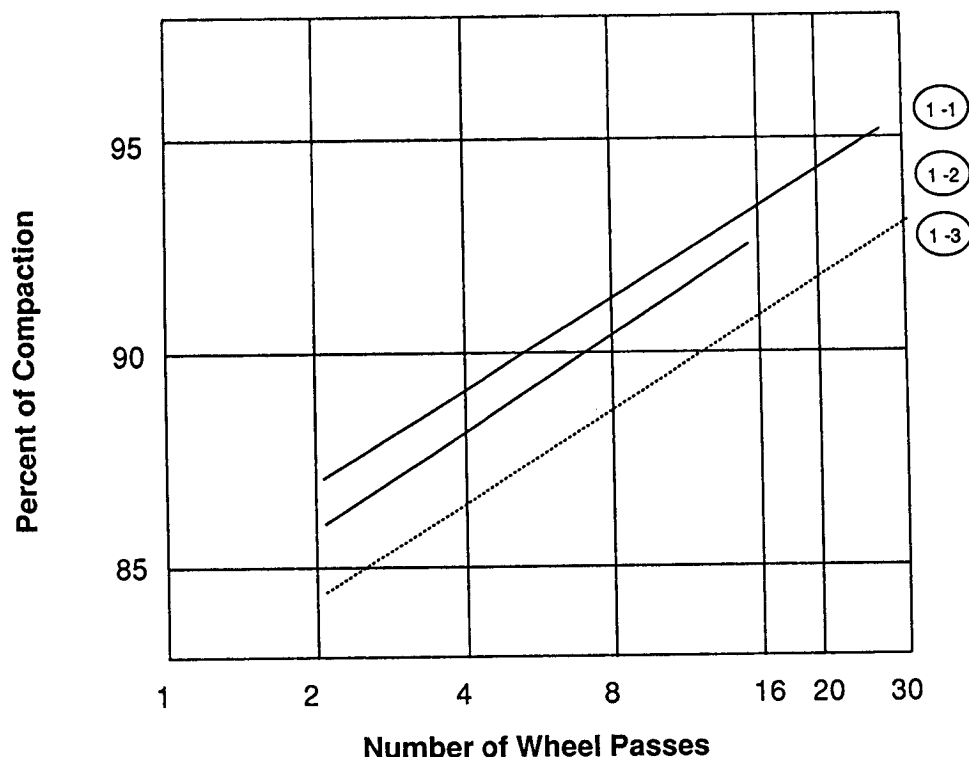


**Figure 2.12. Results with compaction bed**

These results tend to prove that there are transformations that can be made between gyratory compactor curves and compaction curves.

These transformations are quite simple: they are either of the translation or affinity type in semi-logarithmic coordinates. Because of this, if a number of simulator passes is set it is possible to know what percent compaction will be obtained at the end of that number of passes for a material from a simple gyratory compactor test. Depending on the nature of the tested material, the number of corresponding gyrations is calculated from the set number of passes. The percent compaction then is read on the gyratory compactor curve for the tested material. Not taking into account the dispersion, this average compaction is what would be attained for the selected number of passes. If the best of several different mixes for percent compaction is sought, this method has simply to be applied several times (Figure 2.13). This correlation enhances the value of the gyratory compactor. Not only the mix can be chosen based on its percent compaction for a given number of passes, but also based on the general appearance of the compaction curve.

### **2.3.3 SHRP's Gyratory Compactor Approach**

After considering the research on available compactors for the Superpave mix design system, SHRP selected a gyratory compactor operating with a similar protocol as the French LCPC compactor.

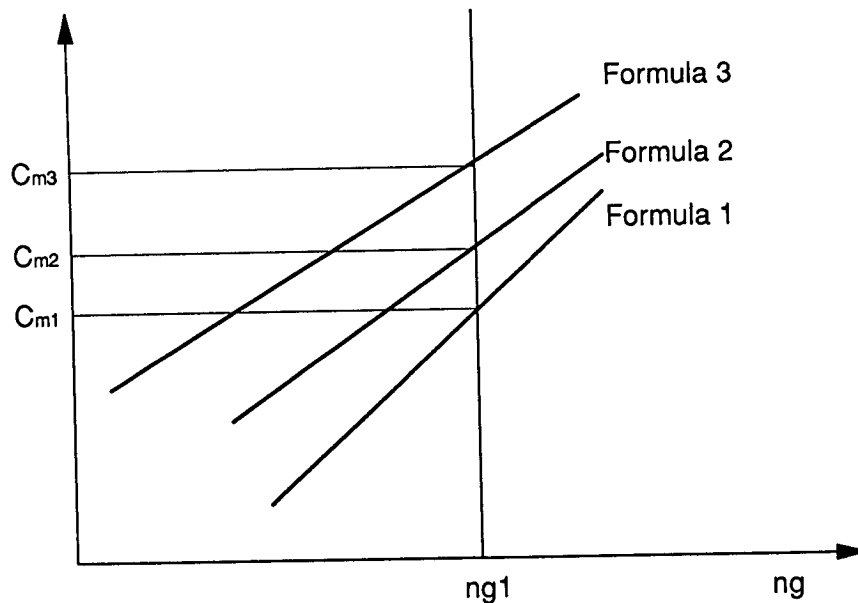


**Figure 2.13. Percent compaction as a function of simulator passes**

**Revolutions per Minute.** The French gyratory compactor protocol stipulates 6 rpm. SHRP's objective was to reduce the compaction time by increasing the number of rpm, if possible. Consequently, an experimental design was developed to compare the mix optimum asphalt content, air voids, VMA, VFA and density based on the gyrations of 6, 15, and 30 rpm.

The RB aggregate and AAK-1 asphalt from SHRP's Materials Reference Library were used as the mix components. The asphalt contents evaluated were at the optimum and  $\pm 1$  percent from this optimum value. Figures 2.14, 2.15, and 2.16 show the percent theoretical maximum density versus the number of gyrations for the various rpm and asphalt contents. Very little difference is observed among the rpm.

Figures 2.17 and 2.18 are plots of volumetric properties versus asphalt contents. Table 2.2 presents a summary of data used for the figures. Reviewing Figure 2.17(a), it can be observed that: at the design asphalt content and 30 rpm, the air voids equal 4 percent; at 6 rpm the air voids equal 4.4 percent; and at 15 rpm the air voids equal 4.5 percent. These values were statistically the same. Based on these results, SHRP selected a speed of 30 rpm instead of the French 6 rpm. The increase in rpm significantly reduces the laboratory compaction time to prepare mix design specimens.

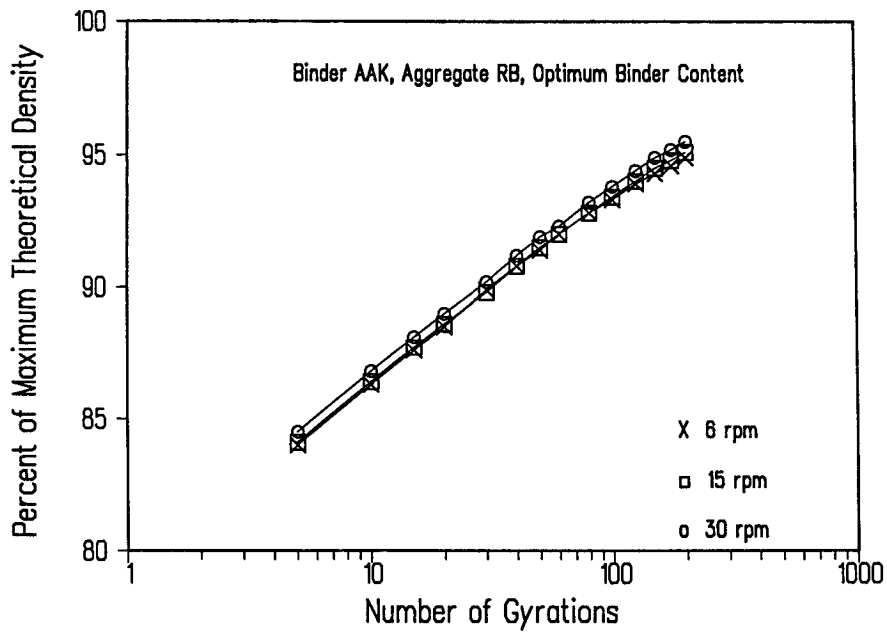


**Figure 2.14. Comparison of maximum density versus number of gyrations at optimum asphalt content**

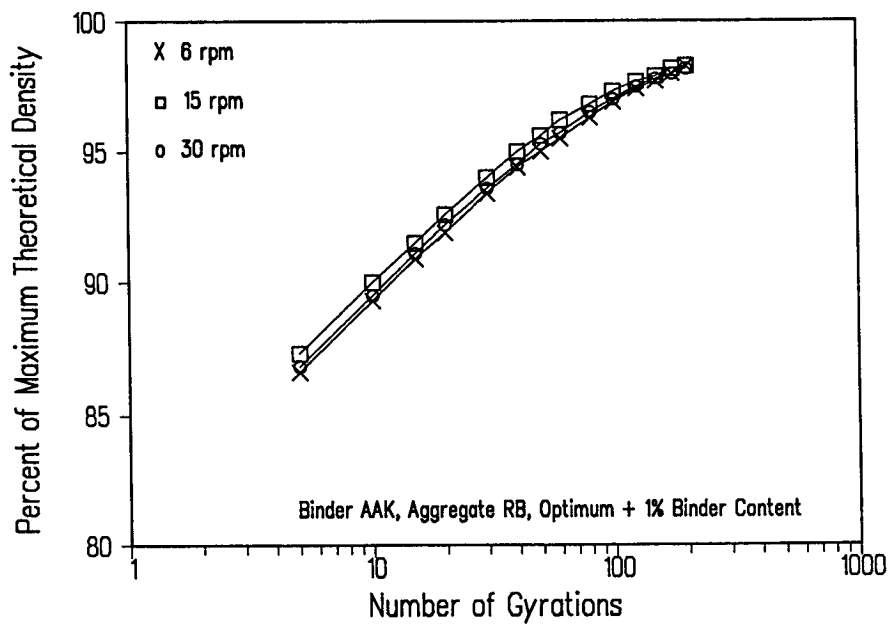


**Figure 2.15. Comparison of maximum density versus number of gyrations at 1 percent greater than optimum asphalt content**

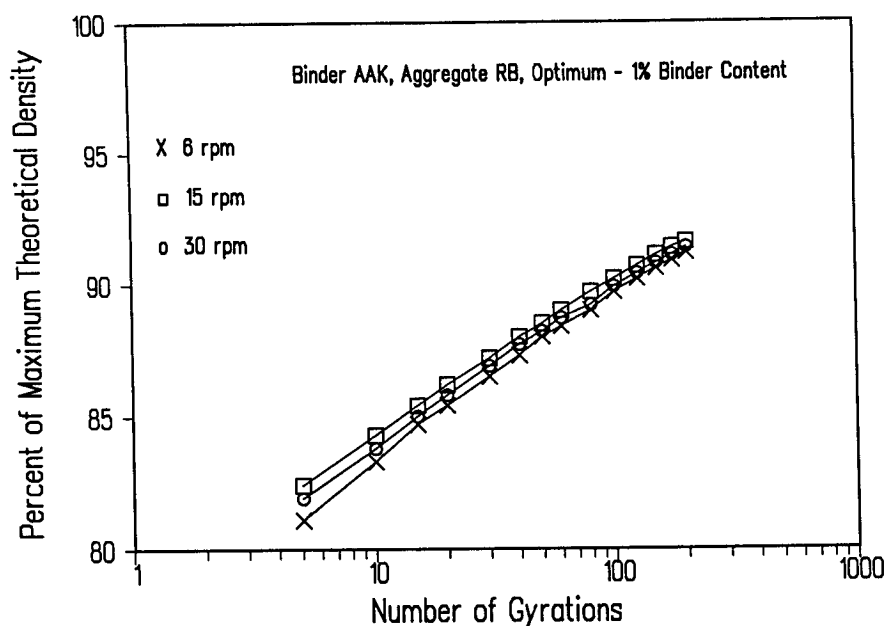


**Figure 2.16. Comparison of maximum density versus number of gyrations at 1 percent less than optimum asphalt content**

**Table 2.2. Summary of gyratory compaction data for 6, 15, and 30 rpm**

AC (%)	Bulk Specific Gravity (BSG)	Unit Weight (lb/ft <sup>3</sup> )	Maximum Specific Gravity (MSG)	Air Voids (%)	VMA (%)	VFA (%)
<b>6 rpm</b>						
3.0	2.409	150.3	2.644	8.9	15.0	40.8
4.0	2.467	153.9	2.602	5.2	13.9	62.6
5.0	2.497	155.8	2.561	2.5	13.7	81.8
<b>15 rpm</b>						
3.0	2.406	150.1	2.644	9.0	15.1	40.5
4.0	2.454	153.1	2.602	5.7	14.3	60.3
5.0	2.507	156.5	2.561	2.1	13.4	84.3
<b>30 rpm</b>						
3.0	2.403	150.0	2.644	9.1	15.2	40.2
4.0	2.467	153.9	2.602	5.2	13.9	62.5
5.0	2.502	156.1	2.561	2.3	13.6	83.0

Aggregate Bulk Specific Gravity = 2.750  
 Aggregate Effective Specific Gravity = 2.780

Asphalt Absorption = 0.4%  
 Asphalt Specific Gravity = 1.03

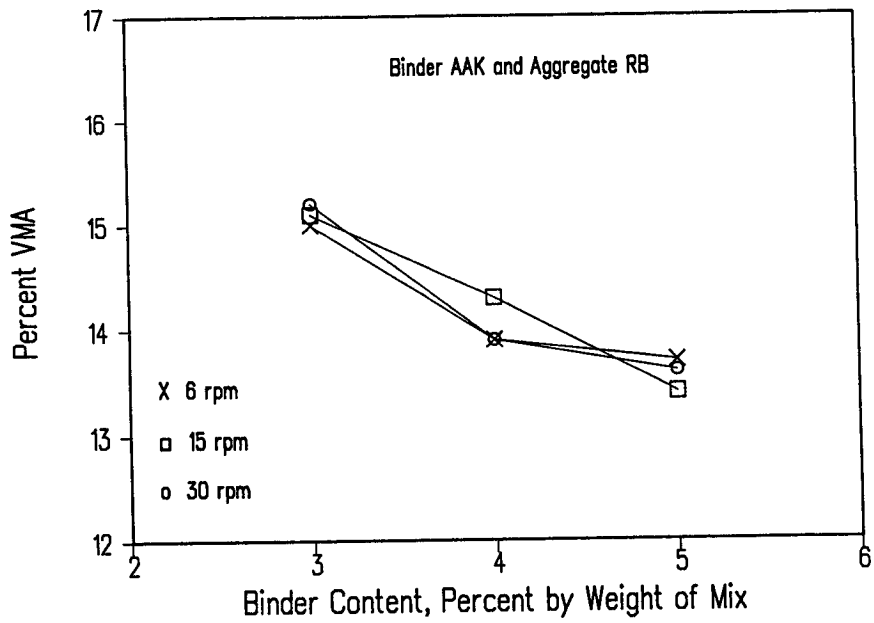
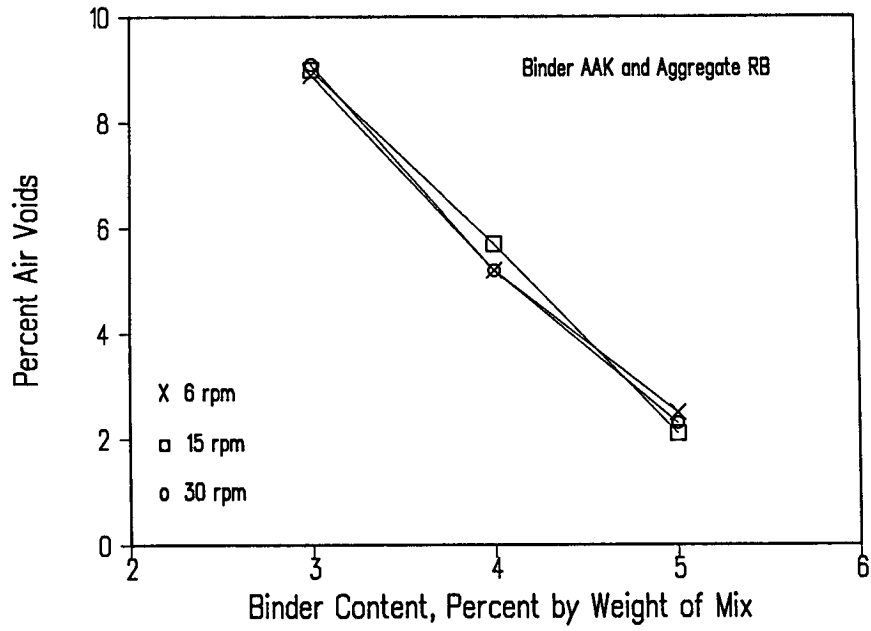


**Figure 2.17. Air voids and VMA as a function of gyratory speed**

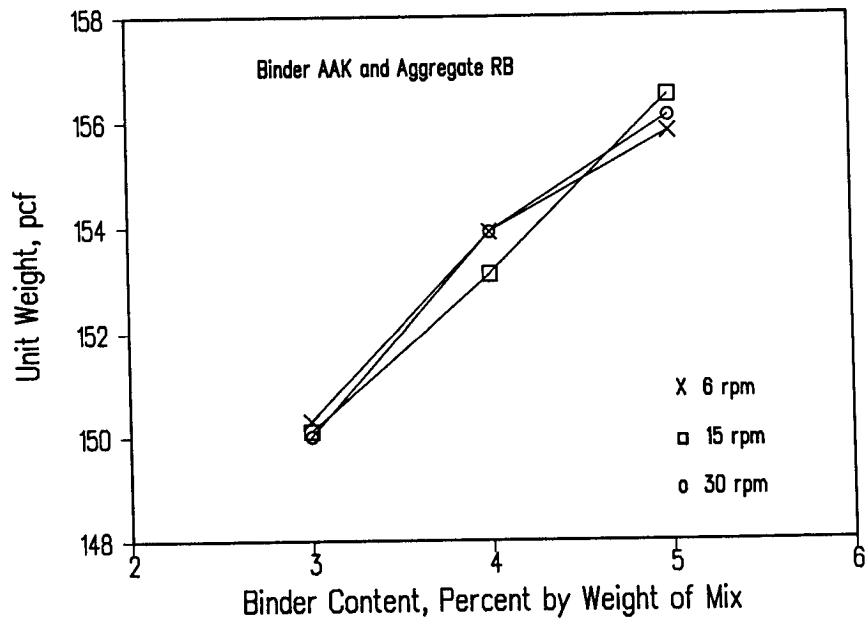
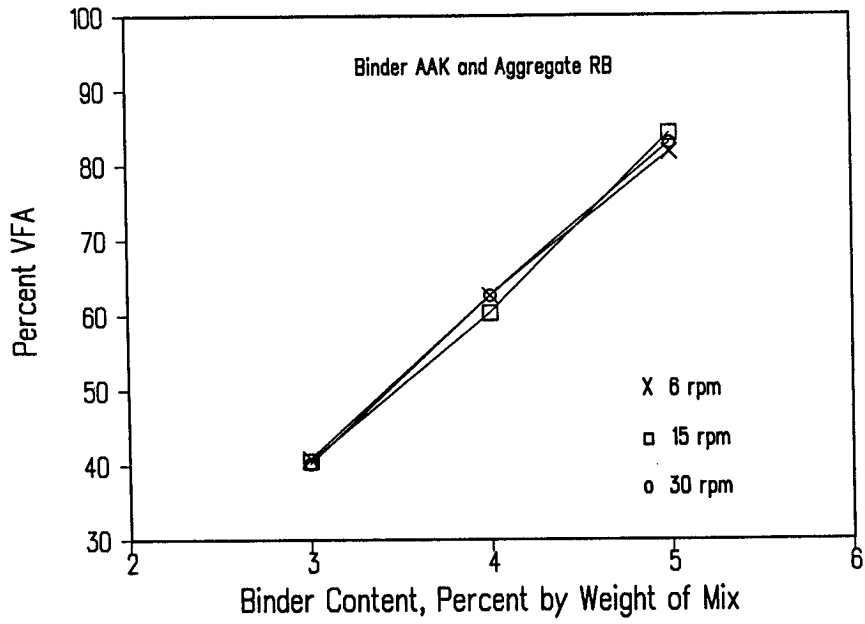


**Figure 2.18. VFA and density as a function of gyratory speed**

**Comparisons of Gyrotory Compactors.** The SHRP A-001 contractors conducted an experiment to determine if it was sufficient to specify the angle of gyration, speed of rotation (30 rpm), and vertical pressure (0.6 MPa [87 psi]). In summary, the experiment progressed as follows:

1. Performed an experiment to compare the modified Texas gyrotory compactor to a SHRP gyrotory compactor.
2. Concluded that the two machines compact differently.
3. Measured the angle of gyration, more precisely, for both machines.
4. Investigated the effect of angle of gyration on the densification parameters.
5. Determined an acceptable tolerance for the angle of gyration.
6. Compared the modified Texas gyrotory compactor, SHRP gyrotory compactor, and the U.S. Army Corps of Engineers gyrotory compactor.

In the experiment various asphalt aggregate mixes were compacted. The number of controlled variables and levels are shown in Table 2.3. A brief description of each variable and level follows.

**Table 2.3. Controlled variables in compactor comparison experiment**

Controlled Variable	Number of Levels
Compactors	2
Aggregate Blends	4
Asphalts	1
Specimen Sizes	2(1)
AC Contents	3
Replicates	2

The LCPC protocol includes a pressure of 0.6 MPa (87 psi). An earlier study had investigated the rate of gyration using a 6 in. Texas gyrotory compactor that had been modified to meet the LCPC protocol (Moultier 1977). Based on the experimental results of this study, SHRP selected a speed of 30 rpm.

### 2.3.3.1 Compactors

#### **SHRP Gyratory**

This compactor was produced by the Rainhart Company. The compactor can produce 100 mm (4 in.) diameter and 150 mm (6 in.) diameter specimens. The vertical pressure can be adjusted, but was fixed for this experiment at 0.6 MPa (87 psi). Speed of rotation was fixed at 30 rpm. Angle of gyration can be adjusted but was fixed at 1° for this experiment.

#### **Modified Gyratory**

The modified gyratory used in this experiment was provided by the Asphalt Institute. Modifications were made to a 6-in. gyratory compactor on loan from the Texas Department of Transportation. Specific modifications include a frequency controller that allows selection of gyration speed and a change in angle of gyration to 1°.

### 2.3.3.2 Aggregate Blends

Four aggregate blends were used in this experiment.

- 25 mm (1 in.) nominal mix aggregate blend used in the Superpave design for the base course of Interstate I-65 in Indiana.
- 19 mm (0.76 in.) nominal mix aggregate blend used in the Superpave design for the binder course of Interstate I-43 used in Wisconsin.
- 12.5 mm (0.5 in.) nominal mix aggregate blend used in the Superpave design for the surface course of Interstate I-43 used in Wisconsin.
- 9.5 mm (0.38 in.) nominal mix aggregate blend used in the Superpave design for the surface course of Interstate I-65 used in Indiana.

### 2.3.3.3 Asphalt Cements

One asphalt cement was used in this experiment, an AC-20.

### 2.3.3.4 Specimen Sizes

Two specimen sizes were used in this experiment.



- 150 mm (6 in.) diameter specimens by 110 mm (4.5 in.) high for the SHRP gyratory compactor. Specimens were 150 mm (6 in.) in diameter by 110 mm (4.5 in.) high for the modified Texas gyratory compactor.
- 100 mm (4 in.) diameter specimens by 75 mm (3 in.) high for the SHRP gyratory compactor. (This specimen size cannot be produced by the modified Texas gyratory compactor.)

### 2.3.3.5 Asphalt Contents

Three asphalt contents were used in this experiment.

- **Optimum.** Optimum asphalt contents have been defined from a Superpave mix design for each of the aggregate blends.
- **Optimum Plus.** Optimum asphalt content plus 1 percent.
- **Optimum Minus.** Optimum asphalt content minus 1 percent.

### 2.3.3.6 Replicates

Two replicate specimens were made for each combination of compactor, aggregate blend, specimen size, and asphalt content.

### 2.3.3.7 Factorial

A complete factorial with all cells of the experiment is shown in Table 2.4. All the cells were filled for the SHRP gyratory compactor. For the modified Texas gyratory compactor, specimens were prepared for only one specimen size. The modified Texas gyratory cannot compact 100 mm (4 in.) diameter specimens.

The total number of specimens prepared was 72.

### 2.3.3.8 Compaction Protocol

Gyratory compaction was achieved using the following set of parameters:

- Angle of compaction = 1°.
- Vertical pressure = 0.6 MPa (87 psi).
- Speed of rotation = 30 rpm.

**Table 2.4. Cells of experiment**

Core Sizes	Aggregate Sizes (mm)	SHRP Gyratory			Modified Gyratory		
		Opt -1%	Opt	Opt +1%	Opt -1%	Opt	Opt +1%
150 mm (6 in.) diameter by 110 (4.5 in.) high	25	2	2	2	2	2	2
	19	2	2	2	2	2	2
	12.5	2	2	2	2	2	2
	9.5	2	2	2	2	2	2
100 mm (4 in.) diameter by 75 mm (3 in.) high	25	2	2	2	N/A	N/A	N/A
	19	2	2	2	N/A	N/A	N/A
	12.5	2	2	2	N/A	N/A	N/A
	9.5	2	2	2	N/A	N/A	N/A

Mixing temperature was that at which the viscosity of the unaged asphalt binder is  $170 \pm 20$  cSt. Compaction temperature was chosen as that for which viscosity of  $280 \pm 30$  cSt is measured on unaged binder. All mixes were short-term aged for 4 hours in a forced draft oven at  $135^{\circ}\text{C}$  ( $275^{\circ}\text{F}$ ).

Maximum theoretical specific gravities of the short-term aged mixes were known prior to compaction. Height of the specimen was measured during the compaction process after 5, 10, 15, 20, 30, 40, 50, 60, 80, 100, 125, 150, 175, 200, and 230 gyrations.

### 2.3.3.9 Response Variables

Results of height measurements taken during the compaction process were used to calculate specimen density expressed as percent maximum (theoretical) specific gravity. A plot was made of percent maximum theoretical specific gravity versus log of the number of gyrations as shown in Figure 2.19.

The compaction or densification curve is characterized by three parameters. C10 is the percent maximum specific gravity after 10 gyrations. C230 is the percent maximum specific gravity after 230 gyrations and K is the slope of the densification line. A comparison of C10, C230 and K was made for mixes compacted with the SHRP gyratory compactor and the modified gyratory (Figure 2.20).

Compaction curves for mixes that are identical except for their binder contents are expected to plot as shown in Figure 2.21. This family of curves would be the family of compaction curves obtained during a mix design in which the aggregate properties are held constant and asphalt binder content varies.

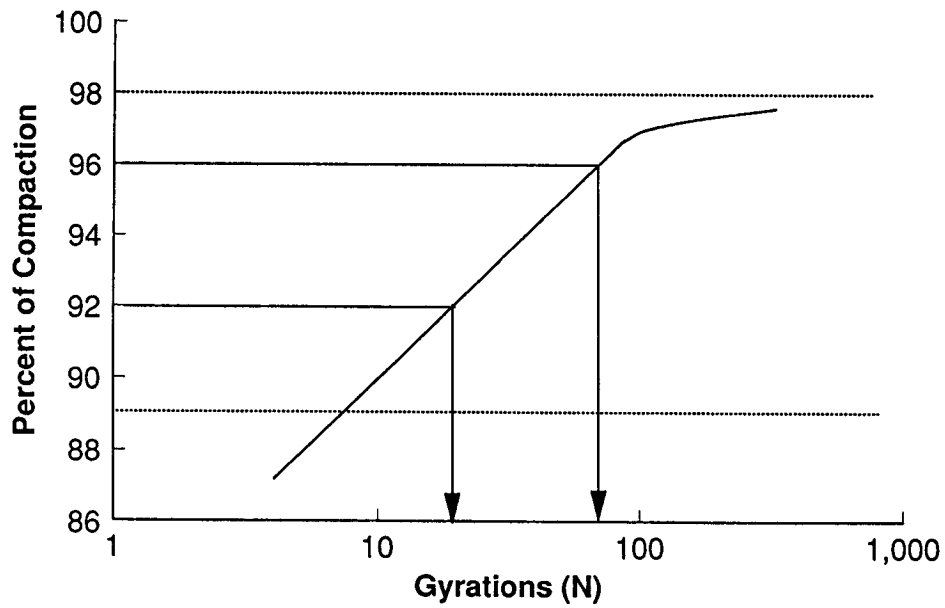


**Figure 2.19. Number of gyrations to define construction and traffic compaction**

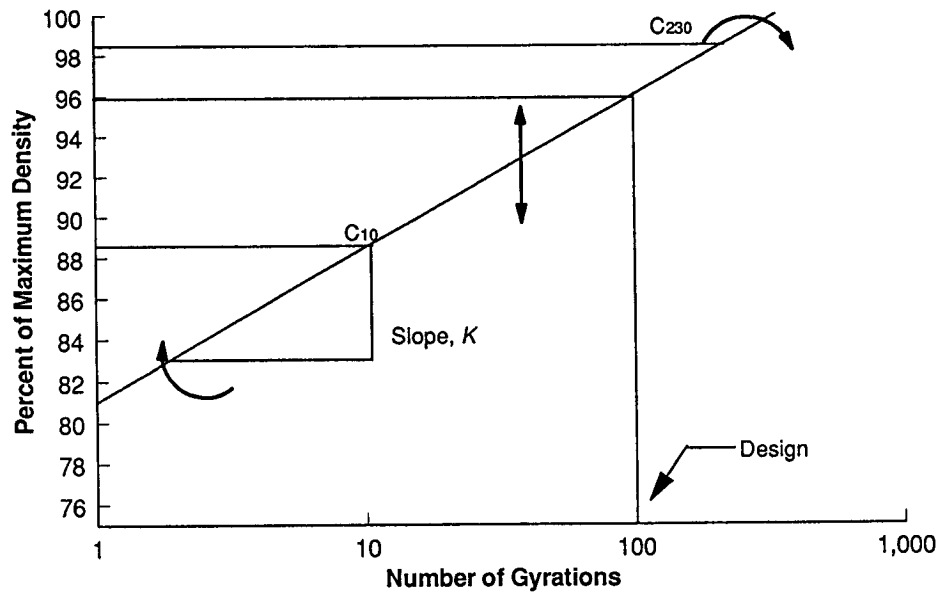


**Figure 2.20. Typical gyratory compaction curve**

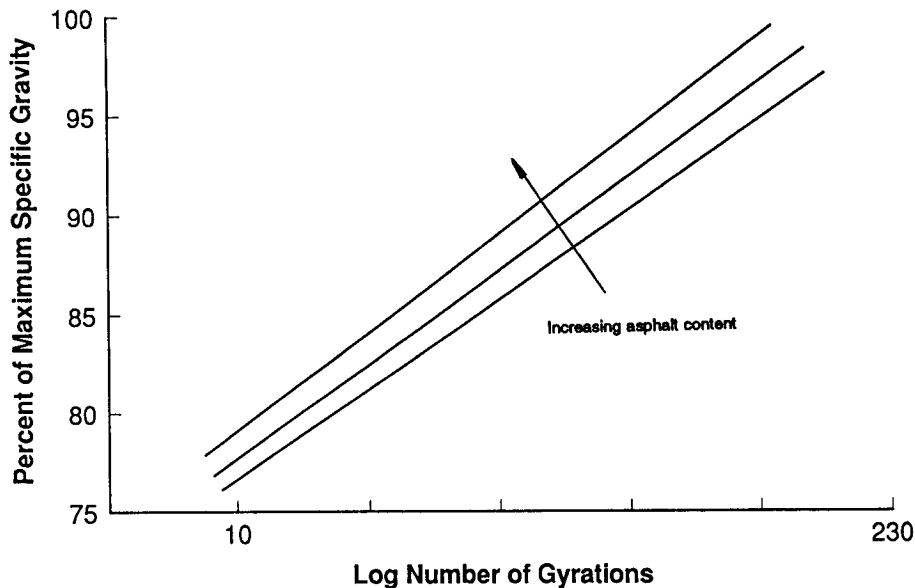


**Figure 2.21. Effect of asphalt content on mix compactability**

In this experiment, mixes that were compacted by the SHRP gyratory compactor were evaluated to determine whether each family of compaction curves would behave in the same manner as the mixes compacted in the modified Texas gyratory compactor.

**U.S. Army Corps of Engineers (USACOE) Gyratory Compactor.** The USACOE gyratory compactor operates with a variable angle of gyration and variable vertical pressure. Both variables can be set to the SHRP protocol. Two differences exist, one of which is considered significant. The speed of rotation is less than 30 rpm. An earlier study showed that speed did not affect the densification curves.

A significant difference lies in the method of applying the angle of gyration. The SHRP gyratory uses a 3-point system to apply the angle. As a result, the angle remains firmly fixed at all times during the compaction process. The USACOE gyratory applies the angle using a 2-point system, thus allowing an additional degree of freedom.

A limited evaluation of a USACOE gyratory compactor was performed using a single mix design compacted at three asphalt contents. The mix was a 19 mm (3/4 in.) nominal mix composed of RB aggregate and AAK-1 asphalt cement from the SHRP Materials Reference Library. The asphalt contents used were Optimum (4 percent), Optimum Plus (5 percent), and Optimum Minus (3 percent). Duplicate specimens were produced for each asphalt content for each compactor. Table 2.5 indicates the cells of the experiment.

**Table 2.5. Cells of USACOE compactor comparison experiment**

% AC	Specimen Size	Gyratory Compactor		
		SHRP	Texas (Mod.)	COE
Optimum Minus	150 mm (6 in.)	2	2	3
	100 mm (4 in.)	2		
Optimum	150 mm (6 in.)	2	2	3
	100 mm (4 in.)	2		
Optimum Plus	150 mm (6 in.)	2	2	3
	100 mm (4 in.)	2		

Note: Number in cell represents number of specimens made.

Triplicate specimens were compacted at each asphalt content on the USACOE gyratory at the Virginia Transportation Research Council. All other specimens were compacted at the Asphalt Institute.

Prior to compaction, the angle of gyration was set to 1° for the SHRP compactor. Both the 100 mm (4 in.) and 150 mm (6 in.) settings were adjusted so that the average angle through one revolution was  $1.00 \pm 0.02^\circ$ . The average densification parameters for the compacted specimens are indicated in Table 2.6.

**Table 2.6. Comparison of densification parameters from gyratory compactors**

% AC	Parameter	Gyratory Compactor			
		SHRP		Texas (Mod.)	COE
		100 mm (4 in.)	150 mm (6 in.)		
Optimum Minus	C10	83.4	84.4	85.4	86.8
	C230	92.0	91.3	92.4	93.7
	K	6.281	5.039	5.100	5.059
Optimum	C10	85.6	86.4	87.1	89.0
	C230	95.2	94.4	95.0	96.5
	K	7.100	5.958	5.858	5.531
Optimum Plus	C10	88.5	88.8	90.0	91.6
	C230	99.0	98.0	99.0	99.4
	K	7.732	6.772	6.598	5.724

Note: The asphalt mix used binder AAK and aggregate RB.

An analysis of variance (ANOVA) was conducted on the data to determine if there were any statistically significant differences in the densification parameters as a function of compactor. All ANOVAs were performed at a confidence level of 95. Comparisons were performed by the t-test.

### 2.3.3.10 Optimum Minus

All response parameters were evaluated for the Optimum Minus mix. There was a significant difference in  $C_{10}$  between the USACOE and the SHRP devices for both the 100 and 150 mm (4 in. and 6 in.) specimens. The  $C_{10}$  for the USACOE machine was higher. There also was a significant difference in  $C_{230}$  from the USACOE compacted specimens and all other compacted specimens. The  $C_{230}$  for the USACOE machine was higher.

Finally, there was a significant difference in the slope,  $K$ , between the SHRP 100 mm (4 in.) specimens and all other compacted specimens. These SHRP specimens produced densification curves with slopes that were higher than the slopes of the other densification curves. In addition, the USACOE compacted specimens were significantly different from the SHRP 150 mm (6 in.) specimens. The slope,  $K$ , was less for the USACOE compactor.

### 2.3.3.11 Optimum Plus

All response parameters were evaluated for the Optimum Plus mix. There was a significant difference in  $C_{10}$  between the USACOE gyratory and all other compacted specimens. The  $C_{10}$  for the USACOE machine was higher. There also was a significant difference between the modified Texas gyratory specimens and all other compacted specimens. The  $C_{10}$  for the Texas device was higher than that of the SHRP device, but lower than the USACOE device.

There also was a significant difference in  $C_{230}$  between the USACOE gyratory specimens and all other compacted specimens. The  $C_{230}$  for the USACOE machine was higher. There was a significant difference in  $C_{230}$  between the SHRP gyratory (150 mm [6 in.] specimens only) and all other compacted specimens. The  $C_{230}$  for the SHRP (150 mm [6 in.]) machine was lower.

Finally, there was a significant difference in the slope,  $K$ , between the SHRP 100 mm (4 in.) specimens and all other compacted specimens. The SHRP 100 mm (4 in.) specimens produced densification curves with slopes that were higher than the slopes of the other densification curves. In addition, the USACOE specimens was significantly different from all other compacted specimens. The slope,  $K$ , was less for the USACOE machine.

### 2.3.3.12 Conclusions

When response parameters  $C_{10}$ ,  $C_{230}$ , and  $K$  were compared, it appeared that the two devices did not compact mixes similarly.

Verification of the fixed parameters indicated that the two devices were not compacting at the same angle. The modified Texas gyratory compactor had an angle of gyration of 0.97 degrees. The SHRP gyratory compactor had angles of 1.14 and 1.30 degrees for the 150 and 100 mm (6 in. and 4 in.) specimens, respectively. The original Superpave mix designs for the blends used in this experiment were compacted on the modified Texas compactor at an angle of 1.27 degrees.

The main differences for all mixes were in the slopes of the compaction curves, K, for each compactor. Plots were made of K versus angle of gyration and a linear correlation was fit to the data. From this information, it was possible to examine the effects of angle of gyration on the slope of the compaction curve. A variation in the angle of compaction of  $\pm 0.02$  degrees resulted in an air voids variation of  $\pm 0.22$  percent at 100 gyrations. This resulted in a  $\pm 0.15$  percent change in the design asphalt content for the 19 mm (0.76 in.) nominal mix.

An additional study was performed to compare the modified Texas gyratory to the SHRP gyratory and USACOE gyratory. All angles were set to  $1.00 \pm 0.02$  degrees. One mix at three asphalt contents was evaluated. The USACOE gyratory, operated at  $1^\circ$  angle of gyration, produced different densification parameters than the SHRP gyratory compactor (both 100 and 150 mm [4 in. and 6 in.] specimens). It was most similar to the modified Texas compactor. The densification curves of the 100 mm (4 in.) specimens produced by the SHRP gyratory compactor had significantly higher slopes than the densification curves from all the other compacted specimens.

The following conclusions are made based on the results of this study:

- Specification of angle of gyration ( $1^\circ$ ), speed of rotation (30 rpm), and vertical pressure (0.6 MPa [87 psi]) alone is not sufficient to produce similar compactors. From the limited study with the USACOE gyratory compactor, it appears that maintaining a firmly fixed angle is a necessity as well.
- The angle of gyration should have a tolerance of  $1.00 \pm 0.02$  degrees.
- Based on limited information, the USACOE gyratory compactor, operated at a  $1^\circ$  angle of gyration, does not produce similar results to the SHRP gyratory compactor. The main difference in the two machines is the method of applying the angle. Firmly fixing the angle on the USACOE machine may eliminate the compaction differences.

#### *2.3.4 Gyratory Compaction Characteristics—Relation to Service Densities of Asphalt Mixes*

Once the design specifications protocol of the SHRP gyratory compactor were validated, it was necessary to establish experimentally the relationship between the number of gyrations and traffic levels. This was accomplished by the SHRP  $N_{\text{design}}$  experiment which was conducted under SHRP contract A-001.

The purpose of the  $N_{\text{design}}$  experiment was to determine the number of gyrations ( $N_{\text{design}}$ ) required to represent various traffic levels in different climates. Thus, gyrations ( $N_x$ ) must relate to traffic levels ( $E_x$ ). This is compatible with information reported in the literature which indicates that the asphalt density under traffic increases linearly with the logarithm of traffic number of passes until it reaches its ultimate density (Busching 1963, Consuegra 1988, Hughes 1989, Hughes 1964).

The SHRP compaction protocol would maintain a constant gyration pressure and a specified number of gyrations to define two levels of compaction: 1) traffic compaction (96 percent of maximum specific gravity [MSG]) and 2) construction compaction (92 percent of MSG), as shown in Figure 2.20. Percent compaction is defined as the ratio of bulk specific gravity (BSG) to maximum specific gravity (MSG).

The design specification of the SHRP gyratory compactor were as follows:

- Angle of Gyration:  $1^\circ$ .
- Speed: 30 rpm.
- Vertical Pressure: 0.6 MPa (87 psi).
- 100 mm (4 in.) and 150 mm (6 in.) diameter molds.

#### 2.3.4.1 $N_{\text{design}}$ Experiment

Two gyration levels were studied:

1. Gyrations ( $N_{\text{design}}$ ) representing compaction ( $C_{\text{design}}$ ) due to current traffic in the wheel path from SHRP GPS projects.
2. Gyrations ( $N_{\text{const}}$ ) representing compaction ( $C_{\text{const}}$ ) due to the initial pavement construction.  $N_{\text{const}}$  is the gyration which represents the field compaction at the end of construction due to rolling.  $C_{\text{const}}$  densities were not available. Out-of-wheel path densities, also were not available, and would not have provided accurate densities since the pavements outside the wheel path densify to some degree due to wander traffic.

The only data available were from cores that were taken from the wheel path. The construction compaction was assumed to be 92 percent of the maximum specific gravity. Thus, an assumption was made in order to complete the design curves. Without this assumption, there would be no data available at zero equivalent single axle loads (ESALs). Therefore, the regression of gyrations ( $N_x$ ) versus traffic ( $E_x$ ) would be difficult to complete.

The 92 percent of MSG is a valid assumption, since these pavements were most likely designed to have an in-place density of 92 percent, or 8 percent air voids. In addition, the



assumption of 8 percent air voids does not significantly effect the initial gyrations, since approximately only 30 gyrations are required to compact the mix from 86 percent to 92 percent of maximum compaction. For example, if 20 to 40 gyrations are used, the corresponding percent compaction is 90 percent to 93 percent, respectively.

The experiment was conducted in the following order.

- Site selection.
- Collection of cores and core data (layer description, gradation, density, asphalt content, and BSG).
- Separation of core layers and lifts.
- Measurement of the BSG of each layer/lift.
- Extraction of asphalt binder and salvage of aggregate.
- Compaction of specimens with salvaged aggregate.
- Measurement of the BSG & MSG of each compacted specimen.
- Plot of densification curves.
- Tabulation of data.
- Analysis.
- Determination of the design gyrations ( $N_{\text{design}}$ ).

The aged asphalt was extracted then remixed with a single AC-20 grade asphalt cement. Various pavement cores were compacted to achieve compaction curves for each core. The testing matrix incorporated asphalt concrete cores representing three ages, three climates, three traffic levels, and upper and lower layers. This required a total of 54 pavement cores (27 original cores and 27 replicate cores). The goal of this testing matrix was to provide sufficient data that would represent the majority of roads that are travelled today and reduce the potential error in the analysis.

Later, it was decided that only cores of pavements older than 12 years would be used. This reduction of levels of factors simplified the experiment without reducing the essential data. Eighteen pavement cores (nine original cores and nine replicate cores) were required to complete the experiment. The 12 in. diameter cores were collected from various SHRP LTPP test sections. They were then stored in the MRL until needed for testing purposes.

### 2.3.4.2 Site Selection

The cores for the  $N_{\text{design}}$  experiment were selected with the following criteria:

- Cores must come from pavements that have been in use for more than 12 years.
- Three climate zones (hot, warm, and cool) must be represented.
- Three traffic levels (high, medium, and low) must be represented.
- Upper and lower layers should exist.
- Cores must be large enough to produce replicate specimens.

The cores from pavements with more than 12 years of traffic use represented pavements that have densified to their design percent air voids (100 percent [ $C_x$ ]). One assumption in this experiment is that pavements were designed to have final air voids of 3 percent to 5 percent and the pavements were placed at 7 percent to 9 percent air voids. This is a reasonable assumption, since most pavements are required to have these densities.

The cores also represent three climatic zones (hot, warm, and cool). Since the asphalt binder has viscoelastic properties, the asphalt concrete will densify at different rates in various climates. For example, mixes in Arizona (hot climate) will densify more quickly than the same mix with the same asphalt binder placed in Canada (cool climate). The climate zones were defined with the following temperature ( $t$ ) limits in the hottest month of the year.

- Hot:  $t \geq 100^\circ\text{F}$ .
- Warm:  $90^\circ\text{F} \leq t < 100^\circ\text{F}$ .
- Cool:  $t < 90^\circ\text{F}$

Three traffic levels (high, medium, and low) were represented in this experiment. The current accumulated traffic in equivalent single axle loads (ESALs) had to be defined in terms of the 20-year design traffic. The design traffic was calculated by the following equation:

$$\text{20-Year Design Traffic} = 20 \times \left[ \frac{\text{Current Traffic, ESALs}}{\text{Total Years of Service}} \right] \quad (2.20)$$

The ESALs were extracted from the SHRP database. The traffic ( $E_x$ ) levels were defined with the following boundaries:

- Low:  $E_x \leq 10^6$  ESALs.
- Medium:  $10^6$  ESALs  $< E_x \leq 15 \times 10^6$  ESALs.

- High:  $E_x \geq 15 \times 10^6$  ESALs.

Traffic that produces vertical and shear stresses will densify asphalt concrete. The higher the traffic level, the more the pavement layer will densify until it reaches its ultimate density. The ultimate density is defined as the density at which the asphalt concrete pavement will no longer densify under traffic. The ultimate density is not the maximum theoretical density (maximum specific gravity).

As mentioned earlier, the desired ultimate percent compaction is 95 percent to 97 percent of the MSG (5 percent to 3 percent air voids, respectively). A lesser percentage of compaction will produce too many air voids in the mix, which will result in raveling since the pavement will be permeable. Too much compaction will result in a pavement that has no room for the binder to expand. This overcompaction will result in flushing and rutting of the pavement. Usually, a pavement subjected to the design traffic will reach its ultimate density after the third summer.

It was specified that the cores should have upper and lower layers for testing, since the layers will have different densities. Pavement densification also varies with pavement depth. This can be understood if we look at Boussinesq's theory of vertical stress distribution. Vertical stress is directly proportional to depth. Therefore, pavement densification is directly related to pavement depth. Furthermore, the majority of pavement densification occurs mainly in the upper layers of the pavement. Thus, the upper layers were defined as less than or equal to four inches from the surface. The lower layers were defined as greater than four inches from the surface.

Duplicate specimens that are subjected to different traffic loads, but within the traffic level boundaries shown above, must be selected to complete the testing matrix. The amount of essential data is important, since the experiment has significant variability. The original and replicate specimens with different traffic loads should provide two pieces of data within the same traffic level. This will reduce the potential for error in the experiment. It should be noted that replicate specimens were not available for the hot climate (i.e., there was only one specimen per traffic level available). The remaining two climates, cool and warm, had two replicates available.

The above selection criteria will provided a complete testing matrix, shown in Table 2.7 for various climates, traffic levels, and layer depths.

**Table 2.7. Final core selection—experiment matrix**

		Temperature								
		Hot			Warm			Cool		
		Low	Medium	High	Low	Medium	High	Low	Medium	High
Layers	Upper	X	X	X	X	X	X	X	X	X
	Lower	X	X	X	X	X	X	X	X	X

### 2.3.4.3 Determination of the Design Gyration ( $N_{\text{design}}$ )

Three lines were regressed through the data points. This produced curves for the three climates (hot, warm, and cool). By using these design curves, the graph can be entered with a known traffic level in a specific climate and obtain the corresponding design gyration ( $N_{\text{design}}$ ). To increase the degrees of freedom in the analysis, one line was regressed through the data without regard to the climate. This analysis was chosen to provide one dependable line instead of three less dependable lines. By using this single curve, the graph can be entered with a known traffic level in a general climate and obtain the corresponding design gyration ( $N_{\text{design}}$ ). These models provided two choices in choosing the final design curves. SHRP could have chosen 1) design curves representing various traffic levels with three climates (climate-included model), or 2) one curve representing various traffic levels without climate difference (climate-excluded model).

The climate-included model (angle of gyration =  $1^\circ$ ) was chosen for the following reasons:

- The analysis pointed toward using the climate as a qualitative variable.
- The climate-included model produced an acceptable degree of error and variability.
- The climate-excluded produced results (like an average of the climate-included model) that are similar in trend to the warm design curve of the climate-included model.
- Part of the objective of this experiment was to show the influence of climate in the design curves.
- A designation of climate in volumetric mix design, not just asphalt grade, must start somewhere with more research to follow.

The equations represent the climate-included model (angle of gyration =  $1^\circ$ ). The design gyrations versus traffic graph (Figure 2.22) shows a plot of these equations. It should be noted that the experiment included design traffic up to 32,100,000 ESALs. Thus, as represented on the graph, the values greater than 32,100,000 ESALs were extrapolated.

$$\text{Hot:} \quad N_{\text{design}} = 10^{1.34276 + 0.10850 \times \text{LOG (Traffic, ESALs)}} \quad (2.21)$$

$$\text{Warm:} \quad N_{\text{design}} = 10^{1.26454 + 0.11206 \times \text{LOG (Traffic, ESALs)}} \quad (2.22)$$

$$\text{Cool:} \quad N_{\text{design}} = 10^{1.21211 + 0.09148 \times \text{LOG (Traffic, ESALs)}} \quad (2.23)$$

To use the models in Superpave, the temperature zones (hot, warm, and cool), which were determined from monthly maximum air temperature ( $^\circ\text{F}$ ), had to be converted to weekly mean maximum air temperature ( $^\circ\text{C}$ ). The climate zones mid-range temperatures are shown in Table 2.8.

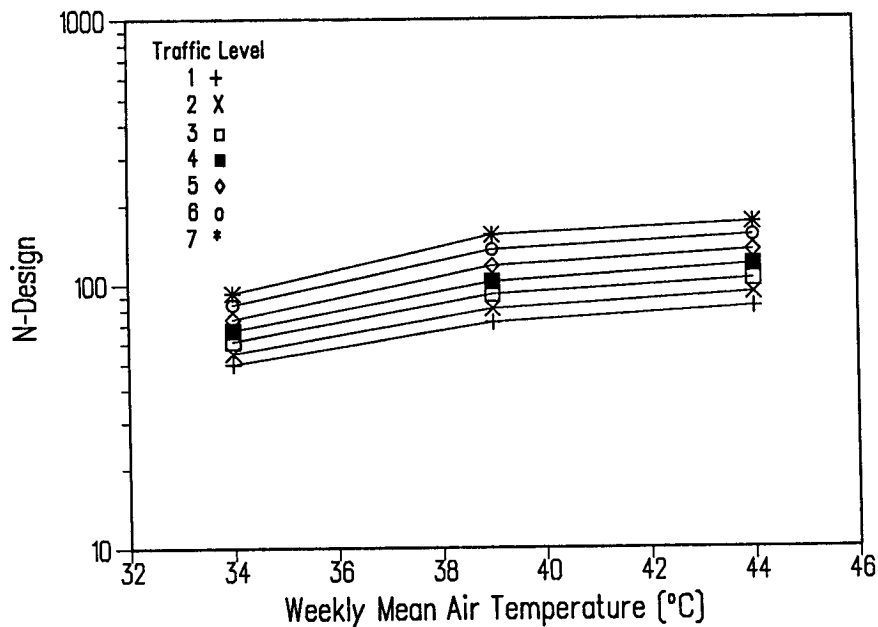


**Figure 2.22. Design gyrations as a function of temperature**

**Table 2.8. Design gyrations determined from monthly maximum air temperature**

Traffic Level	Hot 44°C (105°F)			Warm 39°C (95°F)			Cool 34°C (85°F)		
	ESAL Limit			ESAL Limit			ESAL Limit		
	Low	High	Average	Low	High	Average	Low	High	Average
1	77	87	82	67	76	72	47	52	50
2	87	99	93	76	86	81	52	58	55
3	99	111	105	86	98	92	58	64	61
4	111	127	119	98	108	103	64	69	67
5	127	143	135	108	127	118	59	79	74
6	143	162	153	127	145	136	79	88	84
7	162	183	172	145	164	155	88	97	93

The temperatures shown in Table 2.8 were then converted to the range of temperatures shown in Table 2.9. The design gyrations for these temperatures were developed from Figure 2.22.

**Table 2.9. Temperature conversion**

Climate Zone	Monthly Air Temperature (°F)	Weekly Air Temperature (°C)
Hot	105	44
Warm	95	39
Cool	85	34

These temperatures were entered into equation 2.24. This equation represents the conversion from monthly to weekly mean maximum air temperature for the United States. This equation had an  $R^2$  of 0.90. Therefore the conversions listed in Table 2.9 are judged reliable.

$$\text{Weekly Mean Max, } ^\circ\text{C} = \frac{14.13 + 0.92 (\text{Monthly Mean Max, } ^\circ\text{F}) - 32}{9/5} \quad (2.24)$$

Next, these temperatures in weekly mean maximum air temperature were plotted against the design gyrations at designated 20-year traffic levels. The 20-year design traffic levels to be used in Superpave are defined in Table 2.10. The design gyrations ( $N_{\text{design}}$ ) to represent each of these ESAL limits, which will correspond to a design air voids of 4 percent, are listed in Table 2.8. The  $N_{\text{design}}$  limits (high and low) were averaged for each climate to provide the midrange  $N_{\text{design}}$  for each traffic level (1,2,...). Finally,  $N_{\text{design}}$  was plotted with respect to each traffic level (Figure 2.23).

**Table 2.10. Superpave traffic levels**

Traffic Level	ESAL Limit	Design Air Voids (%)
1	$< 3 \times 10^5$	4
2	$< 1 \times 10^6$	4
3	$< 3 \times 10^6$	4
4	$< 1 \times 10^7$	4
5	$< 3 \times 10^7$	4
6	$< 1 \times 10^8$	4
7	$< 3 \times 10^8$	4

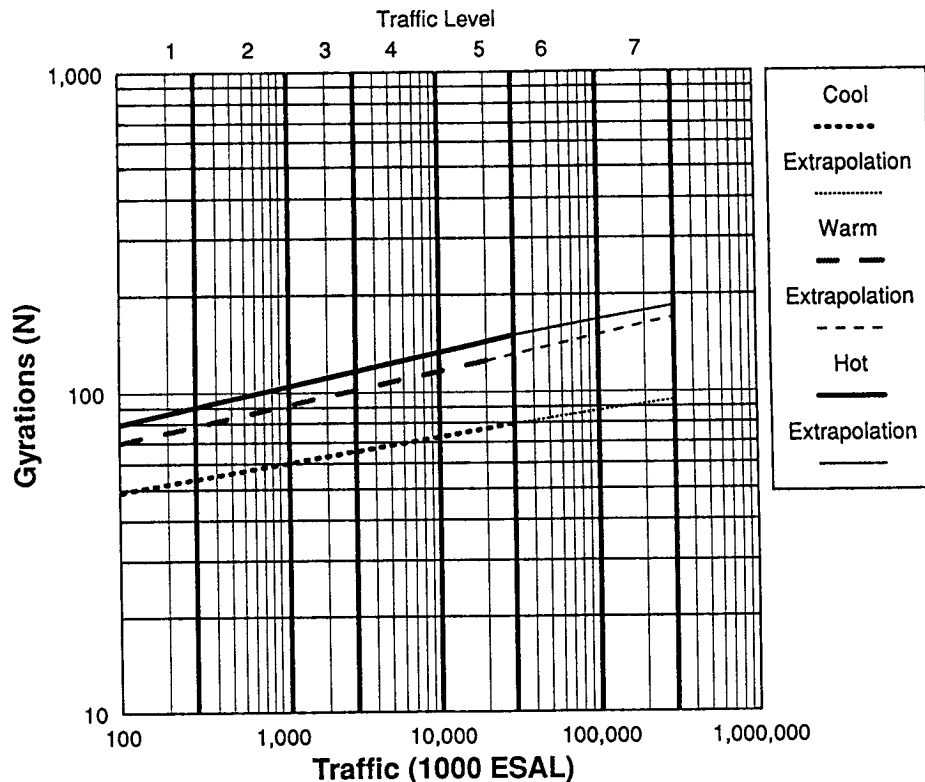


**Figure 2.23. Design gyrations as a function of traffic**

It is now possible to use the design gyrations ( $N_{\text{design}}$ ) obtained from the design curve, Figure 2.23, to determine the design 4 percent compaction ( $C_x$ ) from compaction curves of future mixes. For instance, if one were designing a pavement for Traffic Level 4 and a weekly mean maximum air temperature of  $39^{\circ}\text{C}$ , the  $N_{\text{design}}$  would be 103 gyrations. To achieve the optimum aggregate blend and asphalt content for this mix design, simply enter the design gyration ( $N_{\text{design}}$ ), representing 20-year design traffic, into the compaction curve of the new mix design to obtain the final percent compaction ( $C_x$ ) of that mix (target = 96 percent MSG). Thus, at that specific traffic level (gyration) and climate, the mix will compact to  $C_x$  of the given MSG.

#### 2.3.4.4 Determination of Gyratory Compaction Check Points

The following is a concise step-by-step procedure developing the key gyratory compaction points related to the Superpave mix design.

1. Number of design gyrations for each traffic level in each environmental zone is obtained from Figure 2.22.
2. Use compaction curves to estimate design density curve. See typical curves in Figures 2.24, 2.25, and 2.26.
  - Use density curve as measured.

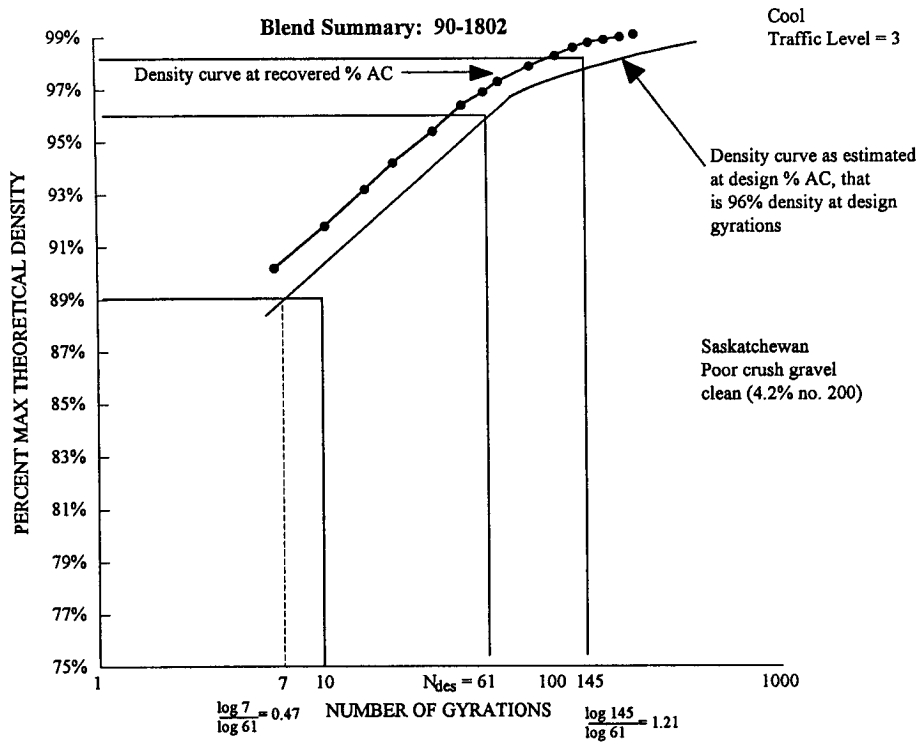


**Figure 2.24. Compaction curve for 90-1802 blend**

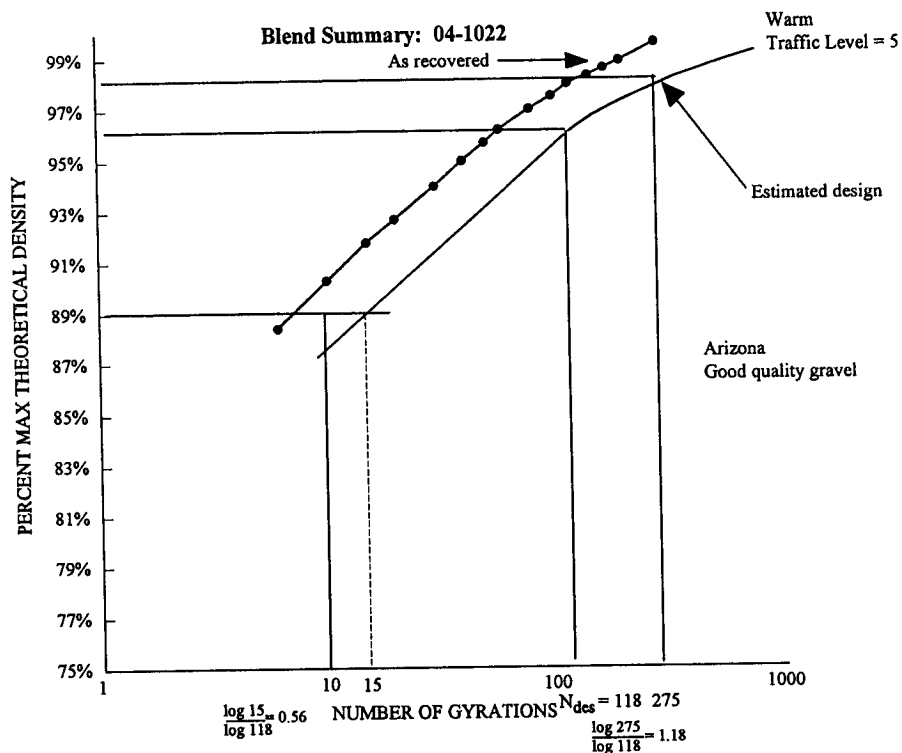


**Figure 2.25. Compaction curve for 04-1022 blend**



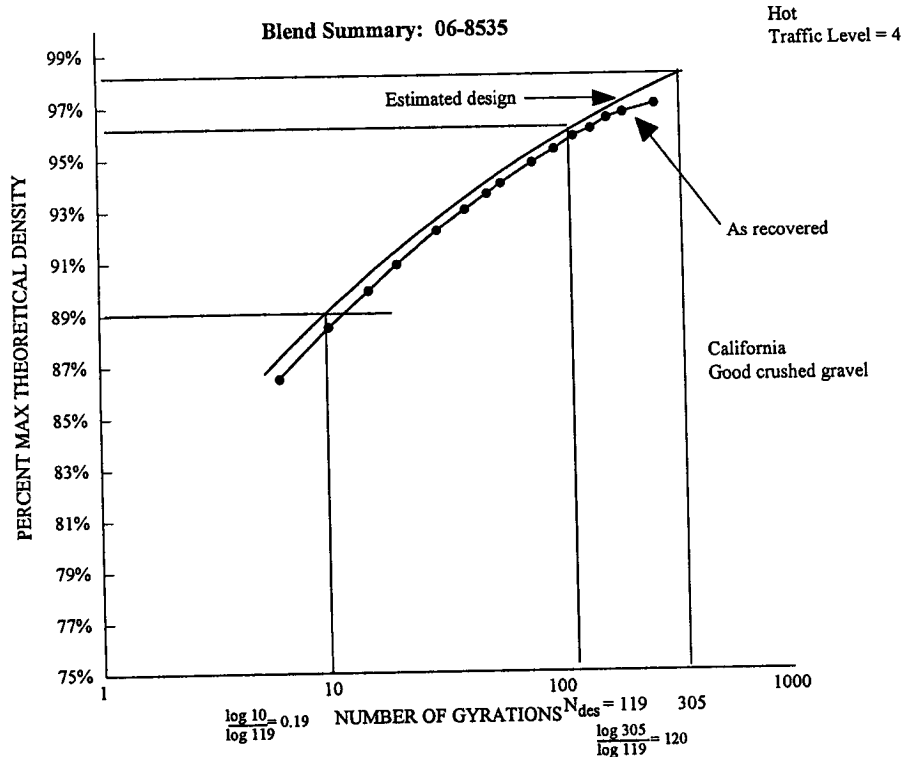


**Figure 2.26. Compaction curve for 06-8535 blend**

- Mark intersection point where density = 96 percent and N = design.
  - Shift compaction curve horizontally until it passes through the intersection point.
3. Determine gyrations where density = 98 percent and compare to design.
- Draw horizontal line at density = 98 percent.
  - At intersection with estimate compaction curve draw vertical line to x-axis, read number of gyrations.
  - Calculate ratio.
- $$\frac{\log (N_{98})}{\log (N_{Design})} \quad (2.25)$$
4. Determine gyrations where density = 89 percent and compare to design.
- Draw horizontal line at density = 89 percent.
  - At intersection with estimated compaction curve draw vertical line to x-axis, read number of gyrations.

- Calculate ratio.

$$\frac{\log (N_{89})}{\log (N_{\text{Design}})} \quad (2.26)$$

5. Determine  $N_{89}$ .

In the French method of mix design,  $N_{89}$  is 10 gyrations, i.e., at 10 gyrations, mix density must be less than 89 percent of theoretical maximum specific gravity.

Ten gyrations remains fixed, regardless of the number of design gyrations. Typical example designs often use  $N_{\text{design}} = 80$  gyrations. Hence

$$\frac{\log 10}{\log 80} = 0.53 \quad (2.27)$$

In some ways the French example is not helpful. For example, if  $N_{\text{design}} = 150$  then the ratio is 0.62. It is easier to meet the requirements for  $N_{89}$  if  $N_{\text{design}}$  is high than if it is low.

Note also, that the French values for percent maximum specific gravity are based only on calculated volume, without correction for surface irregularities.

In the SHRP method  $N_{89}$  should be a function of  $N_{\text{design}}$ . For example, consider a high traffic (level 6 or 5) in a hot environment. A very strong aggregate skeleton is needed, so  $N_{89}$  will be high.

The same strong structure is not needed in a cool climate, where  $N_{\text{design}}$  will be 84 as compared to 153 in the hot environment. Hence  $N_{89}$  can be lower.

SHRP's recommendation is to use the following relationship developed from the  $N_{\text{design}}$  experiments:

$$\log N_{89} = 0.45 \log N_{\text{design}} \quad (2.28)$$

See summary of data in Table 2.9.

$N_{89}$  is the number of gyrations at which the estimated design curve will pass through 89 percent MSG

$$\frac{\log N_{89}}{\log N_{\text{Design}}} \quad (2.29)$$

On average  $\log N_{89} = 0.47 \log N_{\text{design}}$ .

- Sites with lower values have weak aggregate structures, either rounded gravel, sandy mix or high fine content (passing the No. 200 sieve).

Based on the data, SHRP recommends a value of 0.45, i.e.,  
 $\log N_{89} = 0.45 \log N_{\text{design}}$ .

- For a given mix design, density should be less than 89 percent at  $N_{89}$  gyrations.

6. Determine  $N_{98}$ .

The current recommendation in Superpave is

$$\log N = 1.15 \log N_{\text{design}} \quad (2.30)$$

In Table 2.11 the average value of  $\log N_{98}/\log N_{\text{design}}$  is 1.22. Typically mixes which would fail at  $N_{89}$  gyrations have a high ratio  $N_{98}/N_{\text{design}}$ .

- This is logical since if  $N_{89}$  check is not met, then slope is too flat.
- If the slope is too flat, and passed through 96 percent density at  $N_{\text{design}}$ , then it will take longer time to reach 98 percent density.
- For mixes which meet  $N_{89}$  the density must be less than 98 percent at  $1.15 \log N_{\text{design}}$  gyrations

**Table 2.11. Results from  $N_{\text{design}}$  experiment**

Site	Temperature	Traffic Level	$N_{\text{design}}$	$N_{89}$	$\text{Log}(N_{89})/\text{Log}(N_{\text{design}})$	$N_{98}$	$\text{Log}(N_{98})/\text{Log}(N_{\text{design}})$
21-1034	Cool	2	55	5	0.40	140	1.23
53-1801	Cool	2	55	7	0.49	94	1.13
90-1802	Cool	3	61	7	0.47	145	1.21
23-1001	Cool	3	61	9	0.53	120	1.16
18-1028	Cool	5	74	5	0.37	225	1.26
41-7018	Cool	5	74	12	0.58	140	1.15
12-4100	Warm	2	81	6	0.41	270	1.27
48-3559	Warm	2	81	2	0.16	580	1.45
48-1070	Warm	3	92	6	0.40	255	1.23
40-1015	Warm	3	92	18	0.64	200	1.17
04-1022	Warm	5	118	15	0.57	275	1.18
32-1030	Hot	2	93	11	0.53	235	1.20
06-8535	Hot	4	119	10	0.48	305	1.20
04-1003	Hot	5	135	11	0.49	460	1.25
Averages					0.47		1.22

7. Table of Key Gyration.

Table 2.12 shows  $N_{89}$ ,  $N_{design}$ , and  $N_{98}$  gyrations for all traffic levels and environmental zones. To use this table as an example, select "Traffic level 4, warm". Then, the following values are selected:

**Table 2.12. Design gyrations for various traffic levels and environmental zones**

Traffic Level	Environment								
	Cool			Warm			Hot		
	$N_{89}$	$N_{design}$	$N_{98}$	$N_{89}$	$N_{design}$	$N_{98}$	$N_{89}$	$N_{design}$	$N_{98}$
1	6	50	90	7	72	137	7	82	159
2	6	55	100	7	81	157	8	93	184
3	6	61	113	8	92	181	8	105	211
4	7	67	126	8	103	206	9	119	244
5	7	74	141	9	118	241	9	135	282
6	7	84	163	9	136	284	10	153	325
7	8	93	184	10	155	330	10	172	372

- Choose asphalt content for 96 percent density at  $N_{design}$  (103 gyrations).
- Check at  $N_{89}$  (8 gyrations) that density is less than 89 percent.
- Check at  $N_{98}$  (206 gyrations) that density is less than 98 percent.

8. Use in Superpave.

Figures 2.27 and 2.28 show design gyrations for different traffic levels and environment.

Cool		< 90°F (32°C)	Monthly maximum
Warm	were defined as	90 to 100°F (32 to 38°C)	air temperature
Hot		> 100°F (38°C)	

Conversions were made from monthly to weekly temperatures to produced the following temperatures:

<u>Temperature</u>	<u>Monthly</u>	<u>Weekly (°F)</u>	<u>Weekly (°C)</u>
Cool	85°F (29°C)	92	34
Warm	95°F (35°C)	102	39
Hot	105°F (41°C)	111	44

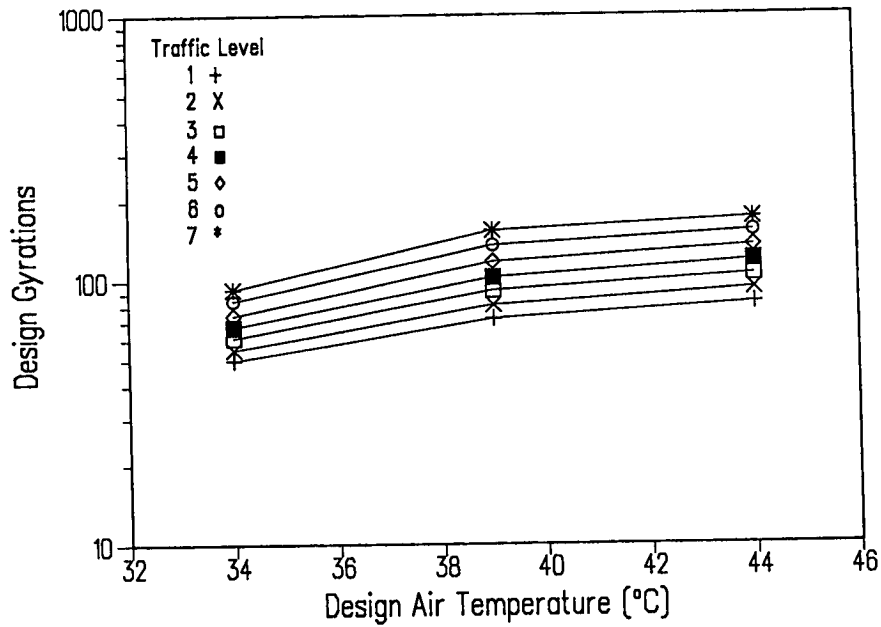


Figure 2.27. Design gyrations ( $N_{\text{design}}$ ) for various temperatures

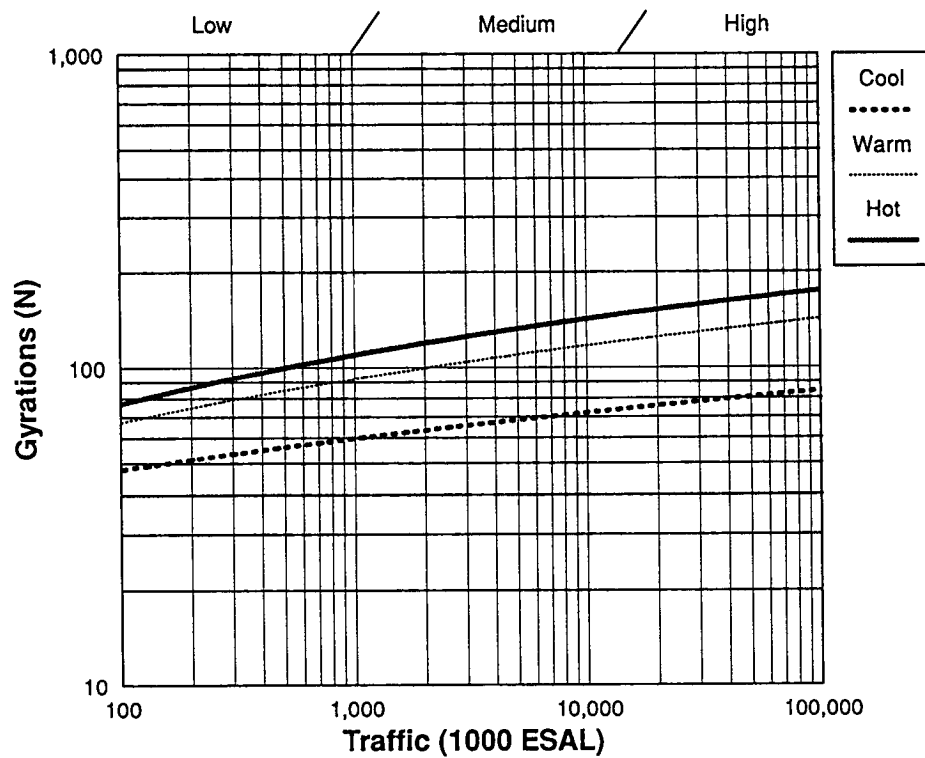


Figure 2.28. Design gyrations for various traffic levels

- User selects weather station from binder statistical weather database (same one used for binder selection).
- Superpave takes air temperature at 50 percent reliability
  - enters chart at correct temperature, and
  - finds  $N_{\text{design}}$  for traffic level.
- Superpave then
  - calculates  $N_{89}$  and  $N_{98}$ , and
  - displays  $N_{89}$ ,  $N_{\text{design}}$ , and  $N_{98}$  to designer.

Note that in the Superpave mix design method,  $N_{89}$  is termed  $N_{\text{init}}$ , and  $N_{98}$  is termed  $N_{\text{max}}$ .

## 2.4 SHRP Gyratory Compactor in Relation to Field Control

Completion of the laboratory phase of mix design is not the last step in the mix design process as envisaged by SHRP. After a job mix formula is obtained, field verification of mix properties and field control of the mix during construction are an integral and essential part of the mix design. One level of mix verification and control suggested by SHRP is to use the gyratory compactor to compact specimens of plant-mixed materials to confirm that volumetric properties, that is air voids, voids in mineral aggregate and voids filled with asphalt, meet the same criteria used to select the job mix formula during the laboratory phase of the mix design. Volumetric verification is envisaged to include three items:

- Compaction of mix in gyratory compactor.
- Determination of asphalt content.
- Determination of aggregate gradation.

An experiment conducted under SHRP contract A-001 evaluated the ability of the SHRP gyratory compactor to discern changes in key mix properties. For example, does a change of a key input cause a change in compaction characteristics which can be detected with the gyratory compactor? This experiment was designed to investigate changes in the following input variables:

- Asphalt content.
- Percent passing 75  $\mu\text{m}$  sieve.

- Percent passing 2.36 mm sieve.
- Change in aggregate nominal maximum size.
- Change percentage of natural and crushed sands.

### 2.4.1 Experiment Design

The experiment consisted of compaction of one asphalt-aggregate mix. The number of controlled variables and levels are shown in Table 2.13. A brief description of each variable and level follows.

**Table 2.13. Controlled variables in compactor field control experiment**

Controlled Variable	Number of Levels
Asphalt Content	3
Percent Passing 75 $\mu\text{m}$	3
Percent Passing 2.36 mm (0.09 in.)	3
Nominal Maximum Size	3
Percent Natural Sand	3
Replicates	3

#### 2.4.1.1 Baseline Mix Design

One mix design was used as the baseline case. Properties of the selected mix design were considered to be the medium value for each variable listed in Table 2.13 with one exception. Hence, percent asphalt binder, percent passing 2.36 mm sieve, nominal maximum size and percentage of natural sand of the baseline mix design were considered medium values for each variable. The percent passing the 75  $\mu\text{m}$  sieve of the selected mix was considered the low value for that variable.

The baseline mix design selected for this study was the surface course mix design determined for the SPS-9P project constructed on Interstate Highway 43 near Milwaukee, Wisconsin in August 1992. This mix has a nominal maximum size of 12.5 mm, a low percent passing the 75  $\mu\text{m}$  sieve, and a middle of the band percent passing the 2.36 mm sieve. Two sands are used in this mix, one natural, the other manufactured. Both sands have a maximum size of 9.5 mm. Gradation of the baseline mix is shown in Figure 2.29.

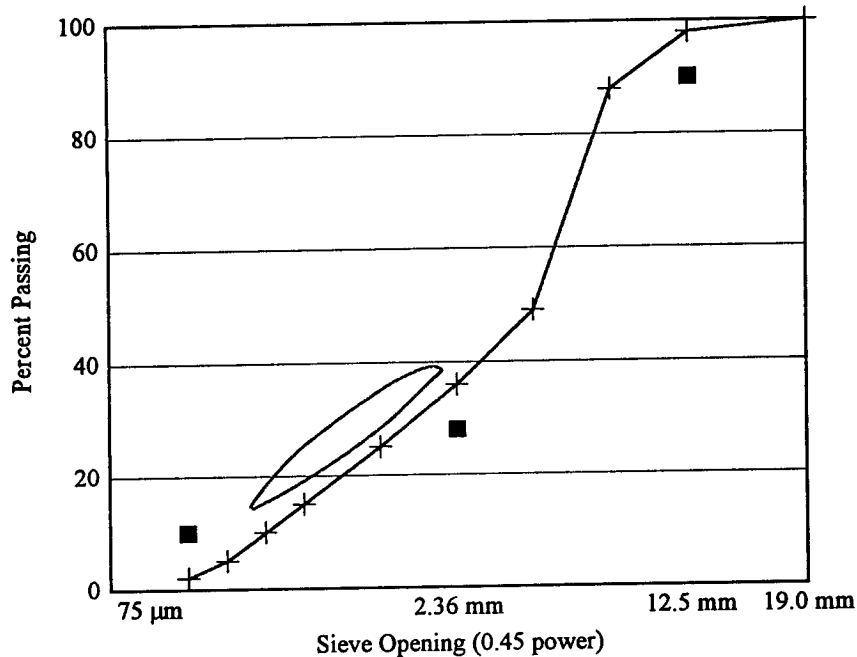


**Figure 2.29. Gradation of baseline mix for field control experiment**

### 2.4.1.2 Asphalt Content

Design asphalt content of the baseline mix was 5.3 percent. Mixes in the field control experiment had three asphalt content levels: high, low, and medium. Three levels were proposed for the experiment as shown in Table 2.14.

**Table 2.14. Definition of asphalt content levels**

Level	Value
1. Low	4.7% (Design minus 0.6%)
2. Medium	5.3% (Design)
3. High	5.9% (Design plus 0.6%)

### 2.4.1.3 Percent Passing 75 μm Sieve

Specification control points for the 75 μm sieve in a 12.5 mm (0.5 in.) nominal maximum gradation are 2 percent to 10 percent. The baseline mix has a relatively low percent passing the 75 μm sieve. Hence, the baseline mix provided the low level of percent passing 75 μm. Gradations are shown in Figure 2.30. Three levels were proposed for the experiment as shown in Table 2.15.



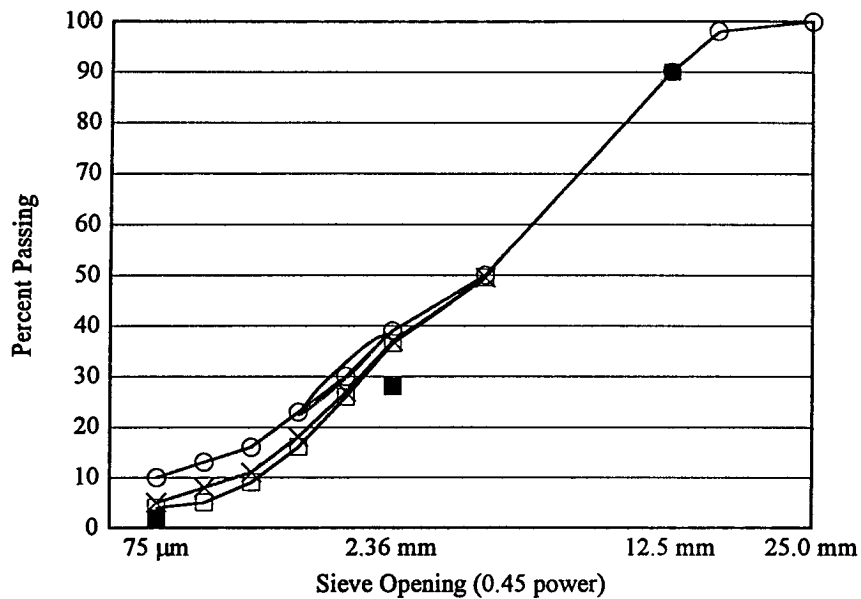


**Figure 2.30. Gradation of mixes with variable percent passing the 75 μm sieve**

**Table 2.15. Definition of levels for percent passing 75 μm sieve**

Level	Value
1. Low	3.8% (Design)
2. Medium	6.0% (Median Control Point)
3. High	9.7% (Maximum Control Point)

#### 2.4.1.4 Percent Passing 2.36 mm Sieve

The baseline mix has a level of percent passing the 2.36 mm sieve near the center of the allowable range from 28 percent to 39 percent. Gradations are shown in Figure 2.31. Three levels were proposed for the experiment as shown in Table 2.16.

#### 2.4.1.5 Nominal Maximum Size

The baseline mix has a nominal maximum size of 12.5 mm. Gradations are shown in Figure 2.32. Three levels were proposed for the experiment as shown in Table 2.17.

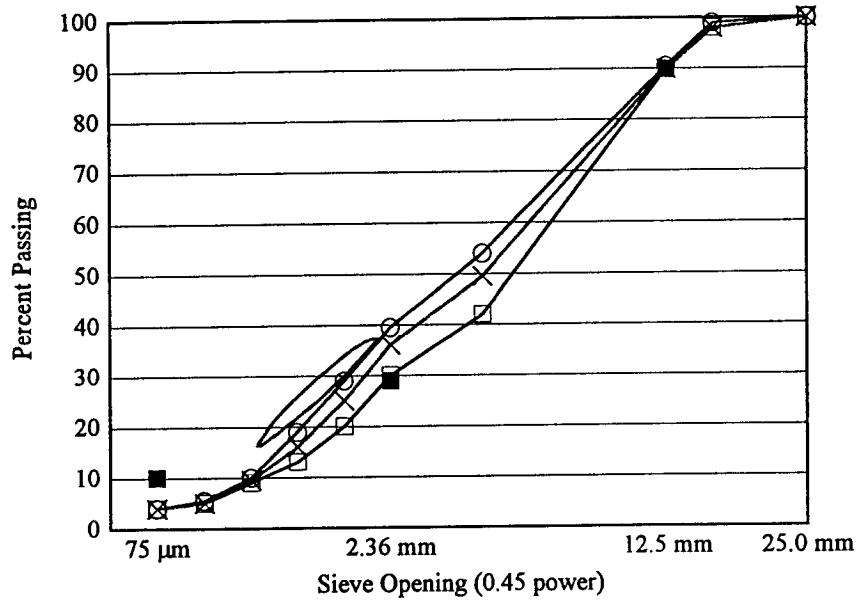


**Figure 2.31. Gradation of mixes with variable percent passing the 2.36 mm sieve**

**Table 2.16. Definition of levels for percent passing 2.36 mm sieve**

Level	Value
1. Low	29.3% (Minimum Control Point)
2. Medium	35.2% (Design)
3. High	38.9% (Maximum Control Point)

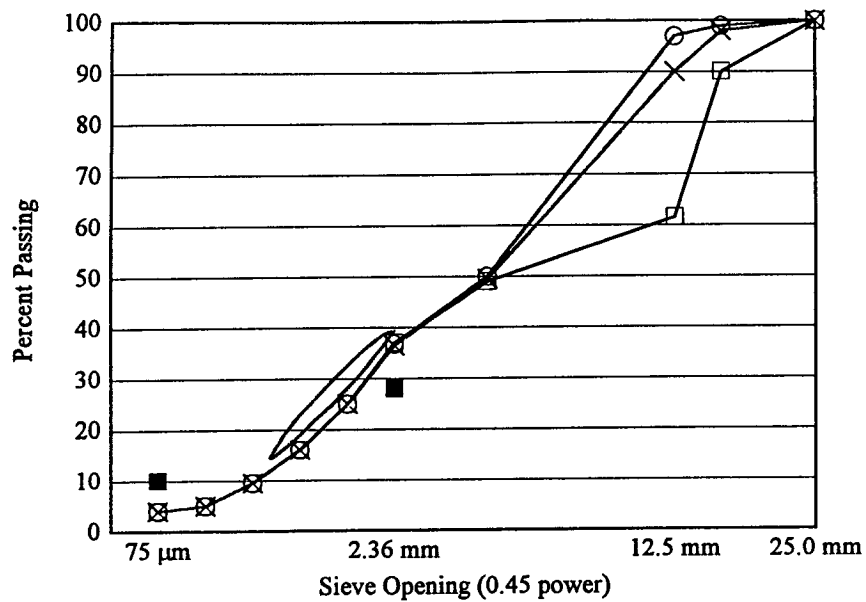


**Figure 2.32. Gradation of mixes with variable nominal maximum size**

**Table 2.17. Definition of levels for nominal maximum size**

Level	Value
1. Low	9.5 mm (Nominal maximum size one size smaller than design)
2. Medium	12.5 mm (Design nominal maximum size)
3. High	19.0 mm (Nominal maximum size one size larger than design)

#### 2.4.1.6 Percent Natural Sand

The proportion of fine aggregate (smaller than 2.36 mm sieve) was varied between natural and manufactured sand. The percentage of fine aggregate remained the same in the design; only the relative proportion of manufactured and natural materials changed. Three levels of natural materials changed. Gradations are shown in Figure 2.33. Three levels of natural sand/manufactured sand were proposed for the experiment as shown in Table 2.18.

#### 2.4.1.7 Replicates

Three replicate specimens were made for each combination of asphalt content, percent passing 75  $\mu\text{m}$ , percent passing 2.36 mm, nominal maximum size, and manufactured proportion of fine aggregate.

#### 2.4.1.8 Factorial

The total number of cells existing in the complete experiment is 243. Eleven cells in the matrix were tested as shown in Table 2.19. The total number of specimens made in the experiment was 33.

#### 2.4.1.9 Compaction Protocol

Specimens prepared with the SHRP gyratory compactor were 150 mm (6 in.) in diameter and 115 mm (4.6 in.) high. Densification curves were plotted for each specimen from  $N = 10$  gyrations to  $N = 230$  gyrations. Gyratory compaction was performed using the following set of parameters:

- Angle of compaction: 1.14°.
- Vertical pressure: 0.6 MPa (87 psi).
- Speed of rotation: 30 rpm.

Design asphalt content for the baseline mix was set at 5.3 percent based on the gyratory compaction mix design.

Mixing temperature was that yielding a viscosity of the unaged asphalt binder of 170 + 20 cSt. Compaction temperature was chosen as that yielding a viscosity of 280 + 20 cSt measured on unaged binder. All mixes were short-term aged for 4 hours in a forced draft oven at 135°C (275°F).

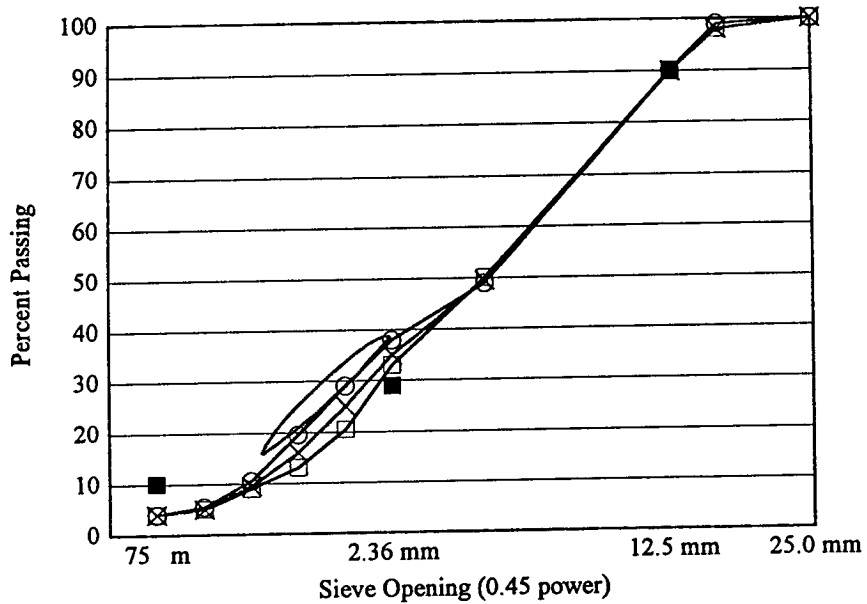


**Figure 2.33. Gradations of mixes with variable percent natural sand**

**Table 2.18. Definition of levels for percent natural sand**

Level	Value
1. Low	0%/50% (Lower proportion of natural sand than design mix)
2. Medium	15%/35% (Design proportion of natural and manufactured sand)
3. High	30%/20% (Higher proportion of natural sand than design mix)
	19.0 mm (Nominal maximum size one size larger than design)

**Table 2.19. Array of conditions used in the field control experiment**

Blend	Asphalt Content	Percent Passing 75 $\mu\text{m}$	Percent Passing 2.36 mm	Nominal Maximum Size	Percent Natural Sand
1	Medium	Low	Medium	Medium	Medium
2	Low	Low	Medium	Medium	Medium
3	High	Low	Medium	Medium	Medium
4	Medium	Medium	Medium	Medium	Medium
5	Medium	High	Medium	Medium	Medium
6	Medium	Low	Low	Medium	Medium
7	Medium	Low	High	Medium	Medium
8	Medium	Low	Medium	High	Medium
9	Medium	Low	Medium	Low	Medium
10	Medium	Low	Medium	Medium	High
11	Medium	Low	Medium	Medium	Low

Note: Definitions of low, medium, and high are shown in Tables 2.14 through 2.18.

#### 2.4.1.10 Response Variables

Results of height measurements taken during the compaction process were used to calculate specimen density expressed as percent maximum specific gravity. A plot was made of percent maximum specific gravity versus log of the number of gyrations, as shown in Figure 2.34 for each mix.

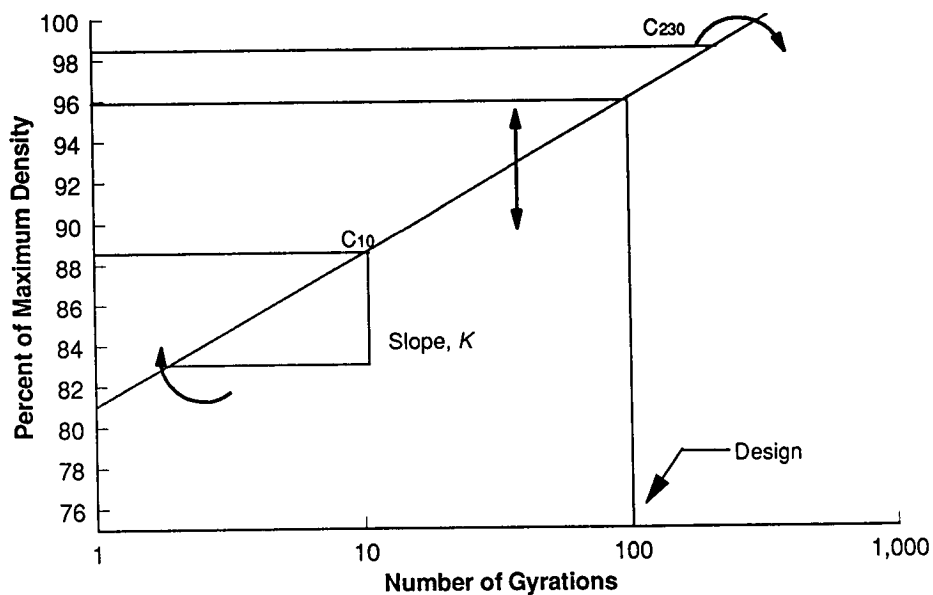


**Figure 2.34. Typical compaction curve for gyratory compacted specimen**

The compaction or densification curve is characterized by three parameters.  $C_{10}$  is the percent maximum specific gravity after 10 gyrations; and  $C_{230}$  is the percent maximum specific gravity after 230 gyrations. The slope of the densification curve,  $K$ , is calculated from the best fit line of all data points assuming that the curve is approximately linear. In situations where density begins to approach 100 percent, and the densification curve begins to bend downward, the slope is calculated from the straight line portion of the curve.

A comparison of  $C_{10}$ ,  $C_{230}$ , and  $K$  was made for mixes compacted with various levels of the treatment variables to determine if changes in asphalt content, gradation or aggregate type can be detected. Expected changes include a shifting of the densification curves either up or down, indicating a more compactible mix or less compactible mix, respectively. In addition, the slope of the densification curve may change, indicating a change in the aggregate structure.

### 2.4.2 Summary of Effects on $C_{10}$ , $C_{230}$ , and $K$

Table 2.20 indicates the response of the compaction curve to the variables in the experiment. The baseline curve is the design case. From this information it appears that the slope of the compaction curve is affected by asphalt content and the percent passing the 75  $\mu\text{m}$  sieve. The position of the curve with respect to the design curve varies as the experiment variables change. Only the nominal maximum particle size has no effect on the design curve.

**Table 2.20. Response of design compaction curve to variables**

Variable With Respect to Design	Translation of Curve ( $\Delta K = 0$ )	Rotation of Curve
Lower % AC	Down	Down
Higher % AC	Up	Up
Median % Passing 75 $\mu\text{m}$ Sieve	Up	None
Higher % Passing 75 $\mu\text{m}$ Sieve	Up	Up
Lower % Passing 2.36 mm (0.09 in.) Sieve	Down	None
Higher % Passing 2.36 mm (0.09 in.) Sieve	Up	None
Lower Nominal Maximum Size	None	None
Higher Nominal Maximum Size	None	None
Lower % Natural Sand	Down	None
Higher % Natural Sand	Up	None

Note: Translation of curve refers to the curve shifting up or down without changing slope. Rotation of curve refers to either an increase in slope (up) or a decrease in slope (down). Translation encompasses both  $C_{10}$  and  $C_{230}$ . Rotation includes the parameter  $K$ .

### 2.4.3 Volumetric Properties

The final objective of this experiment was to evaluate how changes in key variables affect the volumetric properties of the mix. Table 2.21 indicates the results of percent air voids,

**Table 2.21. Volumetric properties at 100 gyrations**

Variable	Blend	% Air Voids	% VMA	% VFA
<b>Asphalt Content</b>				
Low Asphalt Content	2	9.4	18.3	48.6
Baseline	1	7.1	17.5	59.4
High Asphalt Content	3	5.1	17.0	70.0
<b>Percent Passing 75 <math>\mu\text{m}</math> Sieve</b>				
Baseline	1	7.1	17.5	59.4
Medium Percent 75 $\mu\text{m}$	4	3.3	14.1	76.6
High Percent 75 $\mu\text{m}$	5	1.3	12.3	89.4
<b>Percent Passing 2.36 mm (0.09 in.) Sieve</b>				
Low Percent 2.36 mm (0.09 in.)	6	7.7	18.1	57.5
Baseline	1	7.1	17.5	59.4
High Percent 2.36 mm (0.09 in.)	7	6.3	16.7	62.3
<b>Nominal Maximum Size</b>				
Low Nominal Maximum	9	7.5	17.9	58.1
Baseline	1	7.1	17.5	59.4
High Nominal Maximum	8	7.6	17.5	56.6
<b>Percent Natural Sand</b>				
Low Percent Natural Sand	11	9.9	20.0	50.5
Baseline	1	7.1	17.5	59.4
High Percent Natural Sand	10	4.9	15.4	68.2

percent voids in mineral aggregate (% VMA), and percent voids filled with asphalt (% VFA) for each blend at an estimated design of 100 gyrations.

Table 2.21 indicates that all of the volumetric properties change significantly for changes in the variables of asphalt content, percent passing the 75  $\mu\text{m}$  sieve, and percent natural sand. The volumetric properties change slightly with changes in the percent passing the 2.36 mm sieve. The volumetric properties do not change with the nominal maximum particle size.

#### *2.4.4 Summary and Recommendations*

Table 2.22 presents a summary of the experimental results for the comparison of the response variables  $C_{10}$ ,  $C_{230}$ , and K as to the effect of each variable on the design case.

Of the input variables, asphalt content has the strongest effect on the response parameters of the compaction curves. Nominal maximum particle size has the weakest effect on the response parameters of the compaction curves. The percent passing the 75  $\mu\text{m}$  sieve and the ratios of natural and crushed sands also had significant effects on the compaction curves.

In summary, the SHRP gyratory compactor is recommended for field control. The SHRP gyratory compactor specimens change in volumetric properties, as detected through changes in the compaction curves as key input variables change.



**Table 2.22. Response of parameters to input variables**

Increase in Input Variable	C10	C230	K
Percent Asphalt Content	Increases	Increases	Increases
Percent Passing 75 $\mu\text{m}$ Sieve	Increases	Increases	Increases
Percent Passing 2.36 mm Sieve	Increases	Stays the Same	Stays the Same
Nominal Maximum Size	Stays the Same	Stays the Same	Stays the Same
Ratio of Natural/Crushed Sand	Increases	Increases	Stays the Same

## 2.5 Field Validation of SHRP Gyrotory Compactor

Nine pilot SPS-9 projects were constructed in Arizona, Indiana, Maryland, and Wisconsin in 1992 and 1993. Seven different mixes were designed for these projects with the Superpave system. Although the original gyrotory design specified an angle of gyration of  $1^\circ$ , a vertical pressure of 0.6 MPa (87 psi), and 30 rpm, problems were encountered on some SPS-9 mix designs. It became apparent that the  $1^\circ$  angle of gyration provided insufficient compaction effort to provide for the air voids required at  $N_{\text{design}}$ .

Figures 2.35, 2.36, and 2.37 illustrate a significant difference in compaction for different angles of gyration used on the Arizona SPS-9 mix. Similar findings were shown with other SPS-9 mix designs as well. At  $N_{\text{design}}$  equal to 113 gyrations, a significant difference in percent of maximum density is illustrated between an angle of gyration of  $1.27^\circ$  and of  $0.97^\circ$ . Table 2.23 shows the change in percent maximum theoretical density based on 113 and 230 gyrations at the two different angles of gyrations.

This difference is due to the amount of compactive effort imparted to the specimen. This difference in compactive effort affects both the air void contents and the design asphalt contents.

Based on the seven SPS-9 mix designs SHRP selected a fixed angle of gyration of  $1.27^\circ$ , a vertical pressure of 0.6 MPa (87 psi), and 30 revolutions per minute. All the SPS-9 mixes were designed using an angle of  $1.27^\circ$  which provided an air void content at 4 percent for a  $N_{\text{design}}$  of 113 revolutions. The design asphalt content was selected based on these criteria.

## 2.6. Comparison of Experimental Results with Technical Criteria

All the compaction methods examined in the referenced studies yielded mixes that differed substantially in measured engineering properties, all other factors being equal. Lytton et al. (1993), however, indicate that the particular creep test employed was relatively insensitive to the compaction method.

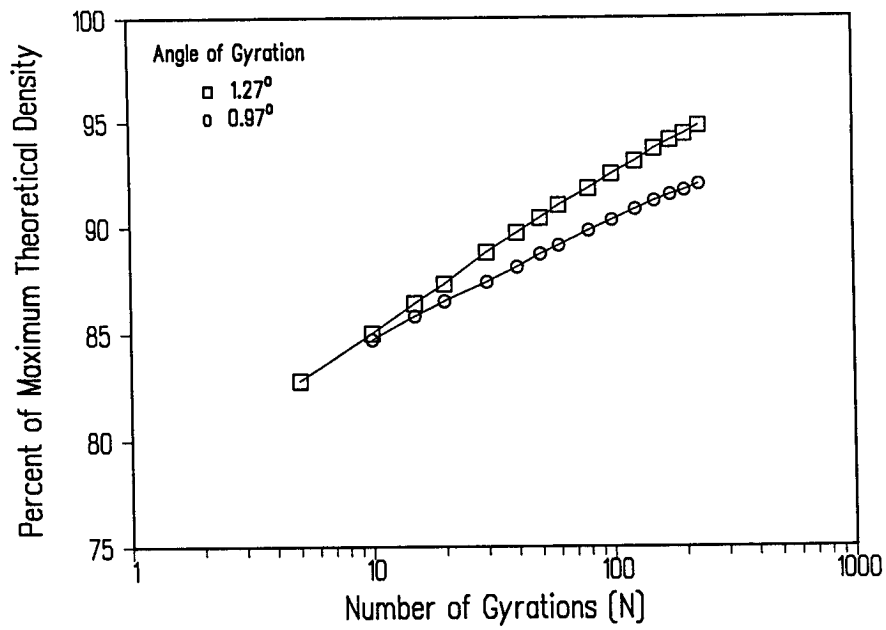


**Figure 2.35. Densification curve for Arizona SPS-9—blend 1**

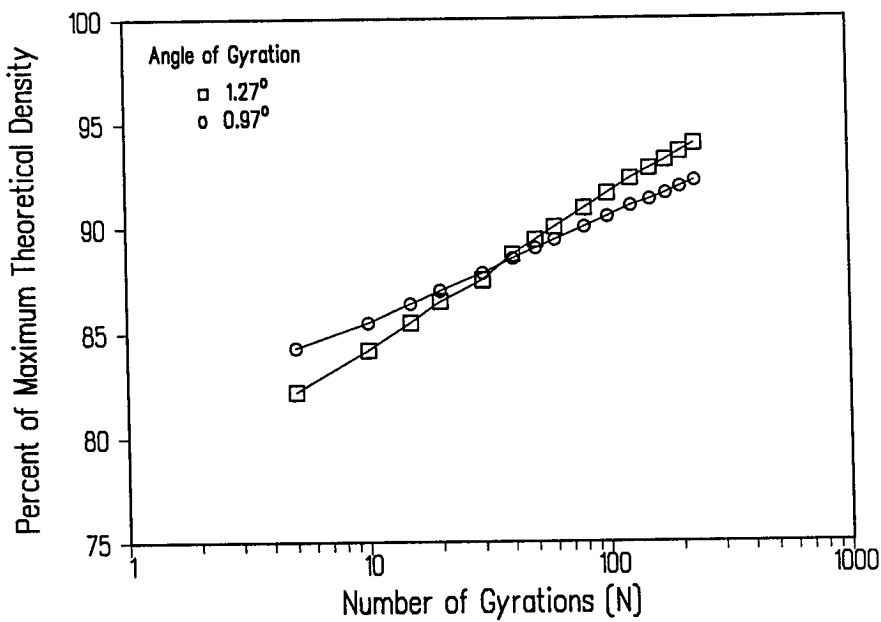


**Figure 2.36. Densification curve for Arizona SPS-9—blend 2**

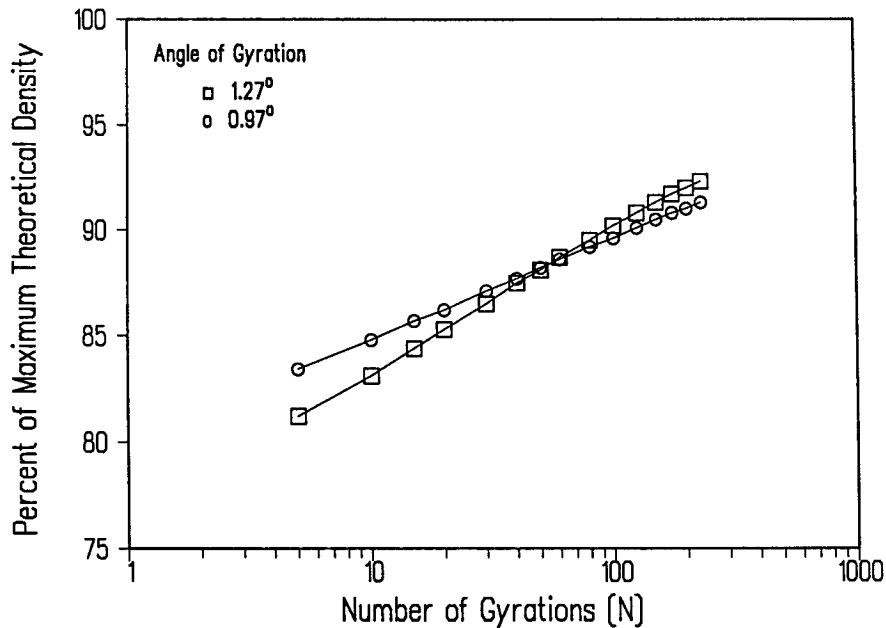


**Figure 2.37. Densification curve for Arizona SPS-9—blend 3**

**Table 2.23. Density as a function of angle of gyration**

Blend Type	Asphalt Content (%)	Number of Gyration			
		C113		C230	
		Angle of Gyration		Angle of Gyration	
		0.97	1.27	0.97	1.27
Percent of Maximum Density					
AZ1	4.2	90.6	92.8	92.2	95.1
AZ2	4.1	90.8	92.0	92.3	94.2
AZ3	4.2	89.9	90.5	91.4	92.6

The data presented by Von Quintus et al. (1991), Lytton et al. (1993) and, to a limited extent, Sousa et al. (1991) establish that the SHRP gyratory (shear) compactor is capable of producing laboratory specimens whose volumetric and engineering properties adequately simulate those of field specimens from a wide variety of pavements.

The results suggest that the steel drum-type rolling wheel compactor may also be an acceptable device for achieving adequate field simulation. Use of the Exxon or LCPC-type, rubber-tired rolling wheel compactor is problematic because of its inability to achieve target

air voids contents (Lytton et al. 1993). The kneading compactor appears to yield more robust laboratory mixes than are obtained from field compaction.

The steel rolling wheel compactor used in the Sousa et al. (1991) study is less suited to field use because it is large and produces heavy slab specimens from which cores must be cut for testing. It is also a labor-intensive piece of apparatus. Several smaller compactors of this type are in use in the United States and Europe that may be more satisfactory as field units, but they were not evaluated in any of the referenced studies.

The SHRP gyratory compactor is a compact, transportable device suitable for use in field laboratories or trailers. In addition, this compactor may be employed as a field control device to monitor how well the as-produced hot mix asphalt conforms to the mix design requirements.

On the basis of the technical criteria, gyratory compaction, specifically in the form of the Texas gyratory compactor, is a clear-cut choice for the SHRP mix design and analysis system, with rolling steel-wheel compaction a close second.

Consideration of operational and financial criteria provide further support for this choice. A gyratory compactor of the "Texas" type is compact, transportable and inexpensive (~\$25,000). One technician can produce finished cylindrical specimens up to 8 inches in diameter in about 30 minutes. It is suitable for both central and field laboratory use. It can be employed both for the design process and field control. Moreover, this type of compactor is amenable for further upgrading.

# 3

## Mix Conditioning Procedures in the Superpave System

This chapter is devoted exclusively to a discussion of the distress-related factors of aging and moisture sensitivity: specifically, the recommended mix conditioning procedures and their validation. A comprehensive review of the entire research effort addressing aging and moisture sensitivity may be found in Bell 1989; Bell et al. 1994; Bell, Wieder, and Fellin 1994; Scholz et al. 1994; Terrel and al-Swailmi 1994; and allen and Terrel 1994.

### 3.1 Aging

Two major effects dominate the aging of asphalt-aggregate mixes: loss of volatile components and oxidation in the construction phase (short-term aging); and progressive oxidation of the in-place mix in the field (long-term aging). Aging results in hardening or stiffening of the mix, altering its performance. This may be beneficial since a stiffer mix will have improved load distribution properties and thus be more resistant to permanent deformation. This hardening, however, makes the mix more susceptible to cracking, ravelling and loss of durability in terms of wear resistance. Although factors such as molecular structuring and actinic light may also affect the aging process, the development of laboratory methods to simulate aging has focused on reproducing the two dominant effects: volatilization and oxidation.

The discussion which follows is based upon research undertaken as part of the A-003A subcontract to Oregon State University which addressed three tasks: 1) aging test/conditioning procedure development, 2) validation of binder properties, and 3) field validation (Bell 1989, Bell et al. 1994, Bell, Wieder, and Fellin, 1994). The following is an overview of the research and a summary of the findings which led to the recommended aging procedure(s) for inclusion in the Superpave mix design and analysis system.

### ***3.1.1 Experimental Design***

Methods of simulating short-term aging on loose mix included oven aging and extended mixing. Methods of simulating long-term aging (LTOA) on compacted specimens included oven aging and oxygen enrichment. As part of the test development and validation effort, as many as 32 mix combinations (8 asphalts and 4 aggregates) were evaluated. Data from at least 16 field sites were also an integral part of the data set. The effects of aging were evaluated by resilient modulus at 25°C (75°F) using both the diametral and triaxial compression modes of testing (ASTM D 4123 and D 3497, respectively.) In all cases, the resilient modulus ratio ( $M_R$ ) (ratio of resilient modulus after aging to the resilient modulus before aging) was the variable used to indicate the degree of aging.

#### **Short-Term Aging**

To simulate the aging which occurs during plant mixing and compaction, the loose mix was held in a forced-draft oven for as long as 15 hours at temperatures of 135°C (275°F) and 163°C (325°F). The aged mix was then compacted to target void contents of 4 or 8 percent.

The extended mixing program used a modified rolling thin film oven test (RTFOT). A loose mix was prepared using the standard mixing procedure, compacted immediately, or subjected to 10, 120, or 360 minutes of additional mixing at either 135°C (275°F) or 163°C (325°F). The aged mix was then compacted to target void contents of 4 or 8 percent.

#### **Long-Term Aging**

In the long-term oven aging (LTOA) procedure, compacted specimens were held in a forced-draft oven at temperatures ranging from 85°C (185°F) to 107°C (225°F) for 1 to 8 days. The "before aging" and "after aging" characteristics were then determined.

The pressure oxidation vessel (POV) used both oxygen and compressed air. The compacted samples were conditioned at temperatures ranging from 25°C (77°F) to 85°C (185°F) for 1 to 8 days. As with the other aging methods, tests were conducted on both unaged and aged samples.

In the triaxial cell aging approach, oxygen or air was passed through a compacted sample and the resilient modulus determined at various times during the conditioning process. A flow rate of 1.2 m<sup>3</sup>/hr (4 ft<sup>3</sup>/hr) was used, which required a pressure of 345 kPa (50 lb/in<sup>2</sup>). Modulus testing was conducted at temperatures of 25° and 60°C (77° and 140°F).

### 3.1.2 Discussion of Results

#### Results—Aging Test/Procedure Development

Data from the short- and long-term oven aging (STOA and LTOA), as well as the extended mixing, generally indicate an increase in aging (as measured by  $M_R$  ratio) with time. Typical results are shown in Figures 3.1 to 3.4. It was observed, however, that extremes in either temperature or aging time often resulted in a decrease in modulus. In Figure 3.2 for example, samples aged for 15 hours at 163°C (325°F) produced a lower  $M_R$  ratio than did samples aged for 6 hours at the same temperature. The 15-hour aging time apparently hardens the binder film to such an extent that compaction to the specified void content is not achievable. The higher void content in these samples resulted in a lower  $M_R$  ratio. As shown in Figure 3.3, levels of  $M_R$  ratio similar to the short-term oven aging were observed with the extended mixing procedure. Operationally, however, the extended mixing procedure is impractical because of the necessity for several ovens or modification to the rolling thin film oven. The LTOA procedure is similar to the one recommended by Von Quintus et al. (1991). It is relatively simple and produces a considerable change in the mixes within a few days, as shown in Figure 3.4.

The use of oxygen in the pressure oxidation vessel produced unexpected results. As the temperature, pressure or aging time increased, the  $M_R$  ratio decreased, most likely due to sample disruption. Researchers concluded that further investigation of this approach, perhaps with a lower pressure and/or confinement, is warranted. Similar decreases in  $M_R$  ratio were observed in pressure oxidation tests with compressed air. Samples tested under the extreme condition (60°C [140°F] and 2069 kPa [300 lb/in<sup>2</sup>]) experienced the greatest deterioration.

Moderate increases in aging were observed in the triaxial aging method as indicated by an increasing  $M_R$  ratio. It appears that this method is the most viable for realistic long-term oxidative aging. It is also much safer than the pressure oxidation approach since the required pressure is significantly lower.

Based on the work conducted in the test development phase, the following conclusions were drawn and used as the foundation for subsequent research conducted in the validation phase:

- STOA and extended mixing procedures for loose mix can cause a four-fold increase in resilient modulus.
- Although extended mixing appears to produce more uniform aging than does oven aging, it may hinder productivity because of the necessity for several ovens.
- LTOA at 107°C (225°F), which causes a six-fold increase in  $M_R$  ratio, produces unrealistic aging of the specimen.
- The results from the pressure oxidation test program using either oxygen or compressed air show a general trend of decreasing modulus with increasing

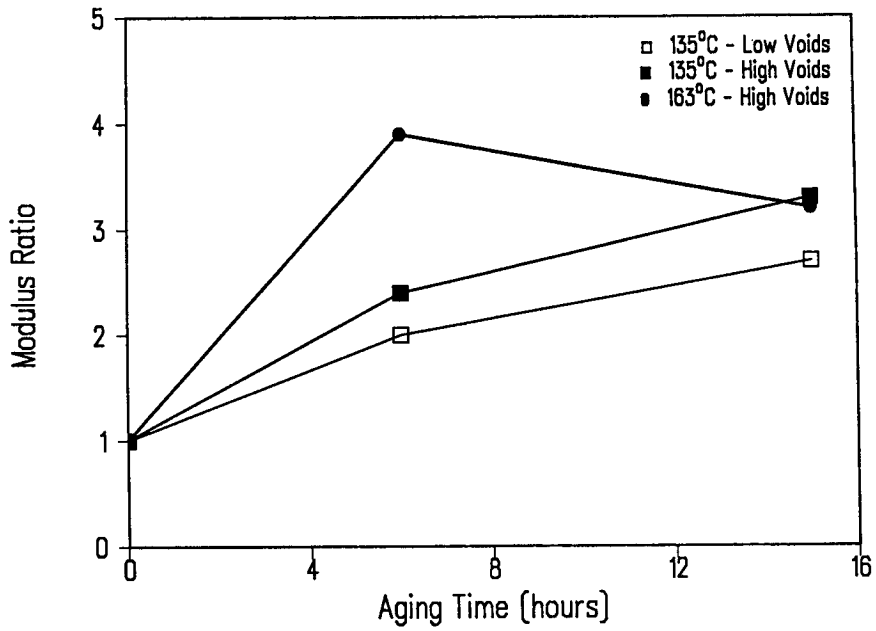


**Figure 3.1. Short-term oven aging (high voids)**

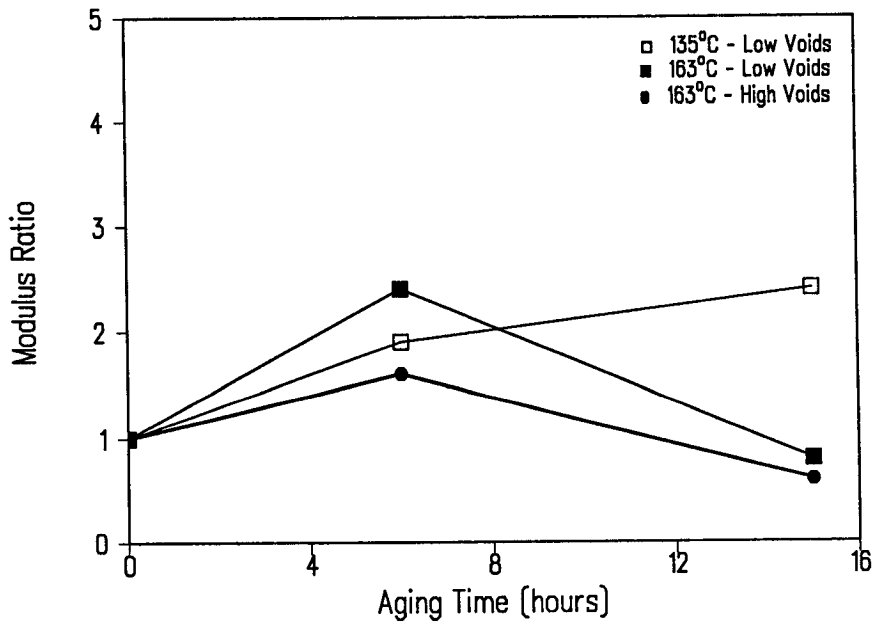


**Figure 3.2. Short-term oven aging (low voids)**



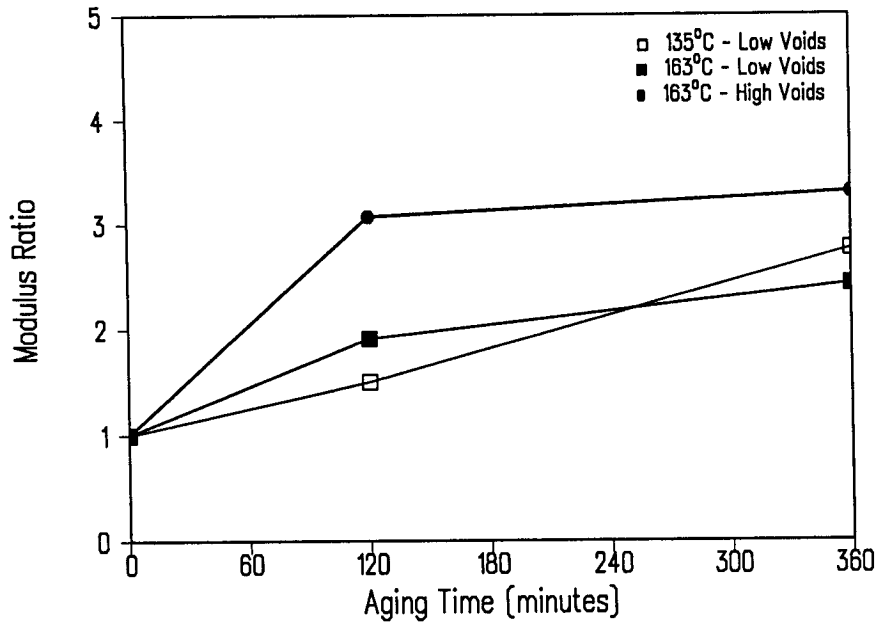


**Figure 3.3. Aging by extended mixing**

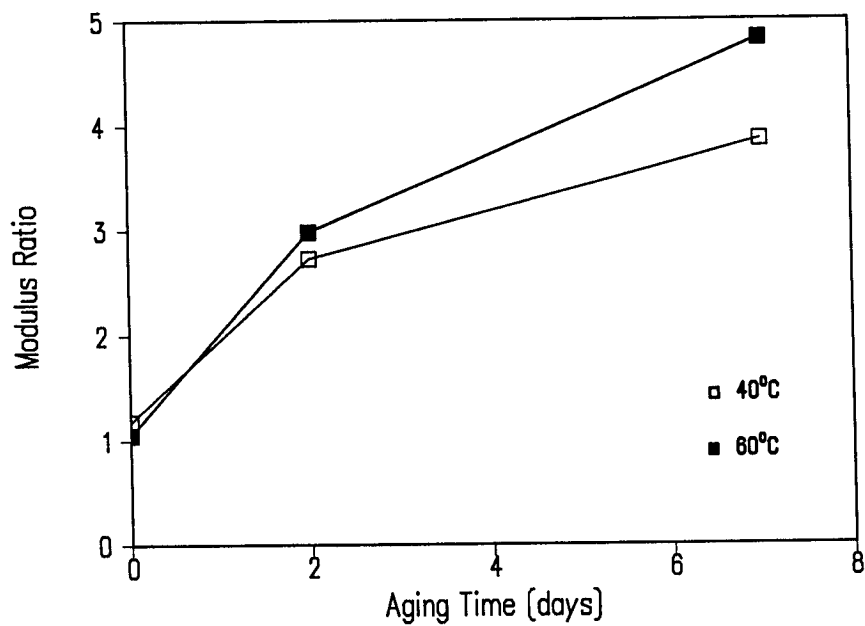


**Figure 3.4. Long-term oven aging (LTOA)**

severity of treatment (i.e., time, temperature, and pressure). This decrease in modulus is attributed to sample disruption when the pressure is relieved. It is hypothesized that the use of a lower pressure would produce the expected results.

- The triaxial cell aging, which increases modulus by 50 to 100 percent, is safer and probably the most realistic for long-term oxidative aging.

In view of the preceding, the aging procedures shown below were used in subsequent validation work.

- For short-term aging loose mix was held in a forced draft oven for 4 hours at 135°C (275°F).
- For long-term aging, both oven aging and low-pressure oxidation in a triaxial cell were advanced. For LTOA temperatures of 85°C (185°F) and 100°C (212°F) were used; for low pressure oxidation (LPO), 60°C (140°F) or 85°C (185°F). Compacted samples were age-conditioned from one to eight days.

## Results—Validation of Binder Properties

As indicated in the proposed binder specification, there is no direct provision for evaluating asphalt durability other than the effect of aging (short- or long-term) on binder properties to control fatigue, permanent deformation and thermal cracking. Fatigue and thermal cracking are controlled on binders that are long-term aged in the pressure aging vessel (PAV) while rutting is controlled on binders which are short-term aged using the Rolling Thin Film Oven Test (RTFOT).

The discussion herein presents the results of tests on 32 different mixes. The mixes were evaluated after both short- and long-term aging with the mix stiffness ratios compared to stiffness (viscosity) ratios of the binders, the intent being to determine whether binder tests alone are adequate to predict the durability of asphalt-aggregate mixes. All specimens used for the long-term aging experiment were first short-term aged at 135°C (275°F) for 4 hours before compaction. Four long-term aging procedures were examined: low-pressure oxidation at 60°C (140°F) and 85°C (185°F), LTOA at 85°C (185°F) for five days, and LTOA at 100°C (212°F) for two days.

As with the mix, binder data can be used to calculate an aging ratio based on the aged viscosity at 60°C (140°F) compared to the original viscosity at 60°C (140°F). The asphalts can be then ranked in order of aging susceptibility. Shown in Figure 3.5 are mix rankings based on short-term aging and the asphalt rankings based on thin film oven (TFO) aging. It should be noted that TFO aging is analogous to short-term mix aging. It is clear that there is little relationship between the mix rankings and the asphalt rankings. Figure 3.6 shows the rankings for mixes based on long-term aging by low pressure oxidation at 85°C (185°F), and

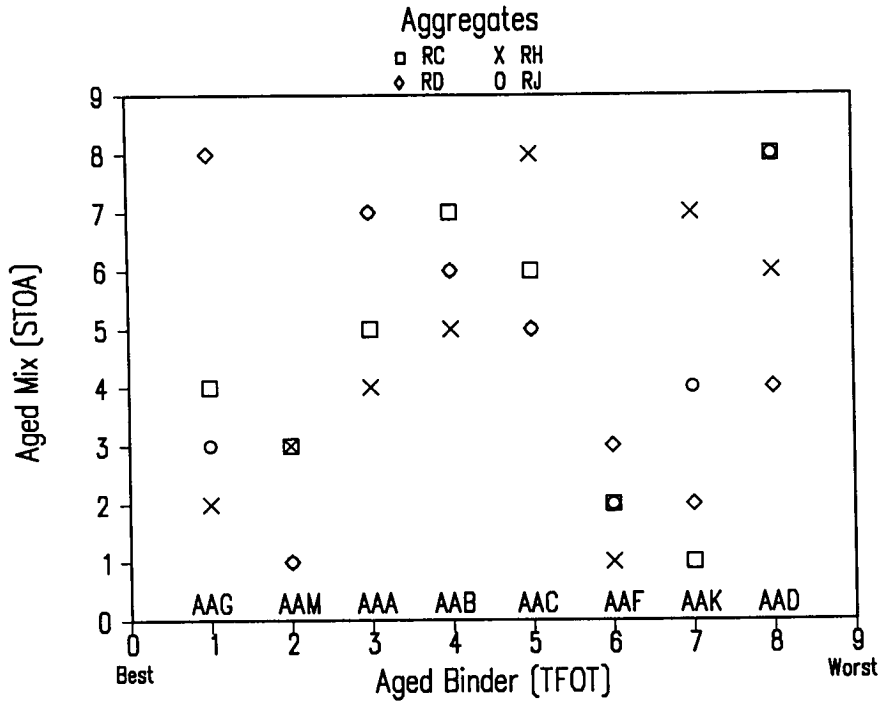


Figure 3.5. Comparison of short-term aging of binders and mixes

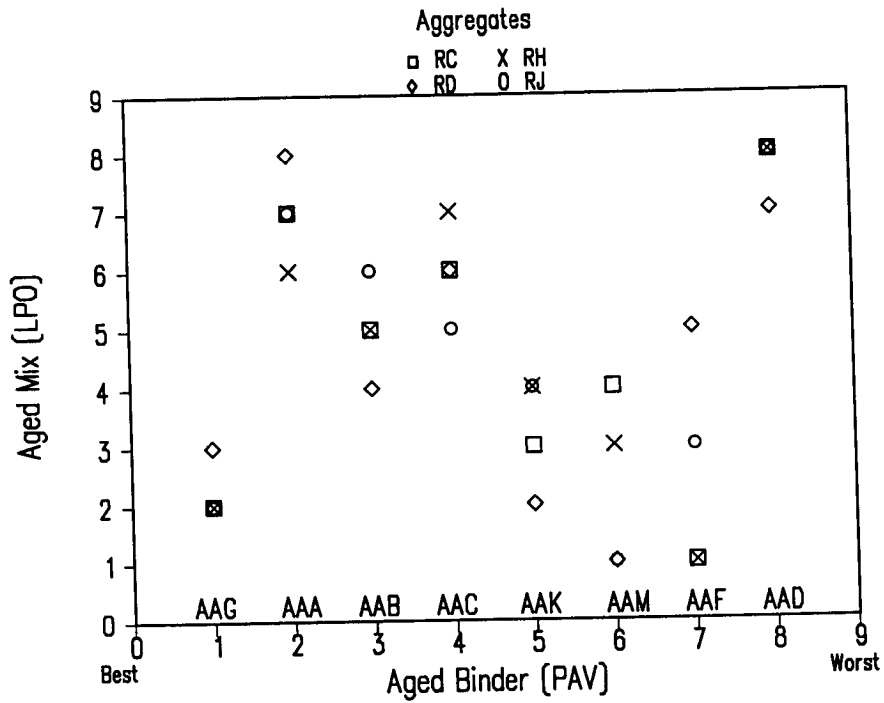


Figure 3.6. Comparison of long-term aging of binders and mixes

rankings for PAV-aged binders. As was the case for short-term aging, there is little similarity between the rankings for long-term aging of asphalt mixes and asphalt alone.

Clearly, the aging of the asphalt alone is not a reliable indicator of the degree to which a mix will age. The data presented underscore the need for mix conditioning testing to ensure a reliable measure of the aging susceptibility of the asphalt-aggregate mix. The difference in binder aging and mix aging is attributed to the chemical interaction between the aggregate and the asphalt.

Based on the preceding one may conclude that the aging of asphalt-aggregate mixes is influenced by both components of the mix: aging of the asphalt alone does not appear to be adequate to predict mix performance because of the apparent mitigating effect that the aggregate has on aging.

## Results—Field Validation

Following site selection and material collection, cores from the field sites were trimmed and analyzed to determine air void content. Whenever possible, asphalt content and aggregate gradation, as determined by extraction from prior studies, were retrieved for use in this effort. Laboratory specimens were prepared in accordance with field core gradations, asphalt content and air void level. The lab-compacted specimens were then subjected to the following aging treatments: STOA at 135°C (275°F) for 4 hours; LTOA at 85°C (185°F) for 2, 4, and 8 days; and LTOA at 100°C (212°F) for 1, 2, and 4 days. Modulus testing, in either the indirect tensile or triaxial mode, was then conducted on both field and lab compacted cores.

As illustrated in Figure 3.7 the modulus values measured on field cores are independent of pavement age. Of all treatments, the moduli of unaged, STOA and LTOA-1 (100°C [212°F]) showed the best correlation with field moduli (Figures 3.8, 3.9, and 3.10). Application of the student t-test to these three lab moduli indicate that the LTOA for one day (LTOA-1) (100°C [212°F]) is not statistically different from the field moduli, and hence, field aging. If the field modulus is normalized by dividing it by the modulus of corresponding unaged specimen, the field data show a reasonable correlation with pavement age, as evidenced by the  $R^2$  value of 0.64. (Normalizing the data in this fashion establishes a common baseline for all the specimens regardless of pavement age.) This suggests that time-in-service is the dominant factor affecting pavement aging. Compared to the passage of time, the mix parameters and environment are of minor importance in terms of the degree of aging.

Based on the regression equation shown in Figure 3.11, at a pavement age of zero months the modulus ratio is 1.25, suggesting that the aging which occurs as the result of plant mixing and construction is somewhat more severe than that which occurs as the result of lab mixing and compaction. Moreover, it takes approximately 6 to 6½ years of in-place aging to double the modulus ratio. Comparison of the unaged modulus with STOA and LTOA-1 (100°C [212°F]) moduli, shown in Figures 3.12 and 3.13, respectively, provides

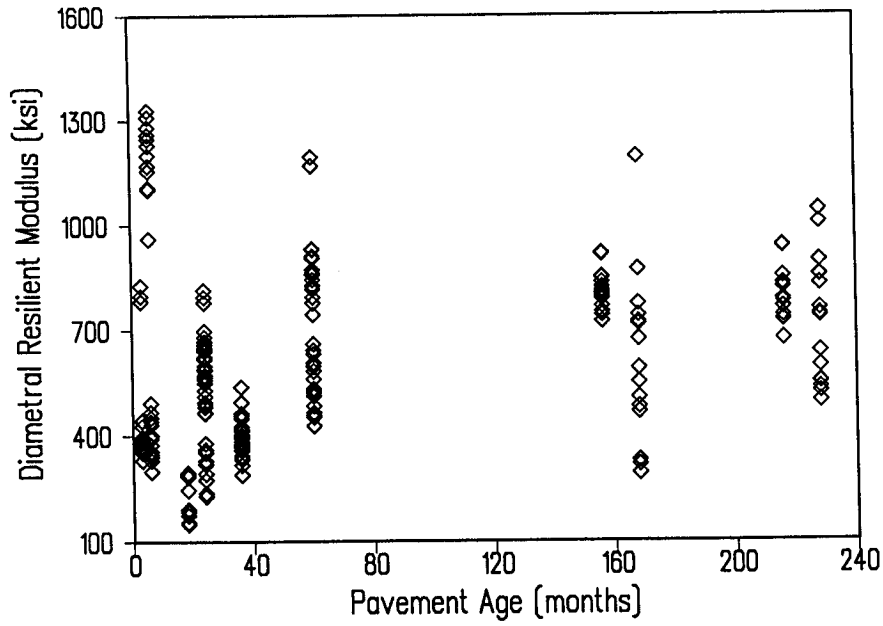


**Figure 3.7. Comparison of pavement age and resilient modulus**

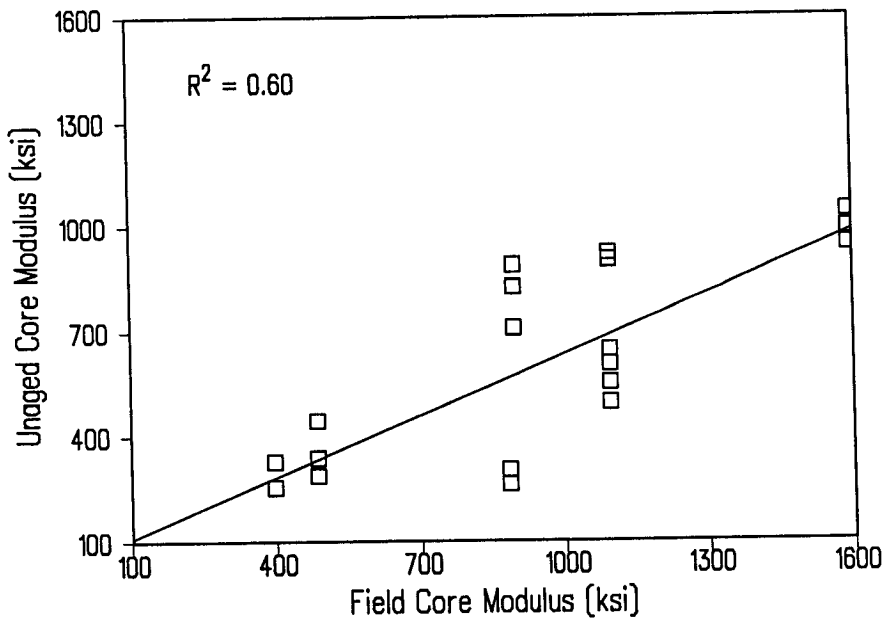


**Figure 3.8. Comparison of field core and unaged core moduli**

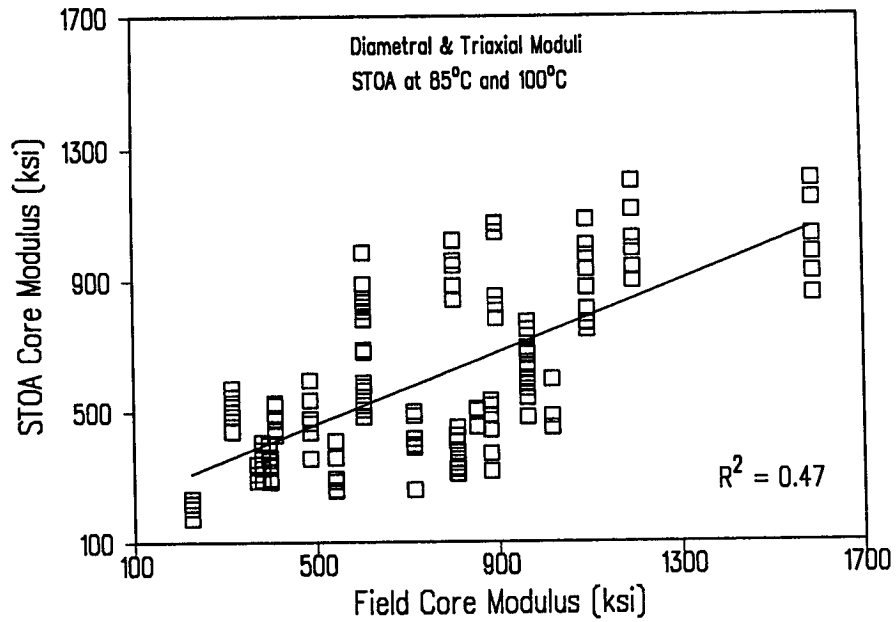


**Figure 3.9. Comparison of field core and short-term oven-aged core moduli**

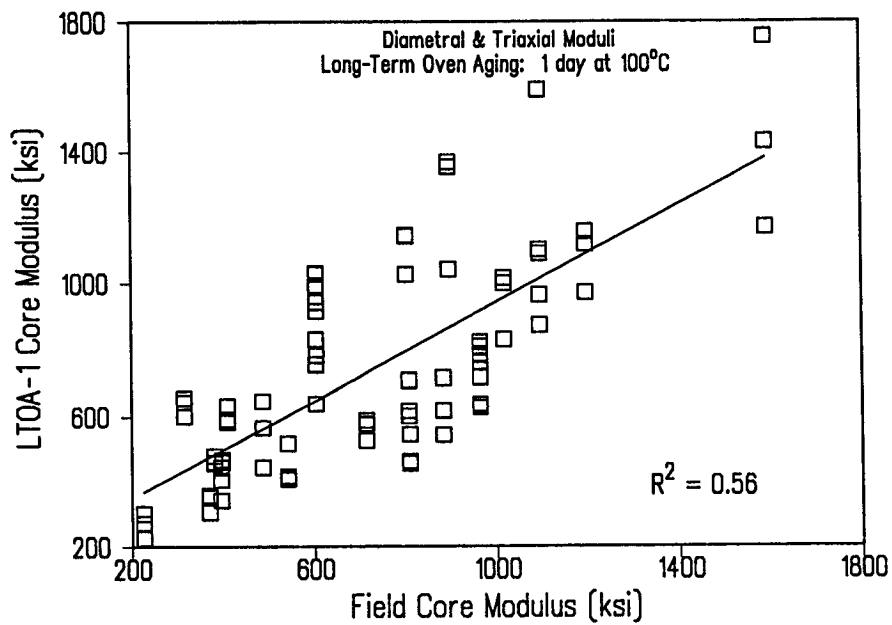


**Figure 3.10. Comparison of field core and long-term oven-aged core moduli**

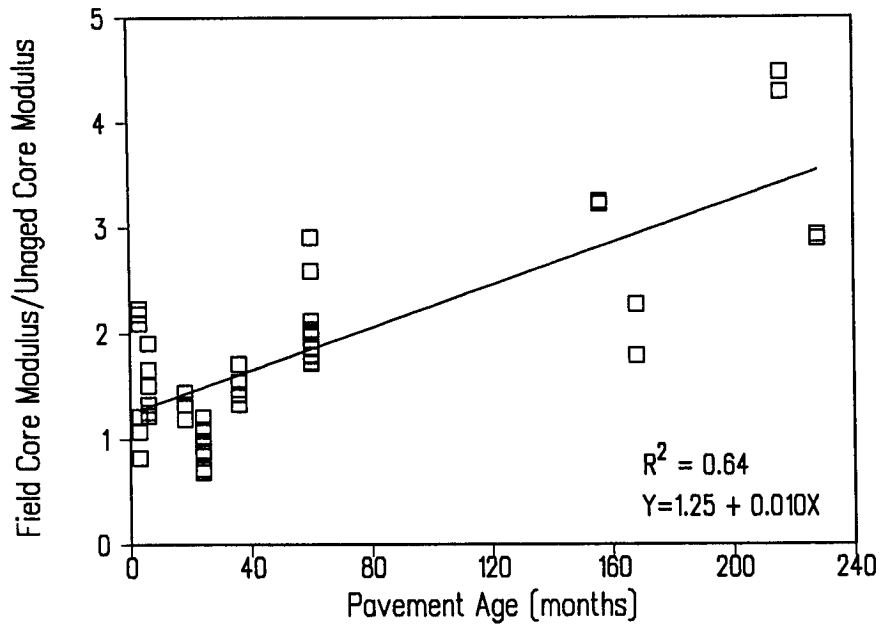


**Figure 3.11. Comparison of pavement age and resilient modulus ratio**

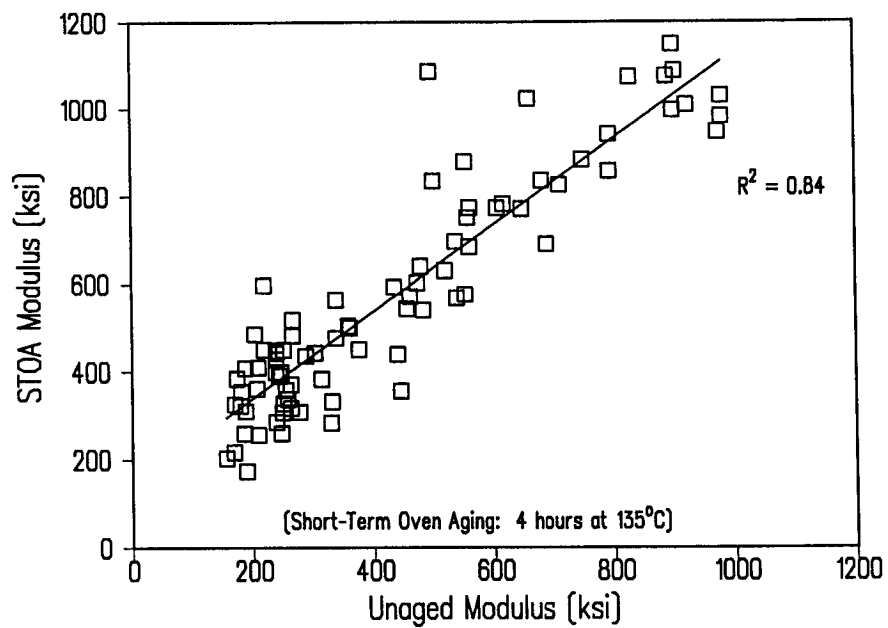


**Figure 3.12. Comparison of unaged and short-term oven-aged moduli**

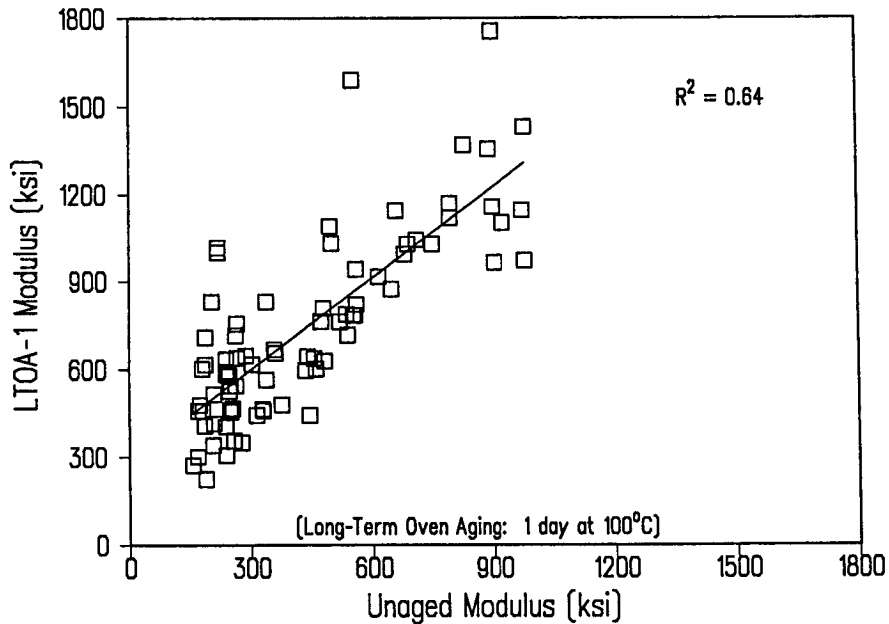


**Figure 3.13. Comparison of unaged and long-term oven-aged moduli**

additional support; i.e., that time is the primary factor determining the extent of aging observed in the lab and in the field. Using the lab aged-to-unaged moduli ratios from Figures 3.12 and 3.13 one can estimate the field aging equivalence of the STOA and LTOA-1 (100°C [212°F]) procedures to be about 4 and 6½ years, respectively.

### 3.1.3 Conclusions and Recommendations

Based on a comprehensive analysis of data drawn from three different but related tasks, it appears that field and laboratory aging is a predictable process that is largely time-dependent. In practical terms, material and mix parameters have only a minor influence on the aging process. Accordingly, within the practical limits of the Superpave mix design and analysis system, all mixes are expected to age to the same degree for any given aging procedure.

Laboratory mixing and compaction (the unaged condition) produces specimens aged comparably to those sampled in the field during pavement construction.

The STOA aging procedure is approximately equivalent to 4 years of service in the field; the LTOA-1 at 100°C (212°F), to approximately 6½ years.

The STOA procedure (4 hours at 135°C [275°F]) is recommended as the standard aging procedure for the Superpave system. The LTOA for one day at 100°C (212°F) is included in the Superpave system as an optional procedure in cases where long-term pavement performance is of particular interest (low temperature cracking and fatigue cracking).



With respect to the performance prediction models incorporated in the Superpave system, neither short- nor long-term aging is accounted for directly. The performance prediction models, however, were developed and calibrated based on data generated from the testing of field cores taken from pavements ranging in age from 5 to 25 years. As such, aging is considered indirectly. It should be clearly understood that the calibration coefficients for the permanent deformation model, like those for low temperature and fatigue cracking, are also based on testing aged and traffic-conditioned mixes from field cores. Accordingly, the user should note that the Superpave mix design system recommends testing short-term aged specimens. This is very likely to result in some error in the distress prediction, but will be conservative from the mix design perspective. The SPS-9 studies which require sampling and materials testing over a 14-year time frame should help to define the difference in calibration factors between short-term (laboratory) and long-term (field cores) aged mixes.

### **3.2 Moisture Sensitivity**

Although many factors contribute to the degradation of asphalt concrete pavements, moisture is a critical factor in the deterioration of asphalt mixes. There are two mechanisms by which moisture destroys the integrity of the asphalt concrete matrix: loss of cohesion or strength and stiffness; and failure of the adhesive bond between the aggregate and asphalt.

In the early stages of the research, the A-002A contractor suggested that asphalts might be ranked based on a ratio of size exclusion chromatography (SEC) fractions or carbonyl content (Branthaver et al., 1994). Subsequent work, however, led the A-002A contractor to conclude that predicting moisture damage susceptibility from the binder chemistry alone was not possible.

The A-003B contractor, charged with describing and defining asphalt-aggregate interactions, examined three specific areas: the specific chemistry of asphalt adsorption onto aggregate using model species that are representative of polar functional group types present in asphalts; compatibility of various asphalt-aggregate pairs and their respective sensitivity to water; and the effect that aggregates treated with saline compounds of differing chemistries have on asphalt-aggregate interactions and water sensitivity.

The A-003B researchers concluded that the adsorptive behavior of asphalt and asphalt model components on aggregates is highly specific and primarily affected by aggregate surface chemistry (Curtis et al.). Tests on aggregates pretreated with saline compounds led to the same conclusion. Evaluation of adsorption and aqueous desorption of asphalt model components on aggregates conclusively showed that polar compounds had different affinities for adsorption for different aggregates. The amount and ease by which the polar compounds were removed from the aggregate surface in the presence of water was found to be dependent on the aggregate chemistry as well as the pH and heat history of the particular system.

Net adsorption tests were used to investigate the compatibility and water sensitivity of asphalt-aggregate pairs and clearly showed that the adsorption behavior of asphalt on aggregate was controlled by aggregate chemistry. The A-003B researchers found substantial

differences in adsorption and aqueous desorption behavior among aggregates, but only small, insignificant differences among asphalts. The differences in adsorption and desorption behavior of a particular asphalt, when combined with various aggregates, were far greater than that of a particular aggregate when combined with various asphalts.

Because there are no hypotheses concerning the influence of binder chemistry on moisture damage, the discussion herein is intended to provide an overview of the *development* and *validation* of the laboratory test(s) recommended for use in evaluating the moisture susceptibility of asphalt-aggregate mixes. Results from the limited net adsorption testing are also addressed. A comprehensive discussion of the development and validation efforts may be found in Terrel and Al-Swailmi (1994) and Allen and Terrel (1994).

### 3.2.1 Hypothesis

The effect of water on asphalt concrete mixes has been difficult to assess because of the numerous variables involved, particularly the air voids in the mix. The very existence of these voids as well as their characteristics can play a major role in performance. In the lab, mixes typically are designed at 4 percent total voids, but in the field may be compacted to 8 to 10 percent voids. Accordingly, the test development work was based on the following hypothesis: current mix design methods and construction practice may be a major cause of moisture-related damage. A major effect of air voids is illustrated in Figure 3.14. The curve in Figure 3.14 suggests that the worst behavior in the presence of water occurs in the range where most conventional mixes are compacted. Thus, the term "pessimum voids" is used to describe a void system that is the opposite of optimum.

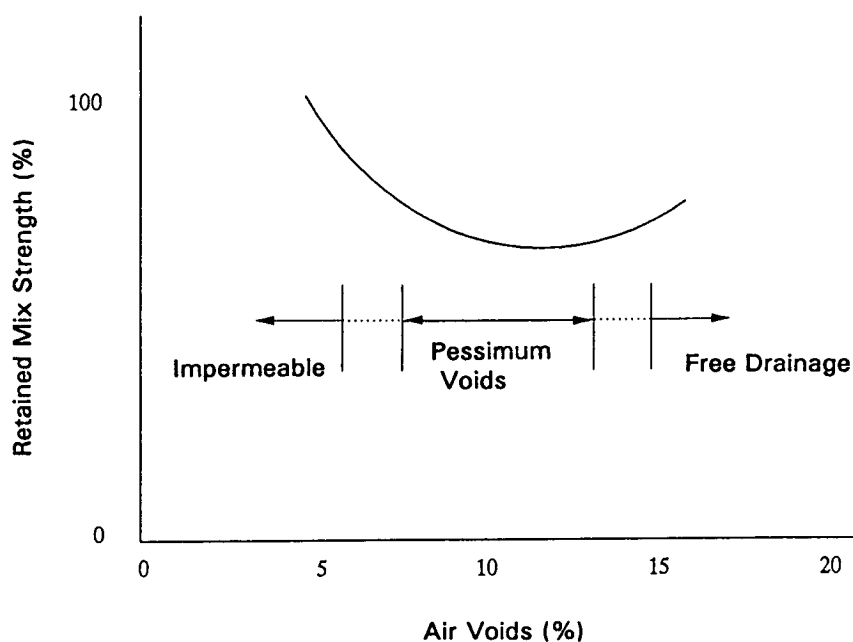


**Figure 3.14. Air void distribution in compacted mix**

### *3.2.2 Experimental Design*

The development of tests to determine the water sensitivity of asphalt concrete mixes began in the 1930s. Since that time, interest in the effect of moisture sensitivity on pavement performance has increased as evidenced by the proliferation of tests used to evaluate the stripping potential of asphalt-aggregate combinations. Traditionally, test procedures have attempted to simulate the strength loss that occurs in the pavement so that mixes which are likely to suffer premature distress as a result of the presence of some form of moisture can be identified prior to construction.

Typical water sensitivity tests include both a conditioning and an evaluation phase. The severity of the conditioning phases may vary, but all attempt to simulate the performance of the mix in the field in the presence of water. The two general methods of evaluating conditioned specimens are visual evaluation and/or subjecting the specimen to some form of strength test. The twofold objective of this research was to develop: 1) a lab conditioning procedure to be used for water sensitivity evaluation during the design process; and 2) for conditioning prior to testing in other modes such as fatigue, rutting, aging and thermal cracking. In developing a laboratory testing/conditioning technique to test the "pessimum voids" hypothesis and evaluate the variables shown in Table 3.1, testing was conducted in the environmental conditioning system (ECS). The ECS was used to develop a test procedure that includes water conditioning and temperature cycling to reproduce field conditions and continuous repeated loading during the conditioning cycles to simulate traffic. A detailed description of the three ECS subsystems (fluid and environmental conditioning and loading) may be found in Terrel et al. (1994). AASHTO T 283 was selected as a bench mark and conducted on many of the same asphalt-aggregate combinations for comparative purposes. To determine the ECS' ability to discriminate among different performance levels, test results were also compared to wheel tracking data and field core specimens.

The ECS experiments included 36 mixes with various combinations of 8 asphalts and 6 aggregates. After core compaction (10 cm (4 in.) in diameter by 10 cm (4 in.) in height) volumetric properties and permeability of the specimen are determined. The specimen is instrumented using linearly variable differential transducers (LVDT) and then mounted in the loading frame for an initial measurement of resilient modulus. The loading frame and specimen are placed in the environmental chamber and connected to the fluid conditioning subsystem. The specimen is then wetted to a near-saturated condition by pulling water through it for 30 minutes. The conditioning procedure includes a series of hot and cold cycles depending on the climatic regime expected in the field. The conditioning procedure for a warm climate includes three wet-hot cycles of 6 hours duration at 60°C (140°F) with continuous repeated loading. The conditioning procedure for a cold climate includes the same procedure for the hot climate plus one freeze cycle at -18°C (-37°F), with no repeated loading during the freeze cycle. Table 3.2 outlines the conditioning information for the hot and cold climates. At the end of each conditioning cycle and after a 2-hour cooling/thawing period to attain a temperature of 25°C (77°F), the  $M_R$  and permeability tests are conducted. Retained  $M_R$  is calculated for each cycle as a ratio of  $M_R$  after conditioning to the original (dry)  $M_R$ . At the conclusion of each conditioning procedure, the  $M_R$  and permeability ratios are determined to show the change with time.

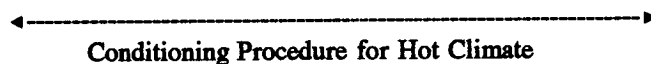
**Table 3.1. Factors considered in the water sensitivity experiment plan**

Variable	Factor
Existing Condition	<ul style="list-style-type: none"> <li>• Compaction</li> <li>• Voids</li> <li>• Permeability</li> <li>• Environmental</li> <li>• Time</li> <li>• Water content</li> </ul>
Materials	<ul style="list-style-type: none"> <li>• Asphalt</li> <li>• Aggregate</li> </ul>
Conditioning	<ul style="list-style-type: none"> <li>• Dry versus wet</li> <li>• Vacuum saturation</li> <li>• Temperature Cycling</li> <li>• Repeated loading</li> <li>• Drying</li> </ul>

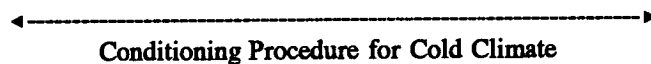
**Table 3.2. Conditioning information chart for warm and cold climates**

Conditioning Factor	Conditioning Stage				
	Wetting*	Cycle-1	Cycle-2	Cycle-3	Cycle-4
Vacuum Level (in of Hg)	20	10	10	10	10
Repeated Loading	No	Yes	Yes	Yes	Yes
Ambient Temp (°C)**	25	60	60	60	-18
Duration	0.5	6	6	6	6

\*Wetting: Wetting the Specimen Prior to Conditioning Cycles



\*\*Inside the Environmental Cabinet



### 3.2.3 Discussion of Results

#### Results—ECS Test Development

Typical results are shown in Figures 3.15 to 3.17. As illustrated in Figures 3.15 and 3.16, the primary component affecting the ECS  $M_R$  ratio is the aggregate. Note that the differences in  $M_R$  ratio are much greater for 1 asphalt tested with 4 aggregates (Figure 3.15)

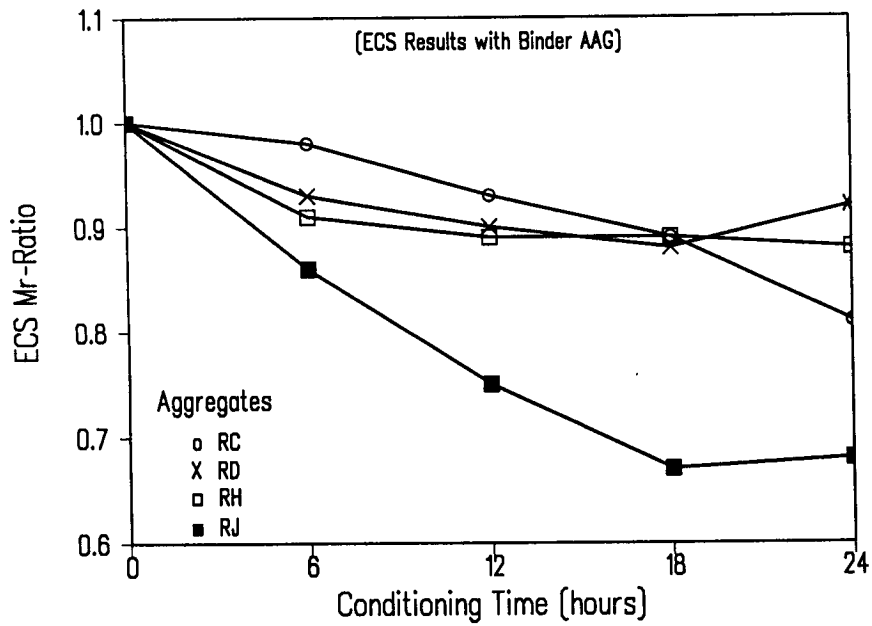


**Figure 3.15. Environmental Conditioning System test results with binder AAG**

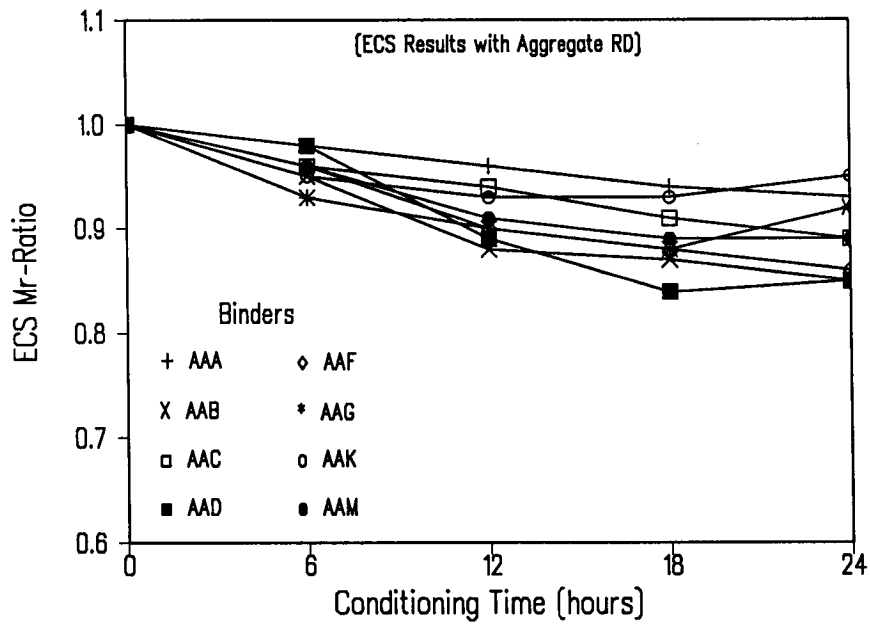


**Figure 3.16. Environmental Conditioning System test results with aggregate RD**

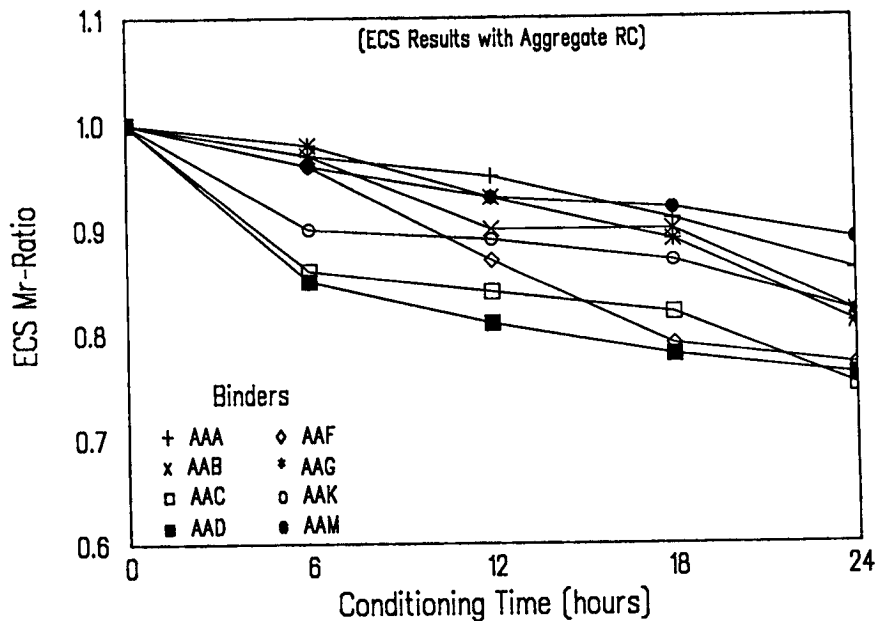


**Figure 3.17. Environmental Conditioning system test results with aggregate RC**

than 1 aggregate tested with 8 asphalts (Figure 3.16). Figure 3.17 shows that after one cycle of ECS conditioning the different asphalts form two groups. Three asphalts (AAK, AAD, and AAC) are at or below an  $M_R$  ratio of 0.9 and susceptible to moisture damage. Furthermore they continue to lose strength with each cycle. Other asphalts that were not markedly affected in the first cycle tend to gradually lose strength with each cycle.

After the first cycle, mixes that have good cohesion properties tend not to be affected by ECS conditioning, while mixes susceptible to cohesion loss tend to lose substantial strength after the first cycle. The A-003A researchers hypothesize that the loss in cohesion may be caused by several factors. Some asphalts absorb water, thus reducing the viscosity. After the refining process some asphalts may contain salt which dissolves in hot water. Asphalt mixes may absorb water into the aggregate pore structure, as well as the voids in the mix, and at the asphalt-aggregate interface. Those mixes that are susceptible to cohesion loss typically do not show a loss of strength (stiffness) until after the first cycle because it takes at least one conditioning cycle to activate the detrimental forces; i.e., wetting of the mix under vacuum; hot rather than cold water; and repeated loading to force water into the voids. These factors tend to accelerate the change in stiffness, if it is going to occur. Water absorption at room temperature for only a short period prior to temperature cycling and without repeated loading is not severe enough to activate these mechanisms.

Mixes susceptible to moisture damage through the loss of adhesion are typically not evident until the second and third warm cycles. Some adhesion loss probably does occur during each cycle, but may not accumulate enough to be observed until after three or more cycles. In the SHRP research the specimens were not broken open for visual examination until after the

third or fourth cycles, so the extent of stripping after one or two cycles was not observed. If specimens had been broken open following each succeeding cycle, the number of specimens required would have at least quadrupled. This was deemed economically impractical for this experiment. It was also observed in the ECS testing that aggregates of marginal quality or that are highly absorptive may tend to disintegrate in the fourth (freeze) cycle, another moisture damage phenomenon.

As noted above, a modified version of AASHTO T 283 (Modified Lottman) was used in this study for predicting water damage as a basis for comparison to the ECS. More than 100 specimens were prepared and tested for resilient modulus,  $M_R$ . For each test, six specimens were divided into two sets (dry and conditioned). Shown in Figure 3.18 is a summary comparison of the AASHTO T 283 and ECS test results. It is clear that for the mixes tested in this study, there is much greater variability associated with the AASHTO T 283 data. Specifically, the coefficient of variation (CV) for the AASHTO T 283 testing varied between 11 and 39 percent, whereas the CV for the ECS testing did not exceed 10 percent. It should be noted, however, that the AASHTO T 283 and ECS rankings of the asphalt-aggregate combinations were identical. The major difference between the two techniques, in terms of the number of specimens required, is that six specimens are needed to obtain one  $M_R$  ratio in the AASHTO procedure. Using the ECS procedure, three  $M_R$  ratios are obtained by testing a single specimen (four if the freeze cycle is included). It should be noted, however, that other laboratory investigations have yielded more consistent results with AASHTO T 283 when retained tensile strength is used to determine variability (Maupin, 1991). Specifically, a study undertaken by the Virginia Transportation Research Council, measured a within lab CV of 3.5 percent and between lab CV of 6.1 percent. An earlier report by the FHWA (Stewart, 1986) compared six laboratory procedures commonly used to assess moisture susceptibility of asphalt mixes. Included in this experiment was that described in the NCHRP Report 246, often referred to as the Lottman procedure (Lottman, 1982). A total of 16 mixes with known field performance were evaluated. According to the author the most effective procedures were those described in NCHRP Reports 274 (Tunnicliff et al., 1984) and 246 (Lottman, 1982). For the latter however, it was noted that the short-term conditioning procedure was *not* useful for predicting pavement performance. Furthermore, Lottman concluded that with respect to the NCHRP 246 long-term conditioning, the  $M_R$  was more effective for predicting performance than was the tensile strength. The report did not include any data on test variability. Based on the conflicting data presented herein, it is clear that the variability and effectiveness of the test procedures depend on the criterion selected to evaluate moisture susceptibility of asphalt mixes.

In addition to the original comparison testing described in the preceding paragraph, five additional mixes were evaluated in accordance with AASHTO T 283 and the ECS to extend the database. As shown in Figure 3.19 the  $M_R$  as determined from the ECS test was typically greater than the tensile strength ratio determined from AASHTO T 283. Using the recommended minimum tensile strength ratio (TSR) of 0.80, the data would lead one to conclude that all of the mixes would be susceptible to moisture damage. The minimum  $M_R$  ratio of 0.70 recommended by the A-003A researchers (Terrel et al., 1994) indicates that only mixes A and C are likely to have water damage problems. In fact, field performance data have shown that mixes A, B, and C tend to strip unless treated with some type of antistripping agent. When the test data are normalized for void content however (Figure 3.20), the correlation between the two tests is quite good, suggesting that the results are comparable. The fact that all the mixes fail according to the AASHTO T 283 minimum TSR

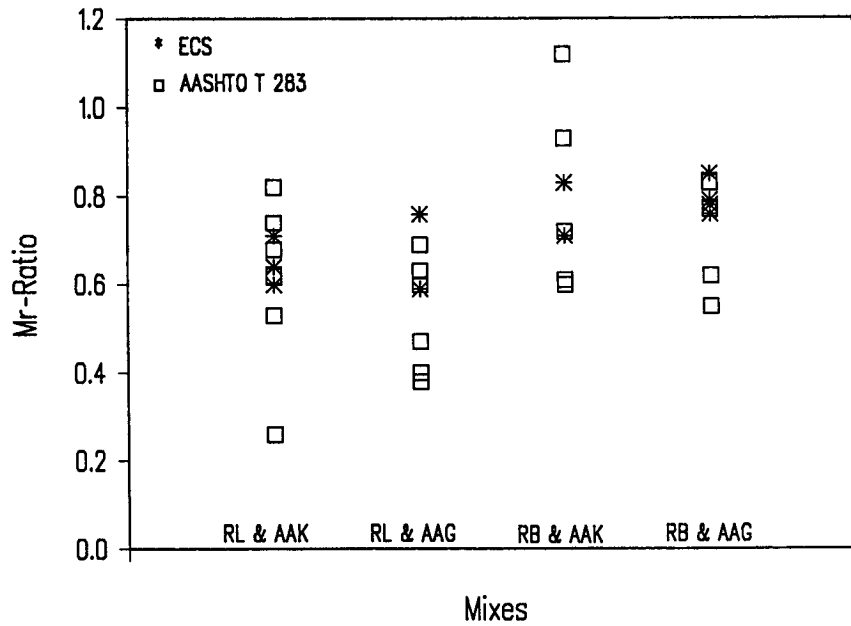


**Figure 3.18. Comparison of AASHTO T 283 and Environmental Conditioning System results for resilient modulus ratio**

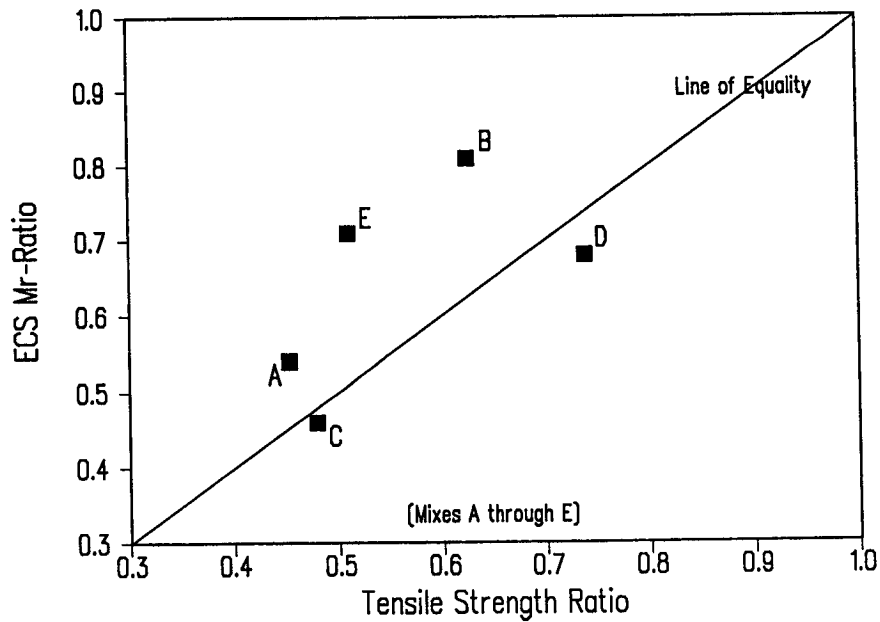


**Figure 3.19. Comparison of AASHTO T 283 and Environmental Conditioning System results for tensile strength and resilient modulus ratios**



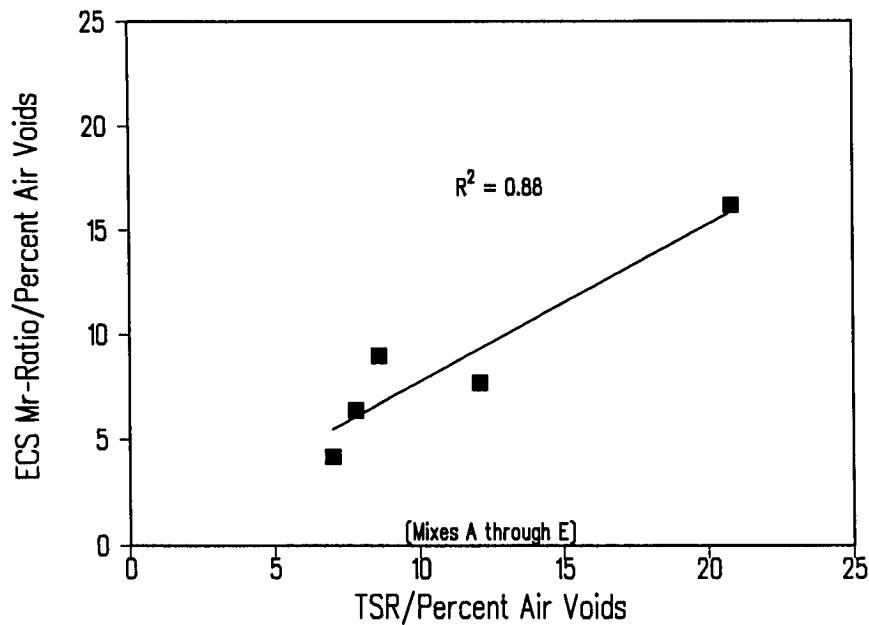


**Figure 3.20. Comparison of AASHTO T 283 and Environmental Conditioning System results normalized for percent air voids**

of 0.80 underscores the need to reevaluate the severity of the test parameters and/or the failure criterion. Furthermore, the fact that the ECS test results ( $M_R$  ratio  $\geq 0.70$ ) agreed with the known performance data in three of the five mixes indicates its potential to identify asphalt-aggregate combinations that are susceptible to moisture damage.

The significant difference between AASHTO T 283 test results in terms of repeatability confirms the importance of simulating the mechanisms of asphalt-aggregate interaction in the presence of water in improving the repeatability of the test. Furthermore, ECS test results show that using one conditioning and testing device to conduct all the tests with the same setup and one specimen orientation decreases the variability of the test results and reduces the error associated with specimen handling. Although there are distinct advantages of the ECS over AASHTO T 283 (measurement of permeability; evaluation of specimens at any void content; and application of repeated loads throughout test duration), at this time the response parameters that are generally used as a measure of moisture sensitivity ( $M_R$  or tensile strength) are the same for both tests, and, when ECS and AASHTO T 283 results are normalized for void content, the results are comparable.

### Results—ECS Field Validation

The purpose of this task was to demonstrate that the ECS test results could discriminate among asphalt concrete mixes based on their performance in full-scale field test sections. Additionally, correlation among the performance of the mixes in several wheel tracking devices and field sections was also a consideration. The validation effort described herein

differs from research associated with the test development phase in that all the mixes evaluated in this task were designed by the local authority in whose jurisdiction the field section was placed. Mix designs in the test development phase were developed by the A-003A contractor (Allen et al., 1994).

Twelve field sites were selected for the field validation effort, including at least two from each of the four SHRP-defined environmental zones. In addition to the original materials and cores from each field site, environmental conditions (temperature and precipitation), traffic loading, and pavement age and condition were used to characterize the test section. The testing program included specimens compacted in the lab by the A-003A contractor and field cores provided by the cooperating agencies. In each testing program the specimens were subjected to water damage followed by measurement of rutting (wheel tracking devices), reduction in modulus (ECS) and visual evaluation of the degree of stripping. The performance parameters, rutting and ratio of conditioned to unconditioned modulus, were used to develop correlations between test procedures. Shown in Figure 3.21 is the relationship between the ECS  $M_R$  ratio and rut depth measured in both the Oregon State University (LCPC) and Elf wheel tracking devices. Three mixes were deleted from the data analysis: one had air voids 200 percent greater than all the other specimens tested; another because it was an open-graded mix; and the third because the data came from only one specimen. As illustrated by Figure 3.21 there is excellent correlation between the ECS  $M_R$ -ratio and the rut depth measured on identical mixes. As seen from the field data shown in Figure 3.22, a final modulus ratio of 0.7 appears to separate mixes which performed well in the ECS, wheel tracking devices and the field from those which performed poorly.

The work performed during the field validation of the ECS test procedure is considered as an initial database of information correlating the performance of field mixes with the ECS and wheel tracking data. The results are very encouraging, as shown in Figures 3.21 and 3.22, but because of the limited amount of materials available and the relatively "young" age of the field sections considered, additional time and testing are needed to better define the role of the ECS in mix design and analysis.

## Results—Net Adsorption Test

As noted in section 3.2, net adsorption tests were used to investigate the compatibility and water sensitivity of asphalt-aggregate pairs. The A-003B researchers found that differences in adsorption and desorption behavior of a particular asphalt, when combined with various aggregates, were far greater than that of a particular aggregate when combined with various asphalts (Curtis et al., 1994). Testing of 32 mixes performed by University of Nevada-Reno under the A-003A contract confirmed this observation as shown in Figures 3.23 and 3.24 (Curtis et al., 1994). Although the net adsorption and ECS tests measure different properties of the asphalt-aggregate interaction, the ECS results on the same 32 mixes were similar in that the differences in  $M_R$  ratio are much greater for one asphalt tested with four aggregates than one aggregate tested with eight asphalts (Figures 3.25 and 3.26).

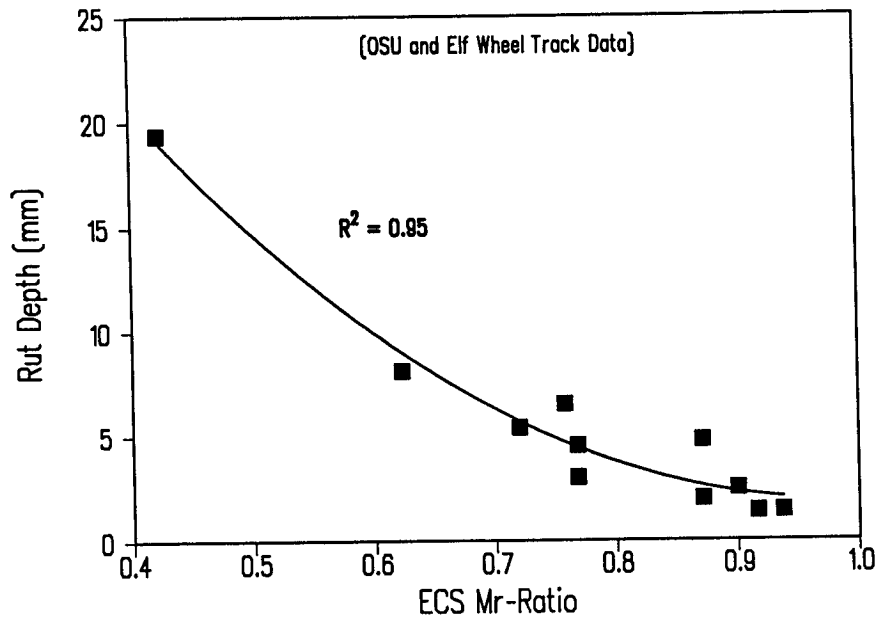


**Figure 3.21. Environmental Conditioning System field validation—wheel track data**

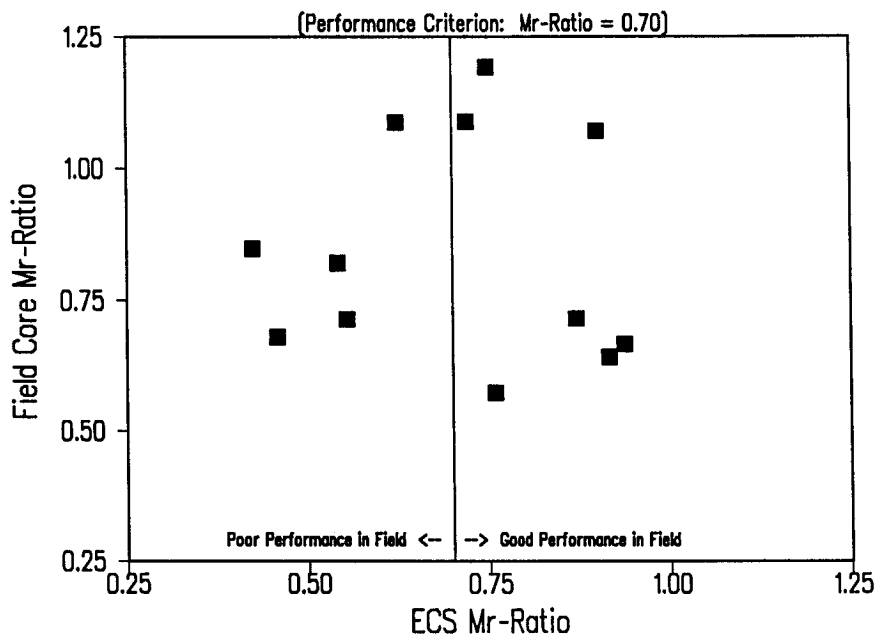


**Figure 3.22. Environmental Conditioning System field validation—performance criterion**

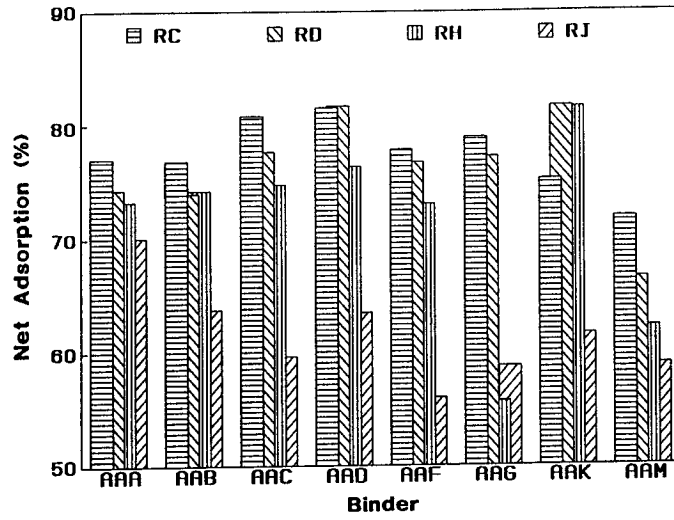


Figure 3.23. Net adsorption test results by binder

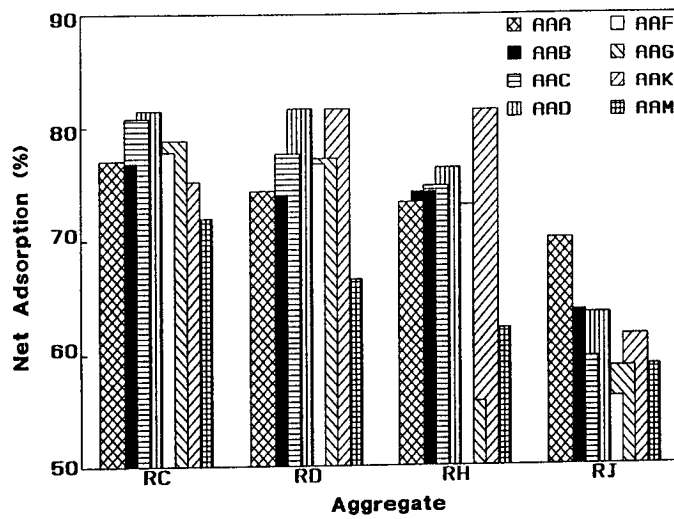


Figure 3.24. Net adsorption test results by aggregate

### 3.3 Conclusions and Recommendations

Based on research conducted by the A-002A, A-003B and A-003A contractors using data generated from several tasks and laboratory tests, performance ranking of mixes by asphalt type or aggregate type alone is not possible due to the significant interaction between asphalt and aggregate. Therefore, the net adsorption, AASHTO T 283, or ECS tests should be used to evaluate specific pairs of asphalt and aggregate. Furthermore, analysis of variance for both the net adsorption and ECS tests confirm that aggregate is the primary component affecting the moisture sensitivity properties of the asphalt-aggregate mix.

Although there are distinct advantages of the ECS over AASHTO T 283 (measurement of permeability; evaluation of specimens at any void content; and application of repeated loads throughout test duration), the response parameters that are generally used as a measure of moisture sensitivity, resilient modulus ( $M_R$ ) or tensile strength, are the same for both tests and when the test data are normalized for void content, the results are comparable. The ECS procedure however, requires fewer specimens for mix evaluation and minimizes the variability by eliminating specimen handling.

In addition to the comparison testing between the ECS and AASHTO T 283 that was part of the original A-003A experimental design, five additional mixes were evaluated to extend the database (Allen et al., 1994). Using recommended values of minimum  $M_R$  ratio or tensile strength ratio (AASHTO T 283), the results were reasonably comparable: the ECS results accurate in three of five cases; AASHTO T 283 accurate in two of five cases. The discrepancy between what is predicted based on the laboratory tests (both the ECS and AASHTO T 283) and the known field performance data underscores the need to reevaluate the severity of the test parameters and/or the failure criterion. In view of the preceding, the AASHTO T 283 is recommended for routine mix design and analysis in the Superpave framework, although the ECS is acknowledged to be a suitable alternative. The net adsorption test is recommended as a screening device only, primarily for preliminary source control/selection of aggregate. Finally, it is clear that a controlled program of materials collection, construction of field sections and subsequent coring to provide a larger data base is needed to further validate and refine the role of the ECS conditioning and test procedure for mix design.

With respect to the performance prediction models incorporated in the Superpave system, they can be used to evaluate the effect of moisture on mix performance by calculating the expected cracking and rutting for both dry and moisture-conditioned specimens. To do this, however, requires that the material properties of the mix be measured in a moisture-conditioned state as opposed to those measured in the dry or original state. The material properties used in the pavement performance models are measured on dry specimens, not moisture-conditioned specimens. Thus, rutting and cracking predictions are not calculated from moisture-conditioned specimens. It should also be noted that calibration factors within the pavement performance models were determined from the testing of dry specimens and field cores. The pavement performance models have been calibrated to take into consideration moisture-sensitive mixes such that distress predictions would be conservative.

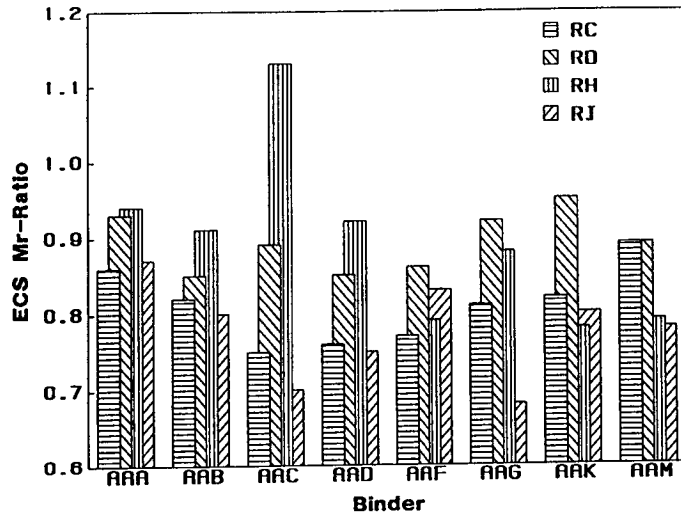


Figure 3.25. Environmental Conditioning System resilient modulus results by binder

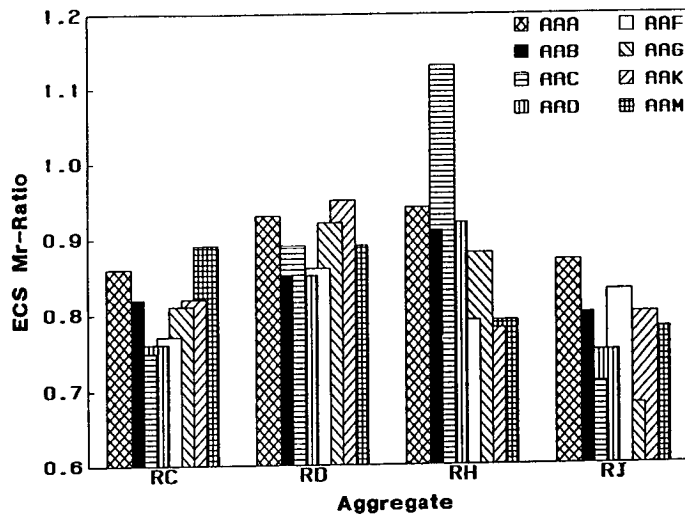


Figure 3.26. Environmental Conditioning System resilient modulus results by aggregate

## References

Allen, W.L., and R.L. Terrel. *Field Validation of the Environmental Conditioning System*. Report no. SHRP-A-396. Strategic Highway Research Program, National Research Council, Washington, DC: 1994.

Bell, C.A. *Summary Report on Aging of Asphalt-Aggregate Systems*. Report no. SHRP-A-305. Strategic Highway Research Program, National Research Council, Washington, DC: 1989.

Bell, C.A., Y. Ab-Wahab, M. Cristi, and D. Sosnovske. *Selection of Laboratory Aging Procedures for Asphalt-Aggregate Mixtures*. Report no. SHRP-A-383. Strategic Highway Research Program, National Research Council, Washington, DC: 1994.

Bell, C.A., A.J. Wieder, and M.J. Fellin. *Laboratory Aging of Asphalt-Aggregate Mixtures: Field Validation*. Report no. SHRP-A-390. Strategic Highway Research Program, National Research Council, Washington, DC: 1994.

Bonnot, J. "Asphalt Aggregate Mixtures." *Transportation Research Record* 1096, pp. 42-51, 1986.

Branthaver, J., J. Petersen, R. Robertson, J. Duvall, S. Kim, P. Harnsberger, T. Mill, E. Ensley, F. Barbour, J. Schabron. *Binder Characterization and Evaluation—Volume 2: Chemistry*. Report no. SHRP-A-368. Strategic Highway Research Program, National Research Council, Washington, DC: 1994.

Brown, B. B. *Delphi Process: A Methodology Used for the Elicitation of Opinions of Experts*. Report no. P-3925. RAND Corporation, Washington, DC: 1968.

Busching, H. W. "Stability Relationships of Gyratory-Compacted Bituminous Mixtures." Master's thesis, Purdue University, West Lafayette, IN: 1963.

Button, J. W., D. W. Little, V. Jagadam, and O. J. Pendleton. "Correlation of Selected Laboratory Compaction Methods with Field Compaction." Texas Transportation Institute, Texas A&M University, College Station: 1992.

Consuegra, A. E. "Comparative Evaluation of Laboratory Compaction Devices Based on Their Ability to Produce Mixtures with Engineering Properties Similar to Those Produced in the Field." Master's thesis, Texas A&M University, College Station: 1988.

Curtis, C., K. Ensley, and J. Epps. *Fundamental Properties of Asphalt-Aggregate Interactions Including Adhesion and Absorption*. Report no. SHRP-A-341. Strategic Highway Research Program, National Research Council, Washington, DC: 1993.

Dalkey, N. C. *Delphi*. Report no. P-3704. RAND Corporation, Washington, DC: 1967.

Dalkey, N. C. and O. Helmer. *The Use of Experts for the Estimation of Bombing Requirements—A Project Delphi Experiment*. Report no. RM-727-PR. RAND Corporation, Washington, DC: 1951.

Hughes, C. S. *Compaction of Asphalt Pavement*. NCHRP Report 152. Transportation Research Board, National Research Council, Washington, DC: 1989.

Hughes, R. E. "Use of a Gyrotory Testing Machine to Apply Simulated Traffic to Bituminous Concrete." Master's thesis, Purdue University, West Lafayette, IN: 1964.

Kennedy, T. W., et al. *Superpave System: The Product of the SHRP Asphalt Research Program*. Strategic Highway Research Program, National Research Council, Washington, DC: 1994. Forthcoming.

Linstone, H. A., and M. Turoff. *The Delphi Method: Techniques and Applications*. Addison-Wesley, Reading, MA: 1975.

Lottman, R. P. "Predicting Moisture-Induced Damage to Asphaltic Concrete — Field Evaluation." NCHRP Report No. 246. Transportation Research Board, 1982.

Maupin, G.W. *The Variability of the Indirect Tensile Stripping Test*. Report no. FHWA/VA-91-5. Federal Highway Administration, U.S. Department of Transportation.

Moultier, R. "Utilization and Possibilities of the Gyrotory Shear Compacting Press." *Liaison Bulletin of the Bridge and Road Laboratories Special Issue: Bitumens and Bituminous Concrete* (December 1977).

Scholz, T.V., R.L. Terrel, A. Al-Joaib, J. Bea. *Asphalt Binder Validation—Water Sensitivity*. Report no. SHRP-A-402. Strategic Highway Research Program, National Research Council, Washington, DC: 1994.

Smith, D. E., et al. "Use of a Modified Delphi Method to Develop Specifications for Aggregates and Asphalt-Aggregate Mixtures for the Strategic Highway Research Program." Working paper. Strategic Highway Research Program, National Research Council, Washington, DC: November 30, 1992.



Sousa, J. B., J. Harvey, L. Painter, J. A. Deacon, and C. L. Monismith. *Evaluation of Laboratory Procedures for Compacting Asphalt-Aggregate Mixtures*. Report no. SHRP-A-UWP-91-523. Strategic Highway Research Program, National Research Council, Washington, DC: 1991.

Stuart, K. *Evaluation of Procedures Used to Predict Moisture Damage in Asphalt Mixtures*. Report no. FHWA-RD-86-091. Federal Highway Administration, U.S. Department of Transportation, 1986.

Terrel, R. L., and S. Al-Swailmi. *Water Sensitivity of Asphalt-Aggregate Mixtures Test Development*. Report no. SHRP-A-403. Strategic Highway Research Program, National Research Council, Washington, DC: 1994.

Tunncliff, D. G. and R. E. Root. "Use of Antistripping Additives in Asphalt Concrete Mixtures. NCHRP Report No. 274, Transportation Research Board, 1984.

Von Quintus, H. L., J. A. Scherocman, C. S. Hughes, and T. W. Kennedy. *Asphalt-Aggregate Mixture Analysis System*. NCHRP Report 338. TRB, National Research Council, Washington, DC: 1991.